UNIVERSIDADE FEDERAL DO PARANÁ

SHUQIN WANG

MÉTODO DE GALERKIN DESCONTÍNUO PARA DOIS PROBLEMAS DE CONVECÇÃO-DIFUSÃO

Curitiba, Setembro de 2015.

UNIVERSIDADE FEDERAL DO PARANÁ
SHUQIN WANG

MÉTODO DE GALERKIN DESCONTÍNUO PARA DOIS PROBLEMAS DE CONVECÇÃO-DIFUSÃO

Tese de Doutorado apresentada ao Programa de Pós-Graduação em Matemática Aplicada da Universidade Federal do Paraná, como requisito parcial à obtenção do Título de Doutor em Matemática.

Orientador: Prof. Dr. Jinyun Yuan.
Co-orientador: Prof. Dr. Yujiang Wu.

Curitiba, Setembro de 2015.

Ministério da Educação
Universidade Federal do Paraná
Setor de Ciências Exatas/Departamento de Matemática
Programa de Pós-Graduação em Matemática - PPGM
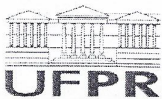
ATA DA 6ª DEFESA DE TESE DE DOUTORADO

Aos três dias do mês de agosto de 2015, no Anfiteatro B, Bloco das PCs, da Universidade Federal do Paraná, foi instalada pelo Professor Yuan Jin Yun, a Banca Examinadora para a Sexta Defesa de Tese de Doutorado em Matemática. Estiveram presentes ao Ato, professores, alunos e visitantes.

A banca examinadora, homologada pelo Colegiado do Programa de Pós-Graduação em Matemática, ficou constituída pelos professores: Prof. Dr. João Luís Gonçalves, Prof. Dr. Saulo Pomponet Oliveira e Prof. Dr. Geovani Nunes Grapiglia, do Programa de Pós-Graduação em Matemática, Prof. Hai-Qiong Zhao, da Shanghai University of International Bussiness and Economics, e o Prof. Dr. Yuan Jin Yun, orientador do projeto de tese, a quem coube a presidência dos trabalhos.

Às dez horas, a banca iniciou seus trabalhos, convidando a candidata **SHUQIN WANG** a apresentar seu Projeto de Tese intitulado: "MÉTODO DE GALERKIN DESCONTÍNUO PARA DOIS PROBLEMAS DE CONVECÇÃO-DIFUSÃO". Encerrada a apresentação, iniciou-se a fase de arguição pelos membros participantes. Após a arguição, a banca com pelo menos 05 (cinco) membros, reuniu-se para apreciação do desempenho do pós-graduando.

A banca considerou que a pós-graduanda fez uma apresentação com a necessária concisão. A tese apresenta contribuição à área de estudos e não foram registrados problemas fundamentais de estrutura e redação, resultando em plena e satisfatória compreensão dos objetivos pretendidos.
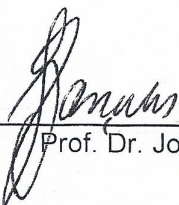
Tendo em vista a tese e a arguição, os membros presentes da banca decidiram pela sua aprovação.

Curitiba, 03 de setembro de 2015.
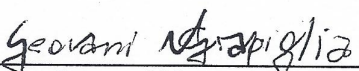
Prof. Dr. Yuan Jin Yun
PPGM – UFPR

Prof. Dr. João Luís Gonçalves
UTFPR

Prof. Dr. Geovani Nunes Grapiglia
PPGM – UFPR

Prof. Dr. Saulo Pomponet Oliveira
PPGM

Prof. Dr. Hai-Qiong Zhao
Shanghai University of International Bussiness
and Economics

Ministério da Educação
Universidade Federal do Paraná
Setor de Ciências Exatas/Departamento de Matemática
Programa de Pós-Graduação em Matemática - PPGM

PARECER DA BANCA EXAMINADORA

Após a apresentação, a banca deliberou pela aprovação da tese da candidata **SHUQIN WANG** devendo, para tanto, incorporar as sugestões feitas pelos membros da banca, no prazo estabelecido pelo regimento correspondente.

Curitiba, 03 de setembro de 2015.

Orientador: Prof. Dr. Yuan Jin Yun
PPGM – UFPR

Prof. Dr. João Luís Gonçalves
UTFPR

Prof. Dr. Geovani Nunes Grapiglia
PPGM – UFPR

Prof. Dr. Saulo Pomponet Oliveira
PPGM – UFPR

Prof. Dr. Hai-Qiong Zhao
Shanghai University of International Bussiness and Economics
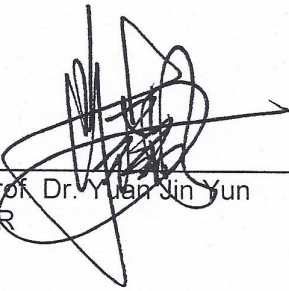
"MÉTODO DE GALERKIN DESCONTÍNUO PARA DOIS PROBLEMAS DE

CONVECÇÃO-DIFUSÃO"

por
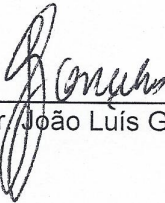
Shuqin Wang

Tese aprovada como requisito parcial para obtenção do grau de Doutor no Programa

de Pós-Graduação em Matemática, pela Comissão Examinadora composta por:
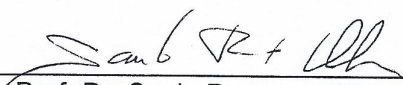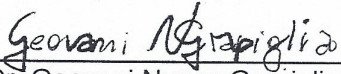
Orientador: Prof. Dr. Yuan Jin Yun
PPGM – UFPR
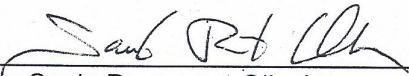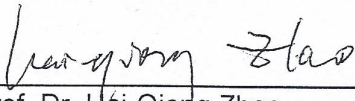
Prof. Dr. João Luís Gonçalves
UTFPR
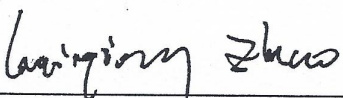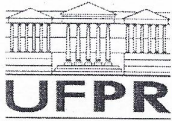
Prof. Dr. Geovani Nunes Grapiglia
PPGM – UFPR

Prof. Dr. Saulo Pomponet Oliveira
PPGM – UFPR

Prof. Dr. Hai-Qiong Zhao
Shanghai University of International Bussiness and Economics

Curitiba, 03 de setembro de 2015.

Aos meus pais e meu irmão.

Acknowledgements

Immeasurable appreciation and deepest gratitude for the help and support from the following persons .

I am extremely thankful to my supervisor **Prof. Jinyun Yuan**, and co-supervisor **Prof. Yujiang Wu** for their support, advices, guidance, valuable comments, suggestions, and care, shelter in doing these researches.

I greatly appreciate **Prof. Weihua Deng**, who responded promptly and enthusiastically to my requests for comments despite his congested schedules.

I thank for all the help from the professors in UFPR, Prof. Saulo, Prof. Geovani, Prof. Elizabeth, Prof. Matioli and other professors who I know.

I am also thankful to my friends in Brazil, Oscar, Kally, Aura, Elvis, Marcos, Diego, Priscila, Leonardo and all the classmates from the Pós.

Above all, thanks to my parents and my brother for their support, understanding and love.

Resumo

Nesta tese consideramos dois tipos de problemas de convecção-difusão, a saber, as equações de Navier-Stokes para meios incompressíveis e dependentes do tempo e as equações de convecção-difusão espaço-fracionária em duas dimensões.

Para as equações de Navier-Stokes usamos o método das características para linearizar equações não-lineares e introduzimos uma variável auxiliar para reduzir a equação de ordem alta a um sistema de primeira ordem. Escolhendo-se cuidadosamente os fluxos numéricos e adicionando os termos de penalização propomos um método de Galerkin descontínuo característico local (CLDG) simétrico e estável. Com essa simetria, é fácil provar estabilidade numérica e estimativas de erros. Experimentos numéricos são realizados para verificar os resultados teóricos. Para os problemas de convecção-difusão espaço-fracionária ainda utilizamos o método das características para tratar a derivada no tempo e os termos convectivos conjuntamente. Para o termo fracionário introduzimos algumas variáveis auxiliares para decompor a derivada de Riemann-Liouville na integral de Riemann-Liouville e na derivada de ordem inteira. Em seguida um método de Galerkin descontínuo hibridizado (HDG) é proposto. Finalmente usamos os métodos analíticos para realizar a análise de estabilidade e estimativas de convergência do esquema HDG.

Pelo nosso conhecimento, este é o primeiro trabalho que combina o método de Galerkin descontínuo característico às equações de Navier-Stokes e às equações convecção-difusão espaço-fracionária em 2D. Estes esquemas também podem ser aplicados e estudados em outros problemas. Os resultados numéricos são consistentes com os resultados teóricos.

Palavras-chave: método das características; método de Galerkin descontínuo; equações de Navier-Stokes; equações de convecção-difusão espaço-fracionária.

Abstract

In this thesis, we consider two kinds of convection-diffusion problems, namely the classical time-dependent incompressible Navier-Stokes equations and the space-fractional convection-diffusion equations in two dimensions.

For Navier-Stokes equations, we use the method of characteristics to make nonlinear equations linear, and we introduce an auxiliary variable to reduce high-order equation to one order system. Carefully choosing numerical fluxes and adding penalty terms, a stable and symmetric characteristic local discontinuous Galerkin (CLDG) method is proposed. With this symmetry, it is easy to perform numerical stability and error estimates. Numerical experiments are performed to verify theoretical results. For the space-fractional convection-diffusion problems, we still use the method of characteristics to tackle the time derivative and convective terms together. For the fractional term, we introduce some auxiliary variables to split the Riemann-Liouville derivative into Riemann-Liouville integral and integer order derivative. Thus a hybridized discontinuous Galerkin method (HDG) is proposed. Finally we use general analytic methods to perform the stability analysis and convergence estimates of the HDG scheme.

As far as we know, this is the first time the discontinuous Galerkin method and the method of characteristics are combined to numerically solve the Navier-Stokes equations and space-fractional convection-diffusion equations in 2D. These schemes can be applied and further studied into other problems as well. The numerical results are consistent with theoretical results.

Keywords: method of characteristics; discontinuous Galerkin method; Navier-Stokes equations; space-fractional convection-diffusion equations.

Contents

List of Figures

List of Tables

List of Symbols

DG   discontinuous Galerkin method

LDG   local discontinuous Galerkin method

CLDG   characteristic local discontinuous Galerkin method

HDG   hybridized discontinuous Galerkin method

$\mathbb{R}^d$ d-dimensional Euclidean space

$\mathbb{C}^d$ d-dimensional complex numbers space

$\|\cdot\|_0$ L^2-norm

$\|\cdot\|_1$ H^1-norm

$\|\cdot\|_{-1}$ the norm of space H^{-1}

$|\cdot|_1$ H^1-semi-norm

$\boldsymbol{v}$ vector function

$\bar{\boldsymbol{v}}$ matrix function

∇u gradient operator for function u

$\nabla \cdot \boldsymbol{u}$ divergence operator for function $\boldsymbol{u}$

Δu Laplace operator for function u

$\mathbb{P}^k$ the space of all polynomials of degree $\leq k$

$\mathscr{E}_h$	the subdivision of domain Ω
E	a triangle or a parallelogram in 2D
$\{v\}$	an average for function v
$[v]$	a jump for function v
$_a\mathcal{I}_x^\mu u(x)$	left Riemann-Liouville fractional integral of function $u(x)$
$_x\mathcal{I}_b^\mu u(x)$	right Riemann-Liouville fractional integral of function $u(x)$
$_aD_x^\nu u(x)$	left Riemann-Liouville fractional derivative of function $u(x)$
$_xD_b^\nu u(x)$	right Riemann-Liouville fractional derivative of function $u(x)$
$_a^CD_x^\nu u(x)$	left Caputo's fractional derivative of function $u(x)$
$_x^CD_b^\nu u(x)$	right Caputo's fractional derivative of function $u(x)$
$J_L^\nu(\mathbb{R})$	left fractional derivative space
$J_R^\nu(\mathbb{R})$	right fractional derivative space
$J_S^\nu(\mathbb{R})$	symmetric fractional derivative space
$J_L^{-\mu}(\mathbb{R})$	left fractional space
$J_R^{-\mu}(\mathbb{R})$	right fractional space
N^+	the set of positive natural numbers

Introduction

In this thesis, we mainly consider two kinds of convection-diffusion problems: the classical time-dependent incompressible Navier-Stokes equations and the space-fractional convection-diffusion equations.

Model one

In 1755, Swiss mathematician Leonhard Euler derived the Euler equations to describe an ideal fluid without consider the effects of viscosity. In 1821, French engineer Claude-Louis Navier introduced the element of viscosity for the more realistic and more difficult problem of viscous fluids. Because of the physical significance of the viscosity coefficient, Claude-Louis Marie Henri Navier's name is associated with the famous Navier-Stokes equations. Untill 1845 Irish mathematician-physicist George Gabrid Stokes published a derivation of the equations in a manner that is currently understood. Then, George Gabrid Stokes's name was attached with the Navier-Stokes equations.

Navier-Stokes equations are useful because they describe many scientific and engineering phenomena. They are used to model weather, ocean currents, water flow in a pipe and air flow around a wing. Navier-Stokes equations are still used to help with the design of aircrafts and cars, the study of blood flow, the design of power stations, the analysis of pollution [4, 6, 17, 18, 30, 37, 44, 46, 56]. The reciprocal of fluid viscosity coefficient ν is called Reynolds number. For very low Reynolds numbers and simple geometries, it is often possible and easy to find explicit formulas for solutions to Navier-Stokes equations in a computation. For high Reynolds numbers, in turbulent flow there begin to be eddies with a wide range of sizes. To capture all these eddies in a computation, one needs a large amount of information, for example, memory and datum. Such flows can be described in many situations, for example, blood flow in large caliber vessels, fluid-structure interaction, aerodynamics, geophysical and astrophysical flow modeling. Despite of half a century of vigorous efforts, there is still a lack of sys-

tematic understanding how different scales interact to form the inertial range from a smooth initial condition. Therefore, the description of the behavior of the solutions of the Navier-Stokes equations at high Reynolds numbers is the heart of the problem. The choice of the singularity problem for the incompressible Navier-Stokes equations as one of the million prize problems highlight the fundamental role that mathematical analysis may play in this topic.

In Chapter 2, we shall design a new scheme to recast the time-dependent incompressible Navier-Stokes equations. Our scheme is based on standard local discontinuous Galerkin method and the method of characteristics. In this work, we devote to recover the solutions with high Reynolds numbers. For the sake of simplicity, we just consider the full Navier-Stokes equations with Dirichlet boundary conditions: these equations can be written by

$$
\begin{cases}
\partial_t \boldsymbol{u} + (\boldsymbol{u} \cdot \nabla)\boldsymbol{u} - \nu \Delta \boldsymbol{u} + \nabla p = \boldsymbol{f}, & (\boldsymbol{x}, t) \in \Omega \times J, \\
\nabla \cdot \boldsymbol{u} = 0, & (\boldsymbol{x}, t) \in \Omega \times J, \\
\boldsymbol{u}(\boldsymbol{x}, t) = 0, & (\boldsymbol{x}, t) \in \partial\Omega \times J, \\
\boldsymbol{u}(\boldsymbol{x}, 0) = \boldsymbol{u}_0(\boldsymbol{x}), & \boldsymbol{x} \in \Omega,
\end{cases} \tag{1}
$$

where Ω is a bounded polygonal domain in $\mathbb{R}^2$ with Lipschitz continuous boundary $\partial\Omega$ and $J = [0, T], 0 < T < \infty$.

Because of the inherent performances of the Navier-Stokes or Stokes equations in characterizing the turbulence in fluids or gases, from finite element method to discontinuous Galerkin method a lot of researches on these topics have been done [4, 15, 17, 18, 29, 31, 32, 37, 51]. As our knowledge, there are few works on discontinuous Galerkin method for solving the time-dependent incompressible Navier-Stokes equations, and much less on local discontinuous Galerkin method (LDG), which motivates us to consider LDG method for the full Navier-Stokes equations. Splitting the nonlinearity and incompressibility, and using discontinuous or continuous Galerkin method in space, Girault et al [29] solved the time-dependent incompressible Navier-Stokes equations using penalty discontinuous Galerkin method [50]. Comparing with the work [29], we use different DG method to discretize spatial space and get better numerical results (see Chapter 2).

In Chapter 2 of this thesis, we use the local discontinuous Galerkin method to discretize the spatial space of the considered equation. It seems that the following advantages can be obtained: 1) by introducing local auxiliary variable, the order of the diffusion term can be reduced. Arising from using penalty terms the symmetric formulation makes stability and error analysis possible; 2) the introduced auxiliary variable

$\bar{\boldsymbol{\sigma}} = \sqrt{\nu}\nabla\boldsymbol{u}$ lessens challenges caused by big Reynolds numbers since $\sqrt{\nu}$ is not as small as ν when ν is small enough. The lucky thing is that we still keep the general advantages of discontinuous Galerkin method, i.e., the high order accuracy, the h_p-adaptivity, and the high parallelizability, etc..

Here we use the method of characteristics [6, 27] to tackle time derivative term and nonlinear convective term together for the considered equation with first order accuracy in time. The method of characteristics has many advantages compared to a high order Runger-Kutta scheme or a high order finite difference scheme, such as 1) efficient in solving the advection-dominated diffusion problems; 2) easily obtaining the existence and uniqueness of the solutions of the discretized system; 3) making nonlinear equations linear and conveniently tackling nonlinear obstacles; 4) easily performing numerical stability analysis.

In summary, the work described in Chapter 2 is an extension of local discontinuous Galerkin methods for the Stokes system [15] with the characteristic local discontinuous Galerkin scheme to the time-dependent incompressible Navier-Stokes equations.

Model two

In Chapter 3, we shall consider the time-dependent space-fractional convection-diffusion problem for u in the form:

$$\begin{cases} \partial_t u + \boldsymbol{b} \cdot \nabla u - c_1 \frac{\partial^\alpha u}{\partial x^\alpha} - c_2 \frac{\partial^\beta u}{\partial y^\beta} = f, & (\boldsymbol{x},t) \in \Omega \times J, \\ u(\boldsymbol{x},t) = 0, & (\boldsymbol{x},t) \in \partial\Omega \times J, \\ u(\boldsymbol{x},0) = u_0(\boldsymbol{x}), & \boldsymbol{x} \in \Omega, \end{cases} \tag{2}$$

where $\Omega \in \mathbb{R}^2$ is rectangular domain with Lipschitz continuous boundary $\partial\Omega$, and $J = [0,T], 0 < T < \infty$, the superdiffusion operators $\frac{\partial^\alpha}{\partial x^\alpha}$ and $\frac{\partial^\beta}{\partial y^\beta}$ will be defined in Chapter 3.

Let us briefly review the development of numerical methods for fractional convection-diffusion equations. Several authors have proposed a variety of higher-order finite difference schemes for solving time-fractional convection-diffusion equations, for example [23, 36, 58, 60], and solving space-fractional convection-diffusion equations [10, 38]. In [40] and [42], W. Mclean and K. Mustapha have used piecewise-constant and piecewise-linear discontinuous Galerkin (DG) methods to solve time-fractional diffusion and wave equations, respectively. However, these methods require more computational costs (see [41]). In order to tackle those problems, in [41] W. Mclean has proposed an efficient

scheme called fast summation by interval clustering to reduce the implementation memory. Furthermore, in [26] Deng and Hesthaven have developed discontinuous Galerkin method for fractional spatial derivatives and given a fundamental frame to combine the discontinuous Galerkin method with fractional operators in one dimension. In [59] Xu and Hesthaven have applied the DG method to fractional convection-diffusion equations in one dimension. In two dimensional case, Ji and Tang [34] have applied the DG method to recast fractional diffusion equations in rectangular meshes with the optimal convergence order $\mathcal{O}(h^{k+1})$ numerically. However, there were no theoretical results. So far very few works have considered fractional problems in triangular meshes. This motivates us to consider a successful DG method for solving fractional problems in triangular meshes.

Fractional differential equations (FDEs) have become more and more popular in applied science and engineering field recently. The history and mathematical background of fractional differential operators are given in [45] with definitions and applications of fractional calculus. This kind of equations has been used increasingly in many fields, for example, in Nature [35] fractional operators applied in fractal stream chemistry and its implications for contaminant transport in catchments, in [39] the fractional calculus motivated in bioengineering, and its application as a model for physical phenomena exhibiting anomalous diffusion, Lévy motion, turbulence [5, 8, 53], etc.

In Chapter 3, we shall design a stable and accurate discontinuous Galerkin method for the considered equation (2). The stability and error analysis are proved in multiple dimensions. This development is built on the extension work on DG for previous work found in [26, 59], where a qualitative study of the high order local discontinuous Galerkin method was discussed and some theoretical results were offered in one space dimension. In order to perform the error analysis, the authors defined some projection operators to prove error results. Unfortunately, we can not extend the defined projection operators into two dimensional case easily (see [26, 59]). Hence, to avoid this difficulty, a different DG method is obtained in Chapter 3 by carefully choosing numerical fluxes and adding penalty terms. The presented hybridized discontinuous Galerkin (HDG) method has the following attractive properties: 1) The HDG method can be used for other fractional problems, for example, fractional diffusion equations; 2) It has excellent provable stability. One can prove the stability in any space dimension; 3) Theoretically, the error estimates are proved more easily with general analytical methods in any space dimension.

The outline of thesis

Let us give a more detailed description of the content of this thesis.

In Chapter 1, firstly, we review some basic definitions of Sobolev spaces and broken Sobolev spaces, some useful lemmas for discontinuous Galerkin method. Then we describe some definitions of fractional calculus and some fractional variational norms and spaces. Finally, we shall introduce the method of characteristics with different cases: the linear case and nonlinear case.

In Chapter 2, by combining the method of characteristics and the local discontinuous Galerkin method and carefully constructing numerical fluxes, we design a variational formulation for the time-dependent incompressible Navier-Stokes equation in $\mathbb{R}^2$. The nonlinear stability of the proposed symmetric variational formulation is proved. Moreover, for general triangulations we derive an a priori estimate for the L^2-norm of the errors in both velocity and the pressure. The proposed scheme works well for a wide range of Reynolds numbers such as $Re = 10^6, 10^8, 10^{12}, 10^{15}, 10^{16}$.

In Chapter 3, a hybridized discontinuous Galerkin method is proposed for solving 2D fractional convection-diffusion equations containing derivatives of fractional order in space on a finite domain. The Caputo's or Riemann-Liouville derivative is chosen as the representation of spatial derivative. Combining the method of characteristics and the hybridized discontinuous Galerkin method, the symmetric variational formulation is constructed. The stability of the presented scheme is proved. An order of $k + 1/2$ is established for some fractional convection-diffusion problems. Some numerical examples are given to illustrate the numerical performance of our method. The first experiment is performed to display the convergence order while the second experiment justifies the benefits of this scheme. Both are tested with triangular meshes.

Finally, in Chapter 4 we conclude these works and give some future perspectives.

Chapter 1

Fundamental definitions and lemmas

Discontinuous Galerkin method was introduced in 1973 by Reed and Hill [49], in the framework of neutron transport (steady state linear hyperbolic equations). A major development of the discontinuous Galerkin method was carried out by Cockburn and collaborators. In a series of papers [15, 16, 19, 21, 22], they established a framework to easily solve nonlinear time-dependent hyperbolic conservation laws, using explicit, nonlinearly stable high-order Runge-Kutta time discretization [22] and discontinuous Galerkin spatial discretization [17, 18].

In this chapter, we shall review some basic definitions and results for mathematical setting of the discontinuous Galerkin (DG) method. Firstly, we describe some Sobolev spaces. Afterwards, we introduce broken Sobolev space, the natural working spaces for DG.

1.1 Sobolev spaces and inequalities

Throughout this section, let Ω denote a bounded polygonal domain in $\mathbb{R}^d, d \in N^+$. The $L^2(\Omega)$ and $L^\infty(\Omega)$ are the classical space of square integrable functions with the inner product $(f, g) = \int_\Omega fg \, dx$ and the space of bounded functions, respectively [14, 50].

$$L^\infty(\Omega) = \big\{ v :\| v \|_{L^\infty(\Omega)} < \infty \big\}, \quad \| v \|_{L^\infty(\Omega)} = ess \ \sup \big\{ |v(x)| : x \in \Omega \big\}.$$

It is well known that $C(\Omega)$ and $C_0^\infty(\Omega)$ are the space of continuous functions and the space of infinitely differentiable functions with compact support, respectively. Generally

6

the Sobolev space $H^s(\Omega)$ for integer s is denoted by

$$H^s(\Omega) = \left\{ v \in L^2(\Omega) : \forall\, 0 \leq |\alpha| \leq s, D^\alpha v \in L^2(\Omega) \right\},$$

where $D^\alpha v = \frac{\partial^{|\alpha|} v}{\partial x_1^{\alpha_1} \cdots \partial x_d^{\alpha_d}}$, $|\alpha| = \sum_{i=1}^d \alpha_i$. Similarly, the space $H^1(\Omega)$ is defined by

$$H^1(\Omega) = \left\{ v \in L^2(\Omega) : Dv \in L^2(\Omega) \right\}.$$

$H_0^1(\Omega)$ denotes the closure of $C_0^\infty(\Omega)$ in $H^1(\Omega)$, and $H^{-1}(\Omega)$ is the dual space of $H_0^1(\Omega)$.

Assume that k is nonnegative integer, $C^k(\bar\Omega) = \left\{ u : \bar\Omega \mapsto \mathbb{R} | D^\alpha u \in C(\Omega), |\alpha| \leq k \right\}$ is the space of k times continuously differentiable functions equipped with the norm

$$\| u \|_{C^k(\bar\Omega)} = \sum_{|\alpha| \leq k} \sup_{x \in \bar\Omega} |D^\alpha u(x)|,$$

where $\bar\Omega$ is the closure of Ω.

Let $0 < \beta \leq 1$, $C^{k,\beta}(\bar\Omega) = \left\{ u \in C^k(\bar\Omega) | \sup_{x \neq y, x, y \in \bar\Omega} \frac{|D^\alpha u(x) - D^\alpha u(y)|}{|x-y|^\beta} < +\infty, |\alpha| = k \right\}$ is the space of $k + \beta$ times Hölder continuous functions equipped with the norm

$$\| u \|_{C^{k,\beta}(\bar\Omega)} = \| u \|_{C^k(\bar\Omega)} + \sup_{x \neq y, x, y \in \bar\Omega} \frac{|D^\alpha u(x) - D^\alpha u(y)|}{|x-y|^\beta}.$$

For any Banach space X let $L^p[0,T;X], 1 \leq p < \infty$, and $L^\infty[0,T;X]$ denote the spaces of $p-$integrable functions with norms

$$\| v \|_{L^p[0,T;X]} = \left(\int_0^T \| v(t) \|_X^p \, \right)^{1/p}, \quad \| v \|_{L^\infty[0,T;X]} = esssup_{t \in [0,T]} \| v \|_X < \infty.$$

Let $H^1[0,T;X]$ denote the space of functions with square integral derivatives with norm

$$\| v \|_{H^1[0,T;X]} = \left(\int_0^T \| v \|_X^2 \, dt + \int_0^T \| \partial_t v \|_X^2 \, dt \right)^{1/2}.$$

Here, we introduce some inequalities [14, 50] that are used many times in our analysis.

- Hölder's inequality:

$$\int_\Omega |f(x)g(x)| dx \leq \left(\int_\Omega |f(x)|^p dx \right)^{\frac{1}{p}} \left(\int_\Omega |g(x)|^q dx \right)^{\frac{1}{q}},$$

where $\frac{1}{p} + \frac{1}{q} = 1$ with $1 \leq p, q < \infty$ and $f \in L^p(\Omega), g \in L^q(\Omega)$. If $p = q = 2$, this inequality becomes Cauchy-Schwarz's inequality.

7

Similarly, Hölder's inequality for sums states that

$$\sum_{k=1}^{n} |a_k b_k| \leq \Big(\sum_{k=1}^{n} |a_k|^p \Big)^{1/p} \Big(\sum_{k=1}^{n} |b_k|^q \Big)^{1/q},$$

where $(a_1, \cdots, a_n), (b_1, \cdots, b_n) \in \mathbb{R}^n$ or $\mathbb{C}^n$.

- Young's inequality:

$$\forall \epsilon > 0, \ \forall a, b \in \mathbb{R}, \ ab \leq \frac{\epsilon}{2} a^2 + \frac{1}{2\epsilon} b^2.$$

Lemma 1.1. *(Poincaré-Friedrichs inequality) [50] The classical Poincaré-Friedrichs inequality in $H^1(\Omega)$ says that there is a constant C such that*

$$\forall \ v \in H^1(\Omega), \quad \| v \|_0 \leq C \big(\| \nabla v \|_0 + \big| \int_{\partial \Omega} v \big| \big). \tag{1.1}$$

Consequently, we have

$$\forall \ v \in H_0^1(\Omega), \quad \| v \|_0 \leq C \| \nabla v \|_0. \tag{1.2}$$

See Chapter 3 of [50].

1.2 Broken Sobolev spaces and fundamental lemmas

As we know, discontinuous Galerkin method is a type of finite element method. They share many properties and results, however discontinuous Galerkin method uses completely discontinuous piecewise polynomial spaces for numerical solutions and test functions. Comparing with classical finite element method, discontinuous Galerkin method have the following attractive properties:

- It can be easily designed for any order of accuracy. In fact, the order of accuracy can be locally determined in each simplex.

- It can handle complicated geometries, i.e, it can be used on arbitrary triangulations, even those with hanging nodes.

- It has high parallelizability.

- It has excellent provable nonlinear stability.
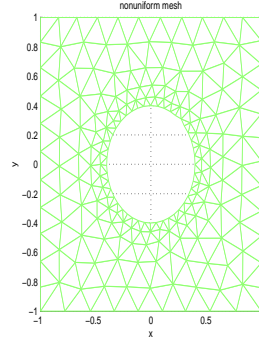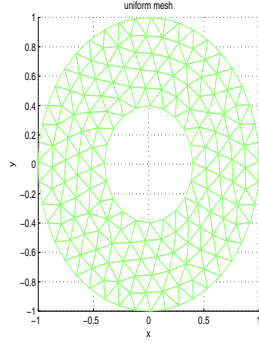
Fig. 1.1: Uniform triangular meshes.   Fig. 1.2: Nonuniform triangular meshes.

The broken Sobolev spaces [50] are natural spaces to work with discontinuos Galerkin method. These spaces depend strongly on the partition of the domain. Let Ω be a polygonal domain subdivided into elements E (see Figures 1.1-1.2). Here E is a triangle or a quadrilateral in 2D. We assume that the intersection of two elements is either empty, or an edge (2D). The mesh is called a regular mesh if

$$\forall E \in \mathscr{E}_h, \quad \frac{h_E}{\rho_E} \leq C,$$

where $\mathscr{E}_h$ is the subdivision of Ω, C is a constant, h_E is the diameter of the element E, i.e., $h_E = \sup_{x,y \in E} \| x - y \|$ and ρ_E is the diameter of the inscribed circle in element E. Throughout this thesis $h = \max_{E \in \mathscr{E}_h} h_E$.

We introduce the broken Sobolev space for any real number s,

$$H^s(\mathscr{E}_h) = \left\{ v \in L^2(\Omega) : \forall E \in \mathscr{E}_h, v|_E \in H^s(E) \right\},$$

equipped with the broken Sobolev norm:

$$\| v \|_{H^s(\mathscr{E}_h)} = \left(\sum_{E \in \mathscr{E}_h} \| v \|^2_{H^s(E)} \right)^{1/2}.$$

Jumps and averages: We denote by $\mathscr{E}_h^B$ the set of edges of the subdivision $\mathscr{E}_h$. Let $\mathscr{E}_h^i$ denote the set of interior edges, $\mathscr{E}_h^b = \mathscr{E}_h^B \setminus \mathscr{E}_h^i$ the set of edges on $\partial\Omega$. With each edge e, we have a unit normal vector $\boldsymbol{n}_e$. If e is on the boundary $\partial\Omega$, then $\boldsymbol{n}_e$ is taken to be the unit outward vector normal to $\partial\Omega$ [50].

9

If v belongs to $H^1(\mathscr{E}_h)$, the trace of v along any side of one element E is well defined. If two elements E_1^e and E_2^e are neighbors and share one common side e, there are two traces of v belonging to e. We assume that the normal vector $\boldsymbol{n}_e$ is oriented from E_1^e to E_2^e, and an average and a jump for v can be defined by

$$\{v\} = \frac{1}{2}(v|_{\partial E_1^e} + v|_{\partial E_2^e}), \quad [v] = (v|_{\partial E_1^e} - v|_{\partial E_2^e}), \ \forall e \in \partial E_1^e \bigcap \partial E_2^e.$$

If e is on $\partial\Omega$, we have

$$\{v\} = [v] = v|_{\partial E}, \quad \forall e \in \partial E \bigcap \partial\Omega.$$

Next, we shall recall some inequalities, which are important tools for theoretical analysis.

Lemma 1.2. *(Continuous Gronwall inequality) [50] Assume that f, g, h are piecewise continuous non-negative functions defined on (a, b), and g is nondecreasing. If there exists a positive constant C independent of t such that*

$$\forall\, t \in (a, b), \quad f(t) + h(t) \leq g(t) + C \int_a^t f(s)ds,$$

then

$$\forall\, t \in (a, b), \quad f(t) + h(t) \leq e^{C(t-a)}g(t).$$

See Chapter 3 of [50].

Lemma 1.3. *(Discrete Gronwall inequality) [50] Let $\Delta t, B, C > 0$ and $(a_n), (b_n), (c_n)$ be sequences of non-negative numbers satisfying*

$$\forall\, n \geq 0, \quad a_n + \Delta t \sum_{i=0}^{n} b_i \leq B + C\Delta t \sum_{i=0}^{n} a_i + \Delta t \sum_{i=0}^{n} c_i,$$

then, if $C\Delta t < 1$,

$$\forall\ n \geq 0, \quad a_n + \Delta t \sum_{i=0}^{n} b_i \leq e^{C(n+1)\Delta t}\left(B + \Delta t \sum_{i=0}^{n} c_i\right).$$

See Chapter 3 of [50].

Theorem 1.4. *(Approximation property) [50] Assume that E is a triangle or parallelo-*

gram in 2D or a tetrahedron or hexahedron in 3D. Let $v \in H^{s+1}(E)$ for $s \geq 0$ and $k \geq 0$. Then, there exists a constant C independent of v and h_E and a function $\tilde{v} \in \mathbb{P}^k(E)$, such that

$$\forall \; 0 \leq q \leq s, \; \| v - \tilde{v} \|_{H^q(E)} \leq C h_E^{min(k,s)+1-q} |v|_{H^s(E)}, \tag{1.3}$$

where $\mathbb{P}^k(E)$ is the space of polynomials of degree less than or equal to k.

See Chapter 2 of [50].

Trace inequalities: [50] Let E be a element with a diameter h_E. Then, $\forall \; e \subset \partial E$ for any function $v \in H^s(E)$, there exists a constant C independent of h_E and v such that

$$\begin{cases} s \geq 1, \| v \|_{L^2(e)} \leq C|e|^{1/2}|E|^{-1/2} \big(\| v \|_{L^2(E)} + h_E \| \nabla v \|_{L^2(E)} \big), \\ \\ s \geq 2, \| \nabla v \cdot \boldsymbol{n}_e \|_{L^2(e)} \leq C|e|^{1/2}|E|^{-1/2} \big(\| \nabla v \|_{L^2(E)} + h_E \| \nabla^2 v \|_{L^2(E)} \big). \end{cases} \tag{1.4}$$

See Chapter 2 of [50].

Lemma 1.5. *(Inverse inequality) [50] There exists a constant C independent of h_E such that for any polynomial function v of degree k defined on E, we have*

$$\forall \; 0 \leq j \leq k, \; \| \nabla^j v \|_{L^2(E)} \leq C h_E^{-j} \| v \|_{L^2(E)}. \tag{1.5}$$

See Chapter 3 of [50].

Next, we shall review two lemmas for our analysis. The first one is the standard approximation result for any linear continuous projection operator Π from $H^{s+1}(E)$ onto $V_h(E) = \{v; v|_E \in \mathbb{P}^k(E)\}$ satisfying $\Pi v = v$ for any $v \in \mathbb{P}^k(E)$. The second one is the standard trace inequality.

Lemma 1.6. *[9] Let $v \in H^{s+1}(E), s \geq 0$ and Π be a linear continuous projection operator from $H^{s+1}(E)$ onto $V_h(E)$ such that $\Pi v = v$ for any $v \in \mathbb{P}^k(E)$. Then, for $m = 0, 1$, we have*

$$\begin{cases} \big| v - \Pi v \big|_{H^m(E)} \leq C h_E^{min(s,k)+1-m} \| v \|_{H^{s+1}(E)}, \\ \\ \| v - \Pi v \|_{L^2(\partial E)} \leq C h_E^{min(s,k)+\frac{1}{2}} \| v \|_{H^{s+1}(E)}. \end{cases} \tag{1.6}$$

Lemma 1.7. *[9] There exists a generic constant C which is independent of h_E such that for any $v \in V_h(E)$ we have*

$$\| v \|_{L^2(\partial E)} \leq C h_E^{-\frac{1}{2}} \| v \|_{L^2(E)} . \tag{1.7}$$

1.3 Fractional calculus

1.3.1 Definitions and properties

This section is devoted to definitions and properties in fractional calculus. The theory of derivatives of non-integer order goes back to the Leibniz's note in his list to L'Hospital [45]. About three centuries, the theory of fractional derivatives developed mainly in a pure theoretical field of mathematics. Until last few decades the integrals of non-integer order were pointed out by many researchers. Those integrals are used for the description of some properties of various real materials and many phenomena in physics, engineering, chemistry [39, 45, 47, 52, 53], etc.

In Chapter 3, we will consider a hybridized discontinuous Galerkin (HDG) method for solving 2D space-fractional convection-diffusion problems. Before giving the numerical method for those fractional equations, we have to review several definitions and lemmas for calculus. In the following we recall some definitions of fractional integrals, derivatives, and their properties.

Definition 1.1. [28, 47, 59] For any $\mu > 0$, the left (right) Riemann-Liouville fractional integral of function $u(x)$ defined on (a, b) is denoted by

(1) Left Riemann-Liouville fractional integral:

$$_a\mathcal{I}_x^\mu u(x) = \int_a^x \frac{(x - \xi)^{\mu-1}}{\Gamma(\mu)} u(\xi) d\xi,$$

(2) Right Riemann-Liouville fractional integral:

$$_x\mathcal{I}_b^\mu u(x) = \int_x^b \frac{(\xi - x)^{\mu-1}}{\Gamma(\mu)} u(\xi) d\xi,$$

where $\Gamma(\mu) = \int_0^\infty e^{-t} t^{\mu-1} dt$, which is Euler's gamma function.

Definition 1.2. [28, 47, 59] For any $\nu > 0, n - 1 < \nu < n, n \in N^+$, the left (right) Riemann-Liouville fractional derivative of function u defined on (a, b) is denoted by

(1) Left Riemann-Liouville fractional derivative:

$$_aD_x^\nu u(x) = \frac{d^n}{dx^n} \int_a^x \frac{(x-\xi)^{n-\nu-1}}{\Gamma(n-\nu)} u(\xi)d\xi,$$

(2) Right Riemann-Liouville fractional derivative:

$$_xD_b^\nu u(x) = (-1)^n \frac{d^n}{dx^n} \int_x^b \frac{(\xi-x)^{n-\nu-1}}{\Gamma(n-\nu)} u(\xi)d\xi.$$

Definition 1.3. [59] For any $\nu > 0, n-1 < \nu < n, n \in N^+$, Caputo's left and right fractional derivatives of function $u(x)$ on (a,b) are defined by

$$_a^C D_x^\nu u(x) = \int_a^x \frac{(x-\xi)^{n-\nu-1}}{\Gamma(n-\nu)} \frac{d^n u(\xi)}{d\xi^n} d\xi, \tag{1.8}$$

$$_x^C D_b^\nu u(x) = \int_x^b \frac{(\xi-x)^{n-\nu-1}}{\Gamma(n-\nu)} \frac{(-1)^n d^n u(\xi)}{d\xi^n} d\xi. \tag{1.9}$$

Property 1. *[26, 28, 59] (Adjoint property) For any $\mu > 0$, the left and right Riemann-Liouville fractional integral operators are adjoints, namely*

$$\int_a^b {}_a\mathcal{I}_x^\mu u(x)v(x)dx = \int_a^b u(x)_x\mathcal{I}_b^\mu v(x)dx, \quad \forall u, v \in L^2(a,b). \tag{1.10}$$

Property 2. *[28] (Inverse property) For any $\mu > 0$, assume that the function $u \in C^\infty(a,b)$, where $(a,b) \subset \mathbb{R}$. Then the following equalities hold*

$$_aD_x^\mu {}_a\mathcal{I}_x^\mu u(x) = u(x), \quad _xD_b^\mu {}_x\mathcal{I}_b^\mu u(x) = u(x),$$
$$_a\mathcal{I}_x^\mu {}_aD_x^\mu u(x) = u(x), \quad \forall \ u(x) \ such \ that \ \overline{supp(u)} \subset (a,\infty),$$
$$_x\mathcal{I}_b^\mu {}_xD_b^\mu u(x) = u(x), \quad \forall \ u(x) \ such \ that \ \overline{supp(u)} \subset (-\infty,b).$$

Property 3. *[28] (Semigroup property) For any $\mu_1, \mu_2 > 0$, assume that the function*

13

$u \in L^p(a, b), p \geq 1$, where $(a, b) \subset \mathbb{R}$. Then the following equalities hold

$$_a\mathcal{I}_x^{\mu_1} {}_a\mathcal{I}_x^{\mu_2} u(x) = {}_a\mathcal{I}_x^{\mu_1 + \mu_2} u(x), \ \forall \ x \in (a, b),$$
$$_x\mathcal{I}_b^{\mu_1} {}_x\mathcal{I}_b^{\mu_2} u(x) = {}_x\mathcal{I}_b^{\mu_1 + \mu_2} u(x), \ \forall \ x \in (a, b).$$

Property 4. *[28] (Fourier transform property) For any $\mu > 0$, assume that the function $u \in L^p(\mathbb{R}), p \geq 1$. Then the Fourier transform of the left and right Riemann-Liouville fractional integrals satisfy the following equations*

$$\mathcal{F}(_{-\infty}\mathcal{I}_x^\mu u(x)) = (i\omega)^{-\mu} \hat{u}(\omega),$$
$$\mathcal{F}(_x\mathcal{I}_\infty^\mu u(x)) = (-i\omega)^{-\mu} \hat{u}(\omega),$$

where $\hat{u}(\omega)$ denotes the Fourier transform of u, i.e.

$$\hat{u}(\omega) = \int_{\mathbb{R}} e^{-i\omega x} u(x) dx.$$

Property 5. *[28] (Fourier transform property) For any $\nu > 0$, assume that the function $u \in C_0^\infty(\Omega), \Omega \subset \mathbb{R}$. Then the Fourier transform of the left and right Riemann-Liouville fractional derivatives satisfy the following*

$$\mathcal{F}(_{-\infty}D_x^\nu u(x)) = (i\omega)^\nu \hat{u}(\omega),$$
$$\mathcal{F}(_xD_\infty^\nu u(x)) = (-i\omega)^\nu \hat{u}(\omega).$$

1.3.2 Fractional spaces and lemmas

In this subsection, we will recall some fractional derivative spaces setting for variational solutions. In order to define associated fractional derivative spaces, we assume that $u \in C_0^\infty(a, b), (a, b) \subset \mathbb{R}$. We extend u by zero outside of the interval (a, b).

Definition 1.4. [28] (Fractional derivative spaces) For any $\nu > 0$, define the norms
(1) Left fractional derivative space:

$$\| u \|_{J_L^\nu(\mathbb{R})} := \big(\|_{-\infty} D_x^\nu u(x) \|_{L^2(\mathbb{R})}^2 + \| u \|_{L^2(\mathbb{R})}^2 \big)^{\frac{1}{2}},$$

where

$$|u|_{J_L^\nu(\mathbb{R})} := \|_{-\infty} D_x^\nu u(x) \|_{L^2(\mathbb{R})}.$$

14

(2) Right fractional derivative space:

$$\| u \|_{J_R^\nu(\mathbb{R})} := \big(\| {}_x D_\infty^\nu u(x) \|_{L^2(\mathbb{R})}^2 + \| u \|_{L^2(\mathbb{R})}^2 \big)^{\frac{1}{2}},$$

where

$$|u|_{J_R^\nu(\mathbb{R})} := \| {}_x D_\infty^\nu u(x) \|_{L^2(\mathbb{R})} .$$

Let $J_L^\nu(\mathbb{R})$ and $J_R^\nu(\mathbb{R})$ be the closures of $C_0^\infty(\mathbb{R})$ with respect to the norms $\| \cdot \|_{J_L^\nu(\mathbb{R})}$ and $\| \cdot \|_{J_R^\nu(\mathbb{R})}$, respectively.

Next we review a norm whose definition is associated with the Fourier transform.

Definition 1.5. [28] For any $\nu > 0$, define the norm

$$\| u \|_{H^\nu(\mathbb{R})} := \big(|u|_{H^\nu(\mathbb{R})}^2 + \| u \|_{L^2(\mathbb{R})}^2 \big)^{\frac{1}{2}},$$

where

$$|u|_{H^\nu(\mathbb{R})} := \| |\omega|^\nu \hat{u} \|_{L^2(\mathbb{R})} .$$

In the analysis of finite element method or discontinuous Galerkin method, we generally make use of the formula $({}_{-\infty}D_x^\nu u, {}_x D_\infty^\nu u)_{L^2(\mathbb{R})}$. For this case, we need the following theorem which is important for combing the fractional spaces and variational spaces.

Theorem 1.8. *[28] For any $\nu > 0, n - 1 < \nu < n, n \in N^+$, assume that u is a real valued function, then*

$$\big({}_{-\infty}D_x^\nu u, {}_x D_\infty^\nu u \big)_{L^2(\mathbb{R})} = \cos(\nu\pi) \| {}_{-\infty} D_x^\nu u \|_{L^2(\mathbb{R})}^2 . \tag{1.11}$$

Remark 1.1. Note that $\cos(\nu\pi) > 0$ when $\nu \in (-\frac{1}{2} + 2m\pi, \frac{1}{2} + 2m\pi), m \in N$. In this case, we can define a norm which is available.

Definition 1.6. [28] (Symmetric fractional derivative space) For any $\nu > 0, \nu \neq m - 1/2, m \in N$. Define the norm

$$\| u \|_{J_S^\nu(\mathbb{R})} := \big(\big| \cos(\nu\pi) \| D^\nu u \|_{L^2(\mathbb{R})}^2 \big|^2 + \| u \|_{L^2(\mathbb{R})}^2 \big)^{\frac{1}{2}},$$

and

$$|u|_{J_S^\nu(\mathbb{R})} := \big| \cos(\nu\pi) \| D^\nu u \|_{L^2(\mathbb{R})}^2 \big|^{\frac{1}{2}},$$

15

where $J_S^\nu(\mathbb{R})$ is the closure of $C_0^\infty(\mathbb{R})$ with respect to $\| \cdot \|_{J_S^\nu(\mathbb{R})}$.

Let $\Omega = (a, b)$ be a bounded open subinterval of $\mathbb{R}$. We now restrict the fractional derivative spaces to Ω.

Definition 1.7. [28] Define the spaces $J_{L,0}^\nu(\Omega), J_{R,0}^\nu(\Omega), H_0^\nu(\Omega), J_{S,0}^\nu(\Omega)$ as the closures of $C_0^\infty(\Omega)$ under their respective norms.

Theorem 1.9. *[28] (Fractional Poincaré-Friedrichs) For $u \in H_0^\nu(\Omega)$, we have*

$$\| u \|_{L^2(\Omega)} \leq C |u|_{H_0^\nu(\Omega)}, \tag{1.12}$$

and for $0 < s < \nu, s \neq n - 1/2, n \in N$

$$|u|_{H_0^s(\Omega)} \leq C |u|_{H_0^\nu(\Omega)}. \tag{1.13}$$

See the proof in [28].

1.4 The method of characteristics

The idea of the method of characteristics dates back to the work of Douglas and Russell [27] in 1982. Later on Arbogast [2, 3] extended the method of characteristics to transport problems. Recently Chen combined the method of characteristics with mixed discontinuous Galerkin method and finite element method for advection-dominated diffusion and degenerate parabolic problems, respectively [11, 12]. In many convection-diffusion problems arising in physical phenomena, convection essentially dominates diffusion. In general, we shall consider the method of characteristics to treat some convection-diffusion problems to reflect the hyperbolic nature of models. The convection-diffusion problems mainly contain two cases: One is the problem with linear convective term, another one is the problem with nonlinear convective term. Next we shall introduce the method of characteristics with those two cases.

1.4.1 The linear convective term

We shall consider applying the method of characteristics to the time-dependent advection diffusion problem for u on the bounded domain $\Omega \subset \mathbb{R}^d, d = 1, 2, 3$, with Lipschtiz

boundary $\partial\Omega$ [2, 24, 27]:

$$\begin{cases} \phi\partial_t u + \boldsymbol{b} \cdot \nabla u - \nabla \cdot (\bar{\boldsymbol{a}}\nabla u) = f, & (\boldsymbol{x}, t) \in \Omega \times J, \\ u(\boldsymbol{x}, t) = g_D, & (\boldsymbol{x}, t) \in \partial\Omega \times J, \\ u(\boldsymbol{x}, 0) = u_0(\boldsymbol{x}), & \boldsymbol{x} \in \Omega, \end{cases} \tag{1.14}$$

where $J = [0, T], 0 < T < \infty$, $\phi(\boldsymbol{x})$ is a function bounded below and above by positive constants, $\boldsymbol{b}(\boldsymbol{x}, t)$ is a bounded vector, $\bar{\boldsymbol{a}}(\boldsymbol{x}, t)$ is a positive semi-definite, bounded, symmetric tensor, $f \in L^2(J; \Omega), g_D \in L^2(J; H^{1/2}(\partial\Omega)), u_0 \in L^2(\Omega)$.

For each positive integer N, let $0 = t^0 < t^1 < \cdots < t^N = T$ be a partition of J into subintervals $J^n = (t^{n-1}, t^n], \Delta t = t^n - t^{n-1}, 1 \le n \le N$, and $u^n = u(\boldsymbol{x}, t^n)$. The time interval of interest is J^n, then the characteristic trace-back of the point $\boldsymbol{x} \in \Omega$ is denoted by $\check{\boldsymbol{x}}(\boldsymbol{x}, t)$, and it satisfies the (time backward) ordinary differential equation

$$\begin{cases} \frac{d\check{\boldsymbol{x}}}{dt} = \boldsymbol{b}(\check{\boldsymbol{x}}, t)/\phi(\check{\boldsymbol{x}}), & t^{n-1} \le t < t^n, \\ \\ \check{\boldsymbol{x}}(\boldsymbol{x}, t^n) = \boldsymbol{x}. \end{cases} \tag{1.15}$$

From equality (1.15) we imply that

$$\begin{aligned} \boldsymbol{x} - \check{\boldsymbol{x}}(\boldsymbol{x}, t^{n-1}) &= \int_{t^{n-1}}^{t^n} \frac{\boldsymbol{b}(\check{\boldsymbol{x}}(\boldsymbol{x}, t), t)}{\phi(\check{\boldsymbol{x}}(\boldsymbol{x}, t))} dt \\ &\approx \Delta t \frac{\boldsymbol{b}(\check{\boldsymbol{x}}(\boldsymbol{x}, t^n), t^n)}{\phi(\check{\boldsymbol{x}}(\boldsymbol{x}, t^n))} \\ &= \Delta t \frac{\boldsymbol{b}(\boldsymbol{x}, t^n)}{\phi(\boldsymbol{x})}. \end{aligned}$$

Let $\psi(\boldsymbol{x}, t) = (\phi^2 + |\boldsymbol{b}|^2)^{1/2}$, $|\boldsymbol{b}|^2 = b_1^2 + \cdots + b_d^2$. Then the characteristic direction associated with the hyperbolic operator $\phi\partial_t u + \boldsymbol{b} \cdot \nabla u$ can be denoted by $\tau(\boldsymbol{x}, t)$, where

$$\partial_\tau = \frac{\phi(\boldsymbol{x})}{\psi(\boldsymbol{x}, t)}\partial_t + \frac{\boldsymbol{b}(\boldsymbol{x}, t)}{\psi(\boldsymbol{x}, t)} \cdot \nabla. \tag{1.16}$$

Then the approximation of the directional derivative $\frac{\partial u(\boldsymbol{x}, t)}{\partial \tau(\boldsymbol{x}, t)}$ at time $t = t^n$ can be

$$\frac{\partial u(\boldsymbol{x}, t^n)}{\partial \tau(\boldsymbol{x}, t^n)} \approx \frac{u(\boldsymbol{x}, t^n) - u(\check{\boldsymbol{x}}(\boldsymbol{x}, t^{n-1}), t^{n-1})}{\left(|\boldsymbol{x} - \check{\boldsymbol{x}}(\boldsymbol{x}, t^{n-1})|^2 + \Delta t^2\right)^{1/2}}.$$

Note that

$$\phi \partial_t u^n + \boldsymbol{b}^n \cdot \nabla u^n = \psi^n \frac{\partial u(\boldsymbol{x}, t^n)}{\partial \tau(\boldsymbol{x}, t^n)}$$
$$\approx \phi \frac{u(\boldsymbol{x}, t^n) - u(\check{\boldsymbol{x}}(\boldsymbol{x}, t^{n-1}), t^{n-1})}{\Delta t}. \qquad (1.17)$$

For the method of characteristics, we need the assumption

$$\phi \in W^{1,\infty}(\Omega), \quad \frac{\boldsymbol{b}}{\phi} \in L^\infty(J; W^{1,\infty}(\Omega)^2),$$

$$0 < c_l \leq \phi(\boldsymbol{x}) \leq c_r < \infty, \quad \left| \frac{\boldsymbol{b}(\boldsymbol{x}, t)}{\phi(\boldsymbol{x})} \right| + \left| \nabla \cdot \left(\frac{\boldsymbol{b}(\boldsymbol{x}, t)}{\phi(\boldsymbol{x})} \right) \right| \leq C, \quad (\boldsymbol{x}, t) \in \Omega \times J, \qquad (1.18)$$

where c_l, c_r, C are some constants. See the details in [2, 3, 24, 27].

In Chapter 3 we will use the above method of characteristics to solve space-fractional convection-diffusion equations in 2D. In this case, $\boldsymbol{b}$ satisfies the assumption (1.18) and $\phi = 1$.

1.4.2 The nonlinear convective term

In this subsection, we focus on applying the method of characteristics to solve some convection diffusion problems with nonlinear convective term. For the sake of simplicity, we consider combining the method of characteristics to the Navier-Stokes equation, i.e.

$$\begin{cases} \partial_t \boldsymbol{u} + (\boldsymbol{u} \cdot \nabla)\boldsymbol{u} - \nu \Delta \boldsymbol{u} + \nabla p = \boldsymbol{f}, & (\boldsymbol{x}, t) \in \Omega \times J, \\ \nabla \cdot \boldsymbol{u} = 0 & (\boldsymbol{x}, t) \in \Omega \times J, \\ \boldsymbol{u}|_{\partial\Omega} = g_D(\boldsymbol{x}, t), & (\boldsymbol{x}, t) \in \partial\Omega \times J, \\ \boldsymbol{u}(\boldsymbol{x}, 0) = \boldsymbol{u}_0(\boldsymbol{x}), & \boldsymbol{x} \in \Omega, \end{cases} \qquad (1.19)$$

where Ω denotes a bounded open subset of $\mathbb{R}^d, d = 2, 3$ with Lipschitz continuous boundary $\partial\Omega$, $\boldsymbol{u}(\boldsymbol{x}, t)$ is the velocity of the fluid, $p(\boldsymbol{x}, t)$ is the kinematic pressure, ν is the kinematic viscosity and $\boldsymbol{f}(\boldsymbol{x}, t)$ is the body force.

Given a fluid flow with the velocity field $\boldsymbol{u}(\boldsymbol{x}, t)$, the trajectory is a solution of the

following suitable differential equation

$$
\begin{cases}
\frac{d\check{\boldsymbol{x}}(\boldsymbol{x},s;t)}{dt} = \boldsymbol{u}(\check{\boldsymbol{x}}(\boldsymbol{x},s;t),t), \\[4mm]
\check{\boldsymbol{x}}(\boldsymbol{x},s;s) = \boldsymbol{x},
\end{cases} \tag{1.20}
$$

where $\check{\boldsymbol{x}}(\boldsymbol{x},s;t)$ is the position at time of particle of fluid which is at point $\boldsymbol{x}$ at time $t = s$, and $\check{\boldsymbol{x}} : (\boldsymbol{x},s;t) \in \Omega \times J \times J \mapsto \check{\boldsymbol{x}}(\boldsymbol{x},s;t)$.

Lemma 1.10. *[55] Assume that $\boldsymbol{u} \in C(C^{0,1}(\bar{\Omega})^d) \cap C(V)$ ($V = \{\boldsymbol{v} \in H_0^1(\Omega)^d | \nabla \cdot \boldsymbol{v} = 0 \text{ in } \Omega\}$). If $|s - t|$ is sufficiently small, then $\boldsymbol{x} \mapsto \check{\boldsymbol{x}}(\boldsymbol{x},s;t)$ is a quasi-isometric homomorphism of Ω onto itself and its Jacobian equals to 1 a.e. on Ω.*

Proof. See the proof in [55]. $\qquad\qquad\qquad\qquad\qquad\qquad\qquad\qquad\qquad\qquad\square$

Define $\psi(\boldsymbol{x},t) = \left(1 + |\boldsymbol{u}|^2\right)^{1/2}$, then the material derivative of $\boldsymbol{u}$ can be rewritten as a derivative in the direction $\tau(\boldsymbol{x},t)$

$$
\partial_t \boldsymbol{u} + (\boldsymbol{u} \cdot \nabla)\boldsymbol{u} = \psi \frac{\partial \boldsymbol{u}}{\partial \tau}. \tag{1.21}
$$

For each positive integer N, let $0 = t^0 < t^1 < \cdots < t^N = T$ be a partition of J into subintervals $J^n = (t^{n-1}, t^n]$, $\Delta t = t^n - t^{n-1}, 1 \le n \le N$, and $u^n = u(x,t^n)$. For $\boldsymbol{x} \in \Omega, s = t^n$, with some deduction we have

$$
\boldsymbol{x} - \check{\boldsymbol{x}}(\boldsymbol{x},t^n;t^{n-1}) = \int_{t^{n-1}}^{t^n} \boldsymbol{u}(\check{\boldsymbol{x}}(\boldsymbol{x},t^n;t),t)dt \approx \Delta t \boldsymbol{u}(\boldsymbol{x},t^n).
$$

Then, the backward difference approximation for direction $\tau(\boldsymbol{x},t^n)$ is that

$$
\frac{\partial \boldsymbol{u}(\boldsymbol{x},t^n)}{\partial \tau(\boldsymbol{x},t^n)} \approx \frac{\boldsymbol{u}(\boldsymbol{x},t^n) - \boldsymbol{u}(\check{\boldsymbol{x}}(\boldsymbol{x},t^n;t^{n-1}),t^{n-1})}{\left(|\boldsymbol{x} - \check{\boldsymbol{x}}(\boldsymbol{x},t^n;t^{n-1})|^2 + \Delta t^2\right)^{1/2}}. \tag{1.22}
$$

Combining equalities (1.21) and (1.22), yields

$$
\partial_t \boldsymbol{u} + (\boldsymbol{u} \cdot \nabla)\boldsymbol{u} \approx \frac{\boldsymbol{u}(\boldsymbol{x},t^n) - \boldsymbol{u}(\check{\boldsymbol{x}}(\boldsymbol{x},t^n;t^{n-1}),t^{n-1})}{\Delta t}. \tag{1.23}
$$

More details can be found in [1, 6, 13, 54, 55, 57].

In Chapter 2, we shall use the method of characteristics to recast the time-dependent incompressible Navier-Stokes equations.

Chapter 2

CLDG method for the incompressible Navier-Stokes equations

2.1 The incompressible Navier-Stokes equations

Based on the assumption that the fluid, at the scale of interest, is a continuum, and the conservation of momentum (often alongside mass and energy conservation), the equation to describe the motion of fluid substances can be derived, which is named after the French engineer and physicist Claude-Louis Navier and the Irish mathematician and physicist George Gabriel Stokes to memory their fundamental contributions. Nowadays, it is still the central equation to fluid mechanics. Let Ω be a bounded polygonal domain in $\mathbb{R}^2$ with Lipschitz continuous boundary $\partial\Omega$ and $J = [0, T]$ is time interval with $T > 0$ is finite quantity. The time-dependent Navier-Stokes equations for an incompressible viscous fluid confined in Ω are [56]:

$$
\begin{cases}
\partial_t \boldsymbol{u} + (\boldsymbol{u} \cdot \nabla)\boldsymbol{u} - \nu \Delta \boldsymbol{u} + \nabla p = \boldsymbol{f}, & (\boldsymbol{x}, t) \in \Omega \times J, \\
\nabla \cdot \boldsymbol{u} = 0, & (\boldsymbol{x}, t) \in \Omega \times J, \\
\boldsymbol{u}(\boldsymbol{x}, t) = 0, & (\boldsymbol{x}, t) \in \partial\Omega \times J, \\
\boldsymbol{u}(\boldsymbol{x}, 0) = \boldsymbol{u}_0(\boldsymbol{x}), & \boldsymbol{x} \in \Omega.
\end{cases} \tag{2.1}
$$

It is well known that the above problem has a unique solution $\boldsymbol{u} \in L^2(J; H_0^1(\Omega)^2) \cap L^\infty(J; L^2(\Omega)^2)$, $p \in W^{-1,\infty}(J; L_0^2(\Omega))$ for $\partial_t \boldsymbol{u} \in L^2(J; \boldsymbol{X}')$, $\boldsymbol{X} = \{\boldsymbol{v} \in H_0^1(\Omega)^2 : \nabla \cdot \boldsymbol{v} = 0\}$, the body force function $\boldsymbol{f} \in L^2(J; H^{-1}(\Omega)^2)$ and $\boldsymbol{u}_0 \in H(div, \Omega)$ [56]. The constant

ν is the fluid viscosity coefficient. Since p is uniquely defined up to an additive constant, we also assume that $\int_\Omega p = 0$. The $(\boldsymbol{u} \cdot \nabla)\boldsymbol{u}$ is a nonlinear convective term and

$$(\boldsymbol{u} \cdot \nabla)\boldsymbol{u} = u_1 \frac{\partial \boldsymbol{u}}{\partial x} + u_2 \frac{\partial \boldsymbol{u}}{\partial y}.$$

2.2   Derivation of the numerical scheme

We first introduce the notations, and then focus on deriving the fully discrete numerical scheme of the time-dependent incompressible Navier-Stokes equations.

2.2.1   Mathematical setting of the Navier-Stokes equations

For the mathematical setting of the Navier-Stokes problems, we describe some Sobolev spaces. The $L_0^2(\Omega)$ is the subspace of $L^2(\Omega)$ with zero mean value, namely

$$L_0^2(\Omega) = \left\{ v \in L^2(\Omega) : \int_\Omega v = 0 \right\}.$$

$\boldsymbol{X}$ denotes by the space of functions of $H_0^1(\Omega)^2$ with zero divergence, namely

$$\boldsymbol{X} = \left\{ \boldsymbol{v} \in H_0^1(\Omega)^2 : \nabla \cdot \boldsymbol{v} = 0 \right\},$$

and $\boldsymbol{X}'$ is its dual space.

The fundamental work spaces for solving the Navier-Stokes equations are $\boldsymbol{X}$ and $\mathbb{M} := L_0^2(\Omega)$.

The inner product and norm of vector functions $\boldsymbol{v} = (v_i)_{1 \le i \le d}$ are defined by

$$(\boldsymbol{u}, \boldsymbol{v}) = \int_\Omega \boldsymbol{u} \cdot \boldsymbol{v}, \quad \| \boldsymbol{v} \|_0 = \left(\sum_{i=1}^d \| v_i \|_{L^2(\Omega)}^2 \right)^{1/2}.$$

The gradient of a vector function $\boldsymbol{v} : \mathbb{R}^d \to \mathbb{R}^d$ and the divergence of a matrix function $\bar{\boldsymbol{\sigma}} : \mathbb{R}^d \to \mathbb{R}^{d \times d}$ are given by

$$\nabla \boldsymbol{v} = \left(\frac{\partial v_i}{\partial x_j} \right)_{1 \le i,j \le d}, \quad \nabla \cdot \bar{\boldsymbol{\sigma}} = \left(\sum_{j=1}^d \frac{\partial \bar{\sigma}_{ij}}{\partial x_j} \right)_{1 \le i \le d}.$$

Consequently, for a vector function $\boldsymbol{v} = (v_i)_{1 \le i \le d}$, we have

$$\Delta \boldsymbol{v} = \nabla \cdot \nabla \boldsymbol{v} = (\Delta v_i)_{1 \le i \le d}.$$

21

The L^2-inner product of two matrix functions $\bar{\boldsymbol{\sigma}}$ and $\bar{\boldsymbol{\tau}}$ is defined by

$$(\bar{\boldsymbol{\sigma}}, \bar{\boldsymbol{\tau}}) = \int_\Omega \bar{\boldsymbol{\sigma}} : \bar{\boldsymbol{\tau}} = \int_\Omega \sum_{1 \leq i,j \leq d} \bar{\sigma}_{ij} \bar{\tau}_{ij},$$

equipped with the norm

$$\| \bar{\boldsymbol{\sigma}} \|_0 = (\bar{\boldsymbol{\sigma}}, \bar{\boldsymbol{\sigma}})^{1/2} = \left(\int_\Omega \bar{\boldsymbol{\sigma}} : \bar{\boldsymbol{\sigma}} \right)^{1/2} = \left(\int_\Omega \sum_{1 \leq i,j \leq d} \bar{\sigma}_{ij}^2 \right)^{1/2}.$$

Obviously, it is a norm. We just prove that it possesses the third property of a norm as follows

$$\begin{aligned}
\| \bar{\boldsymbol{\sigma}} + \bar{\boldsymbol{\tau}} \|^2 &= \int_\Omega (\bar{\boldsymbol{\sigma}} + \bar{\boldsymbol{\tau}}) : (\bar{\boldsymbol{\sigma}} + \bar{\boldsymbol{\tau}}) \\
&= \int_\Omega \sum_{1 \leq i,j \leq d} (\bar{\sigma}_{ij} + \bar{\tau}_{ij})^2 \\
&= \int_\Omega \sum_{1 \leq i,j \leq d} (\bar{\sigma}_{ij}^2 + 2\bar{\sigma}_{ij}\bar{\tau}_{ij} + \bar{\tau}_{ij}^2) \\
&= \| \bar{\boldsymbol{\sigma}} \|^2 + 2(\bar{\boldsymbol{\sigma}}, \bar{\boldsymbol{\tau}}) + \| \bar{\boldsymbol{\tau}} \|^2 \\
&\leq \| \bar{\boldsymbol{\sigma}} \|^2 + 2 \| \bar{\boldsymbol{\sigma}} \| \| \bar{\boldsymbol{\tau}} \| + \| \bar{\boldsymbol{\tau}} \|^2 \\
&\leq (\| \bar{\boldsymbol{\sigma}} \| + \| \bar{\boldsymbol{\tau}} \|)^2.
\end{aligned}$$

2.2.2 CLDG scheme

By introducing an auxiliary variable $\bar{\boldsymbol{\sigma}} = \sqrt{\nu}\nabla\boldsymbol{u}$ [4, 21], we rewrite (2.1) as a mixed form:

$$\begin{cases}
\partial_t \boldsymbol{u} + (\boldsymbol{u} \cdot \nabla)\boldsymbol{u} - \sqrt{\nu}\nabla \cdot \bar{\boldsymbol{\sigma}} + \nabla p = \boldsymbol{f}, & (\boldsymbol{x}, t) \in \Omega \times J, \\
\bar{\boldsymbol{\sigma}} = \sqrt{\nu}\nabla\boldsymbol{u}, & (\boldsymbol{x}, t) \in \Omega \times J, \\
\nabla \cdot \boldsymbol{u} = 0, & (\boldsymbol{x}, t) \in \Omega \times J, \\
\boldsymbol{u}(\boldsymbol{x}, t) = 0, & (\boldsymbol{x}, t) \in \partial\Omega \times J, \\
\boldsymbol{u}(\boldsymbol{x}, 0) = \boldsymbol{u}_0(\boldsymbol{x}), & \boldsymbol{x} \in \Omega,
\end{cases} \qquad (2.2)$$

where $\nu = 1/Re$ is the viscosity coefficient. Obviously, if $\sqrt{\nu}$ is small enough we have $\sqrt{\nu} > \nu$.

Before presenting the variational form, let us clarify the notation: $\boldsymbol{v} \cdot \bar{\boldsymbol{\sigma}} \cdot \boldsymbol{n} := \sum_{i,j=1}^2 v_i \bar{\sigma}_{ij} n_j := \bar{\boldsymbol{\sigma}} : (\boldsymbol{v} \otimes \boldsymbol{n})$. Multiplying the first, the second, and the third equation of (2.2) by the smooth test functions $\boldsymbol{v}, \bar{\boldsymbol{\tau}}, q$, respectively, and integrating by parts over an arbitrary subset $E \in \mathscr{E}_h$, we get the following weak variational formulation, i.e., find

22

the solution $(\boldsymbol{u}, \bar{\boldsymbol{\sigma}}, \boldsymbol{p}) \in \mathbb{V} \times \mathbb{V}^2 \times \mathbb{Q}$ for any functions $(\boldsymbol{v}, \bar{\boldsymbol{\tau}}, q) \in \mathbb{V} \times \mathbb{V}^2 \times \mathbb{Q}$, such that

$$
\begin{cases}
\int_E (\partial_t \boldsymbol{u} + (\boldsymbol{u} \cdot \nabla)\boldsymbol{u}) \cdot \boldsymbol{v} + \int_E \sqrt{\nu}\bar{\boldsymbol{\sigma}} : \nabla \boldsymbol{v} - \int_{\partial E} \sqrt{\nu}\boldsymbol{v} \cdot \bar{\boldsymbol{\sigma}} \cdot \boldsymbol{n}_E \\
\quad - \int_E p\nabla \cdot \boldsymbol{v} + \int_{\partial E} p\boldsymbol{v} \cdot \boldsymbol{n}_E = \int_E \boldsymbol{f} \cdot \boldsymbol{v}, \\[2mm]
\int_E \bar{\boldsymbol{\sigma}} : \bar{\boldsymbol{\tau}} - \int_E \sqrt{\nu}\nabla \boldsymbol{u} : \bar{\boldsymbol{\tau}} = 0, \\[2mm]
\int_E \nabla \cdot \boldsymbol{u} q = 0,
\end{cases}
\tag{2.3}
$$

where $\boldsymbol{n}_E$ is the outward unit normal to ∂E, and

$$
\begin{aligned}
\mathbb{V} &= \left\{ \boldsymbol{v} \in L^2(\Omega)^2 : \boldsymbol{v}|_E \in H^1(E)^2, \forall E \in \mathscr{E}_h \right\}, \\
\mathbb{V}^2 &= \left\{ \bar{\boldsymbol{\sigma}} \in (L^2(\Omega)^2)^2 : \bar{\boldsymbol{\sigma}}|_E \in (H^1(E)^2)^2, \forall E \in \mathscr{E}_h \right\}, \\
\mathbb{Q} &= \left\{ q \in \mathbb{M} : q|_E \in H^1(E), \forall E \in \mathscr{E}_h \right\}.
\end{aligned}
$$

The exact solution $(\boldsymbol{u}, \bar{\boldsymbol{\sigma}}, p)$ will be approximated by the functions $(\boldsymbol{u}_h, \bar{\boldsymbol{\sigma}}_h, p_h)$ belonging to the finite element spaces $\mathbb{V}_h \times \mathbb{V}_h^2 \times \mathbb{Q}_h$:

$$
\begin{aligned}
\mathbb{V}_h &= \left\{ \boldsymbol{v} \in L^2(\Omega)^2 : \boldsymbol{v}|_E \in \mathbb{P}^k(E)^2, \forall E \in \mathscr{E}_h \right\}, \\
\mathbb{V}_h^2 &= \left\{ \bar{\boldsymbol{\sigma}} \in (L^2(\Omega)^2)^2 : \bar{\boldsymbol{\sigma}}|_E \in (\mathbb{P}^k(E)^2)^2, \forall E \in \mathscr{E}_h \right\}, \\
\mathbb{Q}_h &= \left\{ q \in \mathbb{M} : q|_E \in \mathbb{P}^k(E), \forall E \in \mathscr{E}_h \right\},
\end{aligned}
$$

where $\mathbb{P}^k(E)$ denotes the set of all polynomials of degree at most $k \geq 1$ on E. Let $\mathbb{Q}^k(E)$ denote by the space of all polynomials which are of degree $\leq k$ with respect to each variable x or y. And note that $\mathbb{P}^k(E) \subset \mathbb{Q}^k(E)$.

To find $(\boldsymbol{u}_h, \bar{\boldsymbol{\sigma}}_h, p_h) \in \mathbb{V}_h \times \mathbb{V}_h^2 \times \mathbb{Q}_h$ for any functions $(\boldsymbol{v}, \bar{\boldsymbol{\tau}}, q) \in \mathbb{V}_h \times \mathbb{V}_h^2 \times \mathbb{Q}_h, \forall E \in \mathscr{E}_h$ the following holds

$$
\begin{cases}
\int_E (\partial_t \boldsymbol{u}_h + (\boldsymbol{u}_h \cdot \nabla)\boldsymbol{u}_h) \cdot \boldsymbol{v} + \int_E \sqrt{\nu}\bar{\boldsymbol{\sigma}}_h : \nabla \boldsymbol{v} - \int_{\partial E} \sqrt{\nu}\boldsymbol{v} \cdot \bar{\boldsymbol{\sigma}}_h^* \cdot \boldsymbol{n}_E \\
\quad - \int_E p_h \nabla \cdot \boldsymbol{v} + \int_{\partial E} p_h^* \boldsymbol{v} \cdot \boldsymbol{n}_E = \int_E \boldsymbol{f} \cdot \boldsymbol{v}, \\[2mm]
\int_E \bar{\boldsymbol{\sigma}}_h : \bar{\boldsymbol{\tau}} - \int_E \sqrt{\nu}\nabla \boldsymbol{u}_h : \bar{\boldsymbol{\tau}} = 0, \\[2mm]
\int_E \nabla \cdot \boldsymbol{u}_h q = 0,
\end{cases}
\tag{2.4}
$$

where $\bar{\boldsymbol{\sigma}}_h^*$ and p_h^* are to be determined by numerical fluxes. By carefully adding the

penalty terms and choosing the numerical fluxes:

$$\bar{\boldsymbol{\sigma}}_h^* = \{\bar{\boldsymbol{\sigma}}_h\}, \quad p_h^* = \{p_h\}, \tag{2.5}$$

we develop the following numerical scheme:

$$\begin{cases} \big(\partial_t \boldsymbol{u}_h + (\boldsymbol{u}_h \cdot \nabla)\boldsymbol{u}_h, \boldsymbol{v}\big) + (\bar{\boldsymbol{\sigma}}_h, \sqrt{\nu}\nabla\boldsymbol{v}) - (\{\bar{\boldsymbol{\sigma}}_h\}, \sqrt{\nu}[\boldsymbol{v}] \otimes \boldsymbol{n}_e)_{\mathscr{E}_h^B} \\ -(p_h, \nabla \cdot \boldsymbol{v}) + (\{p_h\}, [\boldsymbol{v}] \cdot \boldsymbol{n}_e)_{\mathscr{E}_h^B} + ([\boldsymbol{u}_h], [\boldsymbol{v}])_{\mathscr{E}_h^B} = (\boldsymbol{f}, \boldsymbol{v}), \\[2mm] (\bar{\boldsymbol{\sigma}}_h, \bar{\boldsymbol{\tau}}) - (\sqrt{\nu}\nabla\boldsymbol{u}_h, \bar{\boldsymbol{\tau}}) + (\{\bar{\boldsymbol{\tau}}\}, \sqrt{\nu}[\boldsymbol{u}_h] \otimes \boldsymbol{n}_e)_{\mathscr{E}_h^B} = 0, \\[2mm] (q, \nabla \cdot \boldsymbol{u}_h) - (\{q\}, [\boldsymbol{u}_h] \cdot \boldsymbol{n}_e)_{\mathscr{E}_h^B} + ([p_h], [q])_{\mathscr{E}_h^i} = 0, \end{cases} \tag{2.6}$$

for any functions $(\boldsymbol{v}, \bar{\boldsymbol{\tau}}, q) \in \mathbb{V}_h \times \mathbb{V}_h^2 \times \mathbb{Q}_h$. The exact solution $(\boldsymbol{u}, p)$ of (2.1) is expected to be at least continuous and have homogeneous boundary values. So added penalty terms $(\{\bar{\boldsymbol{\tau}}\}, \sqrt{\nu}[\boldsymbol{u}_h] \otimes \boldsymbol{n}_e)_{\mathscr{E}_h^B}$, $([\boldsymbol{u}_h], [\boldsymbol{v}])_{\mathscr{E}_h^B}$, $(\{q\}, [\boldsymbol{u}_h] \cdot \boldsymbol{n}_e)_{\mathscr{E}_h^B}$ and $([p_h], [q])_{\mathscr{E}_h^i}$ still keep the consistency of the scheme. Moreover, the locality of the discontinuous Galerkin method still remains since the penalty in the second equation is about $\boldsymbol{u}_h$ element-by-element and it is independent of $\bar{\boldsymbol{\sigma}}_h$. These additions make the variational formula symmetric. Then this formula makes the stability and error analysis convenient.

The LDG method is one of several discontinuous Galerkin methods, which was introduced by Cockburn and Shu in [21] as an extension to general convection-diffusion problems of the numerical scheme for the compressible Navier-Stokes equations proposed by Bassi and Rebay in [4].

- In LDG method, the original idea is applied to both $\boldsymbol{u}$ and $\nabla\boldsymbol{u}$ which are now considered independent unknowns. The basic idea for constructing the LDG method is to suitably rewrite the considered equations into a larger, degenerate, first-order system.

- The CLDG method considered in this chapter shares several properties with the LDG method. On each element, both the approximation to $\boldsymbol{u}$ and the approximations to each of the components of $\bar{\boldsymbol{\sigma}}$ belong to the same space. They use discontinuous-in-space approximations, are locally conservative, and approximate the diffusion fluxes with independent variables. The implementation of the LDG method is much simpler than that of standard mixed methods, especially for high-degree polynomial approximations (see [33]).

24

- In LDG method, the local conservativity holds. In order to do that, suitable discrete approximations of the traces of the fluxes on the boundary of the elements are needed which are provided by the so-called numerical fluxes. These numerical fluxes enhance the stability of the method, and the quality of its approximation (see the proof of stability and the numerical experiments).

Throughout this chapter, we use the notations

$$(\boldsymbol{w}, \boldsymbol{v}) = \sum_{E \in \mathscr{E}_h} (\boldsymbol{w}, \boldsymbol{v})_E, \quad (\boldsymbol{w}, \boldsymbol{v})_{\mathscr{E}_h^i} = \sum_{e \in \mathscr{E}_h^i} (\boldsymbol{w}, \boldsymbol{v})_e, \quad (\boldsymbol{w}, \boldsymbol{v})_{\mathscr{E}_h^B} = \sum_{e \in \mathscr{E}_h^B} (\boldsymbol{w}, \boldsymbol{v})_e.$$

Definitions of the bilinear forms:

$$\mathbb{a}(\bar{\boldsymbol{\sigma}}_h, \boldsymbol{v}) = (\bar{\boldsymbol{\sigma}}_h, \sqrt{\nu}\nabla \boldsymbol{v}) - (\{\bar{\boldsymbol{\sigma}}_h\}, \sqrt{\nu}[\boldsymbol{v}] \otimes \boldsymbol{n}_e)_{\mathscr{E}_h^B},$$

$$\mathbb{b}(p_h, \boldsymbol{v}) = -(p_h, \nabla \cdot \boldsymbol{v}) + (\{p_h\}, [\boldsymbol{v}] \cdot \boldsymbol{n}_e)_{\mathscr{E}_h^B},$$

$$\mathbb{c}(\boldsymbol{u}_h, \boldsymbol{v}) = ([\boldsymbol{u}_h], [\boldsymbol{v}])_{\mathscr{E}_h^B},$$

$$\mathbb{d}(p_h, q) = ([p_h], [q])_{\mathscr{E}_h^i}.$$

By integration by parts, the forms $\mathbb{a}(\bar{\boldsymbol{\sigma}}_h, \boldsymbol{v})$ and $\mathbb{b}(p_h, \boldsymbol{v})$ also can be rewritten as

$$\mathbb{a}(\bar{\boldsymbol{\sigma}}_h, \boldsymbol{v}) = -(\nabla \cdot \bar{\boldsymbol{\sigma}}_h, \sqrt{\nu}\boldsymbol{v}) + ([\bar{\boldsymbol{\sigma}}_h], \sqrt{\nu}\{\boldsymbol{v}\} \otimes \boldsymbol{n}_e)_{\mathscr{E}_h^i},$$

$$\mathbb{b}(p_h, \boldsymbol{v}) = (\nabla p_h, \boldsymbol{v}) - ([p_h], \{\boldsymbol{v}\} \cdot \boldsymbol{n}_e)_{\mathscr{E}_h^i}. \tag{2.7}$$

2.2.3 Time discretization

For each positive integer N, let $0 = t^0 < t^1 < \cdots < t^N = T$ be a partition of T into subintervals $J^n = (t^{n-1}, t^n]$, with uniform mesh and the interval length $\Delta t = t^n - t^{n-1}, 1 \le n \le N, \boldsymbol{u}^n = \boldsymbol{u}(\boldsymbol{x}, t^n)$. The characteristic tracing back along the field $\boldsymbol{u}^{n-1}$ of a point $\boldsymbol{x} \in \Omega$ at time t^n to t^{n-1} is approximated by [54]:

$$\dot{\mathrm{x}}(\boldsymbol{x}, t^{n-1}) = \boldsymbol{x} - \boldsymbol{u}^{n-1}\Delta t.$$

Consequently, the approximation for the hyperbolic part of (1.1) at time t^n can be derived by

$$\partial_t \boldsymbol{u}^n + \boldsymbol{u}^n \cdot \nabla \boldsymbol{u}^n \approx \frac{\boldsymbol{u}^n - \dot{\boldsymbol{u}}^{n-1}}{\Delta t},$$

where $\dot{\boldsymbol{u}}^{n-1} = \boldsymbol{u}(\dot{\mathrm{x}}(\boldsymbol{x}, t^{n-1}))$.

25

Lemma 2.1. *(Time truncation error) [54] Let* $E(\boldsymbol{x}, n) = \frac{\boldsymbol{u}^n - \dot{\boldsymbol{u}}^{n-1}}{\Delta t} - (\partial_t \boldsymbol{u}^n + \boldsymbol{u}^n \cdot \nabla \boldsymbol{u}^n),$ *for* $\boldsymbol{u} \in C^4([\Delta t, T]; H^3(\Omega)^2)$ *and* $t^n > \Delta t$, *we have*

$$E(\boldsymbol{x}, n) = -\Delta t \Big(\frac{1}{2} \frac{d^2 \boldsymbol{g}_x^n}{dt^2} + \frac{\partial \boldsymbol{u}}{\partial t} \cdot \nabla \boldsymbol{u}(\boldsymbol{x}, t^n) \Big) + \mathcal{O}(\Delta t^2), \tag{2.8}$$

where $\boldsymbol{g}_x^n(t) = \boldsymbol{u}(\boldsymbol{x} - (t^n - t)\boldsymbol{u}^{n-1}, t).$

So the fully discretized scheme, the CLDG scheme corresponding to the variational formulation (2.6) is to find $(\boldsymbol{u}_h^n, \bar{\boldsymbol{\sigma}}_h^n, p_h^n) \in \mathbb{V}_h \times \mathbb{V}_h^2 \times \mathbb{Q}_h$ for any functions $(\boldsymbol{v}, \bar{\boldsymbol{\tau}}, q) \in \mathbb{V}_h \times \mathbb{V}_h^2 \times \mathbb{Q}_h$ such that

$$\begin{cases} \big(\frac{\boldsymbol{u}_h^n - \check{\boldsymbol{u}}_h^{n-1}}{\Delta t}, \boldsymbol{v} \big) + (\bar{\boldsymbol{\sigma}}_h^n, \sqrt{\nu} \nabla \boldsymbol{v}) - (\{\bar{\boldsymbol{\sigma}}_h^n\}, \sqrt{\nu}[\boldsymbol{v}] \otimes \boldsymbol{n}_e)_{\mathscr{E}_h^B} \\ \quad - (p_h^n, \nabla \cdot \boldsymbol{v}) + (\{p_h^n\}, [\boldsymbol{v}] \cdot \boldsymbol{n}_e)_{\mathscr{E}_h^B} + ([\boldsymbol{u}_h^n], [\boldsymbol{v}])_{\mathscr{E}_h^B} = (\boldsymbol{f}^n, \boldsymbol{v}), \\[2mm] (\bar{\boldsymbol{\sigma}}_h^n, \bar{\boldsymbol{\tau}}) - (\sqrt{\nu} \nabla \boldsymbol{u}_h^n, \bar{\boldsymbol{\tau}}) + (\{\bar{\boldsymbol{\tau}}\}, \sqrt{\nu}[\boldsymbol{u}_h^n] \otimes \boldsymbol{n}_e)_{\mathscr{E}_h^B} = 0, \\[2mm] (q, \nabla \cdot \boldsymbol{u}_h^n) - (\{q\}, [\boldsymbol{u}_h^n] \cdot \boldsymbol{n}_e)_{\mathscr{E}_h^B} + ([p_h^n], [q])_{\mathscr{E}_h^i} = 0, \end{cases} \tag{2.9}$$

where $\check{\boldsymbol{u}}_h^{n-1} = \boldsymbol{u}_h(\check{\mathbf{x}}(\boldsymbol{x}, t^{n-1})) = \boldsymbol{u}_h(\boldsymbol{x} - \boldsymbol{u}_h^{n-1} \Delta t, t^{n-1})$, and $\check{\boldsymbol{u}}_h^0 = \boldsymbol{u}^0.$

We rewrite (2.9) as a compact formulation: Find $(\boldsymbol{u}_h^n, \bar{\boldsymbol{\sigma}}_h^n, p_h^n) \in \mathbb{V}_h \times \mathbb{V}_h^2 \times \mathbb{Q}_h$ for any functions $(\boldsymbol{v}, \bar{\boldsymbol{\tau}}, q) \in \mathbb{V}_h \times \mathbb{V}_h^2 \times \mathbb{Q}_h$ such that

$$\begin{cases} \big(\frac{\boldsymbol{u}_h^n - \check{\boldsymbol{u}}_h^{n-1}}{\Delta t}, \boldsymbol{v} \big) + \mathrm{a}(\bar{\boldsymbol{\sigma}}_h^n, \boldsymbol{v}) + \mathrm{b}(p_h^n, \boldsymbol{v}) + \mathrm{c}(\boldsymbol{u}_h^n, \boldsymbol{v}) = (\boldsymbol{f}, \boldsymbol{v}), \\[2mm] (\bar{\boldsymbol{\sigma}}_h^n, \bar{\boldsymbol{\tau}}) - \mathrm{a}(\bar{\boldsymbol{\tau}}, \boldsymbol{u}_h^n) = 0, \\[2mm] -\mathrm{b}(q, \boldsymbol{u}_h^n) + \mathrm{d}(p_h^n, q) = 0. \end{cases} \tag{2.10}$$

For notational and analytic convenience, we define the following equality

$$\begin{aligned} \mathscr{A}(\boldsymbol{u}_h^n, \bar{\boldsymbol{\sigma}}_h^n, p_h^n; \boldsymbol{v}, \bar{\boldsymbol{\tau}}, q) \\ = \mathrm{a}(\bar{\boldsymbol{\sigma}}_h^n, \boldsymbol{v}) + \mathrm{b}(p_h^n, \boldsymbol{v}) + \mathrm{c}(\boldsymbol{u}_h^n, \boldsymbol{v}) + (\bar{\boldsymbol{\sigma}}_h^n, \bar{\boldsymbol{\tau}}) \\ - \mathrm{a}(\bar{\boldsymbol{\tau}}, \boldsymbol{u}_h^n) - \mathrm{b}(q, \boldsymbol{u}_h^n) + \mathrm{d}(p_h^n, q), \end{aligned} \tag{2.11}$$

and the right side hand

$$\mathscr{F}(\boldsymbol{v}) = (\boldsymbol{f}^n, \boldsymbol{v}). \tag{2.12}$$

Remark 2.1. We take $(\boldsymbol{v}, \bar{\boldsymbol{\tau}}, q) = (\boldsymbol{u}_h^n, \bar{\boldsymbol{\sigma}}_h^n, p_h^n)$ into (2.11), then a semi-norm $|\cdot|_{\mathscr{A}}$ can be

obtained

$$
\begin{aligned}
&\left|(\boldsymbol{u}_h^n, \bar{\boldsymbol{\sigma}}_h^n, p_h^n)\right|_{\mathscr{A}}^2 \\
&= \mathscr{A}(\boldsymbol{u}_h^n, \bar{\boldsymbol{\sigma}}_h^n, p_h^n; \boldsymbol{u}_h^n, \bar{\boldsymbol{\sigma}}_h^n, p_h^n) \\
&= \mathbb{c}(\boldsymbol{u}_h^n, \boldsymbol{u}_h^n) + (\bar{\boldsymbol{\sigma}}_h^n, \bar{\boldsymbol{\sigma}}_h^n) + \mathbb{d}(p_h^n, p_h^n) \\
&= \sum_{e \in \mathscr{E}_h^B} \| [\boldsymbol{u}_h^n] \|_{L^2(e)}^2 + \| \bar{\boldsymbol{\sigma}}_h^n \|_0^2 + \sum_{e \in \mathscr{E}_h^i} \| [p_h^n] \|_{L^2(e)}^2 .
\end{aligned}
\tag{2.13}
$$

2.2.4 Existence and uniqueness of CLDG solution

In order to prove the existence and uniqueness of the approximation solution of the CLDG scheme of problem (2.1), we shall introduce the following mild conditions on the local spaces.

$$
\boldsymbol{u} \in \mathbb{P}^k(E)^2 : \quad \int_E \nabla \boldsymbol{u} : \bar{\boldsymbol{\tau}} = 0, \quad \forall \, \bar{\boldsymbol{\tau}} \in \left(\mathbb{P}^k(E)^2\right)^2, \text{ then } \nabla \boldsymbol{u} = 0 \text{ on } E,
\tag{2.14}
$$

$$
q \in \mathbb{P}^k(E) : \quad \int_E \boldsymbol{v} \cdot \nabla q = 0, \quad \forall \, \boldsymbol{v} \in \mathbb{P}^k(E)^2, \text{ then } \nabla q = 0 \text{ on } E.
\tag{2.15}
$$

Obviously $\nabla \mathbb{P}^k(E)^2 \subset (\mathbb{P}^k(E)^2)^2, \nabla \mathbb{P}^k(E) \subset \mathbb{P}^k(E)^2$. See [9, 15], equations (2.14) and (2.15) are satisfied with $k \geq 1$.

Lemma 2.2. *If the approximation spaces $\mathbb{V}_h \times \mathbb{V}_h^2 \times \mathbb{Q}_h$ are spanned by the polynomial space $\mathbb{P}^k(E)$ with $k \geq 1$, then there exists a unique solution $(\boldsymbol{u}_h^n, \bar{\boldsymbol{\sigma}}_h^n, p_h^n) \in \mathbb{V}_h \times \mathbb{V}_h^2 \times \mathbb{Q}_h$ satisfying (2.9).*

Proof. To ensure the computability of the CLDG scheme for problem (2.1), we begin by showing that the variational formulation (2.9) is uniquely solvable for $(\boldsymbol{u}_h^n, \bar{\boldsymbol{\sigma}}_h^n, p_h^n)$ at each time step n. As (2.9) represents a finite system of linear equations, the uniqueness of $(\boldsymbol{u}_h^n, \bar{\boldsymbol{\sigma}}_h^n, p_h^n)$ is equivalent to the existence.

Setting $\breve{\boldsymbol{u}}_h^{n-1} = \boldsymbol{f} = 0$ and taking $\boldsymbol{v} = \boldsymbol{u}_h^n, \bar{\boldsymbol{\tau}} = \bar{\boldsymbol{\sigma}}_h^n, q = p_h^n$ in (2.10), we have

$$
\frac{1}{\Delta t} \| \boldsymbol{u}_h^n \|_0^2 + \left|(\boldsymbol{u}_h^n, \bar{\boldsymbol{\sigma}}_h^n, p_h^n)\right|_{\mathscr{A}}^2 = 0,
\tag{2.16}
$$

which implies $\boldsymbol{u}_h^n = \boldsymbol{0}, \bar{\boldsymbol{\sigma}}_h^n = \bar{\boldsymbol{0}}$, and $[p_h^n]\big|_e = 0, \forall \, e \in \mathscr{E}_h^i$. We go back to the equation (2.10), there is

$$
\forall \boldsymbol{v} \in \mathbb{V}_h, \quad b(\boldsymbol{v}, p_h^n) = 0.
$$

From identity (2.7), we get

$$b(\boldsymbol{v}, p_h^n) = \sum_{E \in \mathscr{E}_h} \int_E \nabla p_h^n \cdot \boldsymbol{v} = 0, \ \forall \ \boldsymbol{v} \in \mathbb{V}_h.$$

We conclude from equation (2.15) that $\nabla p_h^n = \boldsymbol{0}$ on each $E \in \mathscr{E}_h$, and $\left[p_h^n\right]\big|_e = 0, \forall \, e \in \mathscr{E}_h^i$, that p_h^n is a constant. Since $p_h^n \in \mathbb{M}$, i.e. $\int_\Omega p_h^n d\boldsymbol{x} = 0$, then we have $p_h^n = 0$. $\qquad\square$

2.3 Stability analysis

In this subsection, before presenting and proving the numerical stability result, we shall give the following lemma.

Lemma 2.3. *[6, 12, 27, 54] Define $\check{\mathcal{X}}_{\boldsymbol{x}}^n(t) = \boldsymbol{x} - (t^n - t)\boldsymbol{u}_h^{n-1}, \forall \, t \in [t^{n-2}, t^n], 2 \le n \le N$. If $\Delta t < \frac{1}{2L_n}, L_n = \max_{1 \le i \le n} \| \boldsymbol{u}_h^i \|_{1,\infty}$ on each time step t^n. Then for any function $\boldsymbol{v} \in L^2(\Omega)$ the following inequality holds*

$$\| \check{\boldsymbol{v}} \|_0^2 - \| \boldsymbol{v} \|_0^2 \le C\Delta t \| \boldsymbol{v} \|_0^2, \tag{2.17}$$

where $\check{\boldsymbol{v}} = \boldsymbol{v}(\boldsymbol{x} - \Delta t \boldsymbol{u}_h^{n-1})$, $\boldsymbol{u}_h^{n-1} \in \mathbb{V}_h \subset W^{1,\infty}(\Omega)^2$.

Proof. By the definition of $\check{\mathcal{X}}_{\boldsymbol{x}}^n(t^{n-1}) = \boldsymbol{x} - \Delta t \boldsymbol{u}_h^{n-1} = \check{\mathbf{x}}(\boldsymbol{x}, t^{n-1})$, the Jacobian of this transformation is that

$$J(\check{\mathcal{X}}_{\boldsymbol{x}}^n(t^{n-1})) = \begin{pmatrix} 1 - \partial_x u_{h1}^{n-1}\Delta t & -\partial_y u_{h1}^{n-1}\Delta t \\ -\partial_x u_{h2}^{n-1}\Delta t & 1 - \partial_y u_{h2}^{n-1}\Delta t \end{pmatrix},$$

therefore,

$$\left| J(\check{\mathcal{X}}_{\boldsymbol{x}}^n(t^{n-1})) \right| = 1 + \mathcal{O}(\Delta t),$$

then, we have

$$\begin{aligned} \| \check{\boldsymbol{v}} \|_0^2 - \| \boldsymbol{v} \|_0^2 &= \int_\Omega \boldsymbol{v}(\check{\mathbf{x}})^2 d\boldsymbol{x} - \int_\Omega \boldsymbol{v}(\boldsymbol{x})^2 d\boldsymbol{x} \\ &= \int_\Omega \boldsymbol{v}(\boldsymbol{x})^2 (1 + \mathcal{O}(\Delta t)) d\boldsymbol{x} - \int_\Omega \boldsymbol{v}(\boldsymbol{x})^2 d\boldsymbol{x} \\ &= \mathcal{O}(\Delta t) \int_\Omega \boldsymbol{v}(\boldsymbol{x})^2 d\boldsymbol{x}. \end{aligned}$$

$\qquad\square$

Theorem 2.4. *(Nonlinear stability) The CLDG scheme of (2.9) is nonlinear stable, i.e., for any integer $N = 1, 2, 3, \cdots$, such that*

$$\| \boldsymbol{u}_h^N \|_0^2 + 2\Delta t \sum_{n=1}^{N} \left| (\boldsymbol{u}_h^n, \bar{\boldsymbol{\sigma}}_h^n, p_h^n) \right|_{\mathscr{A}}^2 + \sum_{n=1}^{N} \| \boldsymbol{u}_h^n - \check{\boldsymbol{u}}_h^{n-1} \|_0^2$$

$$\leq C\Delta t \sum_{n=1}^{N} \| \boldsymbol{f}^n \|_0^2 + C \| \boldsymbol{u}^0 \|_0^2,$$

where $\Delta t < \frac{1}{2L_n}, L_n = \max_{1 \leq i \leq n} \| \boldsymbol{u}_h^i \|_{1,\infty}, \boldsymbol{u}^0 = \boldsymbol{u}_h^0, | \cdot |_{\mathscr{A}}$ is defined by (2.13), C is a generic constant.

Proof. Taking $\boldsymbol{v} = 2\Delta t \boldsymbol{u}_h^n$, $\bar{\boldsymbol{\tau}} = 2\Delta t \bar{\boldsymbol{\sigma}}_h^n$ and $q = 2\Delta t p_h^n$ in (2.10), respectively, we get the following equations

$$2(\boldsymbol{u}_h^n - \check{\boldsymbol{u}}_h^{n-1}, \boldsymbol{u}_h^n) + 2\Delta t \left| (\boldsymbol{u}_h^n, \bar{\boldsymbol{\sigma}}_h^n, p_h^n) \right|_{\mathscr{A}}^2 = 2\Delta t \mathscr{F}(\boldsymbol{u}_h^n),$$

and

$$2(\boldsymbol{u}_h^n - \check{\boldsymbol{u}}_h^{n-1}, \boldsymbol{u}_h^n) = \| \boldsymbol{u}_h^n \|_0^2 - \| \check{\boldsymbol{u}}_h^{n-1} \|_0^2 + \| \boldsymbol{u}_h^n - \check{\boldsymbol{u}}_h^{n-1} \|_0^2.$$

Now we estimate the bound of $\| \check{\boldsymbol{u}}_h^{n-1} \|_0^2 - \| \boldsymbol{u}_h^{n-1} \|_0^2$. Since $\mathbb{V}_h$ is a subset of $W^{1,\infty}(\Omega)^2$, from Lemma 2.3 we have

$$\| \check{\boldsymbol{u}}_h^{n-1} \|_0^2 - \| \boldsymbol{u}_h^{n-1} \|_0^2 \leq C\Delta t \| \boldsymbol{u}_h^{n-1} \|_0^2. \tag{2.18}$$

It follows the definition of $\mathscr{F}$, Hölder's inequality and Young's inequality, that

$$\begin{aligned}
\| \boldsymbol{u}_h^n \|_0^2 - \| \boldsymbol{u}_h^{n-1} \|_0^2 + 2\Delta t \left| (\boldsymbol{u}_h^n, \bar{\boldsymbol{\sigma}}_h^n, p_h^n) \right|_{\mathscr{A}}^2 + \| \boldsymbol{u}_h^n - \check{\boldsymbol{u}}_h^{n-1} \|_0^2 \\
\leq C\Delta t \| \boldsymbol{u}_h^{n-1} \|_0^2 + \Delta t \| \boldsymbol{f}^n \|_0^2 + \Delta t \| \boldsymbol{u}_h^n \|_0^2.
\end{aligned} \tag{2.19}$$

Summing up the above equation from $n = 1$ to N, we have

$$\| \boldsymbol{u}_h^N \|_0^2 - \| \boldsymbol{u}_h^0 \|_0^2 + 2\Delta t \sum_{n=1}^{N} \left| (\boldsymbol{u}_h^n, \bar{\boldsymbol{\sigma}}_h^n, p_h^n) \right|_{\mathscr{A}}^2 + \sum_{n=1}^{N} \| \boldsymbol{u}_h^n - \check{\boldsymbol{u}}_h^{n-1} \|_0^2$$

$$\leq C\Delta t \sum_{n=1}^{N} \| \boldsymbol{u}_h^{n-1} \|_0^2 + \Delta t \sum_{n=1}^{N} \| \boldsymbol{f}^n \|_0^2 + \Delta t \sum_{n=1}^{N} \| \boldsymbol{u}_h^n \|_0^2.$$

Then the following holds

$$\| \boldsymbol{u}_h^N \|_0^2 + 2\Delta t \sum_{n=1}^{N} \left| (\boldsymbol{u}_h^n, \bar{\boldsymbol{\sigma}}_h^n, p_h^n) \right|_{\mathscr{A}}^2 + \sum_{n=1}^{N} \| \boldsymbol{u}_h^n - \check{\boldsymbol{u}}_h^{n-1} \|_0^2$$

$$\leq C\Delta t \sum_{n=1}^{N} \| \boldsymbol{u}_h^n \|_0^2 + \Delta t \sum_{n=1}^{N} \| \boldsymbol{f}^n \|_0^2 + (C\Delta t + 1) \| \boldsymbol{u}_h^0 \|_0^2 .$$

From the discrete Gronwall inequality, we have

$$\| \boldsymbol{u}_h^N \|_0^2 + 2\Delta t \sum_{n=1}^{N} \left| (\boldsymbol{u}_h^n, \bar{\boldsymbol{\sigma}}_h^n, p_h^n) \right|_{\mathscr{A}}^2 + \sum_{n=1}^{N} \| \boldsymbol{u}_h^n - \check{\boldsymbol{u}}_h^{n-1} \|_0^2$$

$$\leq e^{CT} \left(\Delta t \sum_{n=1}^{N} \| \boldsymbol{f}^n \|_0^2 + (C\Delta t + 1) \| \boldsymbol{u}_h^0 \|_0^2 \right).$$

Hence, the proof is completed. $\qquad\square$

2.4 Error analysis

In this section, we present and prove error estimates for the CLDG scheme of (2.9). For the sake of simplicity, we introduce some notations:

$$\boldsymbol{\xi}_1^n = \boldsymbol{\Pi}\boldsymbol{u}^n - \boldsymbol{u}_h^n, \quad \boldsymbol{\xi}_2^n = \boldsymbol{\Pi}\boldsymbol{u}^n - \boldsymbol{u}^n, \quad \boldsymbol{e}_u^n = \boldsymbol{\xi}_1^n - \boldsymbol{\xi}_2^n = \boldsymbol{u}^n - \boldsymbol{u}_h^n,$$

$$\bar{\boldsymbol{\eta}}_1^n = \bar{\boldsymbol{\Pi}}\bar{\boldsymbol{\sigma}}^n - \bar{\boldsymbol{\sigma}}_h^n, \quad \bar{\boldsymbol{\eta}}_2^n = \bar{\boldsymbol{\Pi}}\bar{\boldsymbol{\sigma}}^n - \bar{\boldsymbol{\sigma}}^n, \quad \bar{\boldsymbol{e}}_\sigma^n = \bar{\boldsymbol{\eta}}_1^n - \bar{\boldsymbol{\eta}}_2^n = \bar{\boldsymbol{\sigma}}^n - \bar{\boldsymbol{\sigma}}_h^n,$$

$$\zeta_1^n = \Pi p^n - p_h^n, \quad \zeta_2^n = \Pi p^n - p^n, \quad e_p^n = \zeta_1^n - \zeta_2^n = p^n - p_h^n,$$

where $\boldsymbol{\Pi} : \mathbb{V} \mapsto \mathbb{V}_h, \bar{\Pi} : \mathbb{V}^2 \mapsto \mathbb{V}_h^2$ and $\Pi : \mathbb{Q} \mapsto \mathbb{Q}_h$ are linear continuous L^2-projection operators onto the corresponding finite element spaces.

In this chapter, we assume that the solution $(\boldsymbol{u}, p)$ of (2.1) satisfies the following regularity conditions:

$$\boldsymbol{u} \in L^\infty(J; W^{1,\infty}(\Omega)^2) \cap L^\infty(J; H^{k+1}(\Omega)^2) \cap C^4([\Delta t, T]; H^3(\Omega)^2),$$

$$\boldsymbol{u} \in H^1(J; H^{-1}(\Omega)^2), \partial_t \boldsymbol{u} \in L^2(J; H^{k+1}(\Omega)^2), \partial_{tt}\boldsymbol{u} \in L^2(J; L^2(\Omega)^2), \qquad (2.20)$$

$$p \in L^2(J; H^{k+1}(\Omega)) \cap L^2(J; L_0^2(\Omega)),$$

where k is the degree of polynomials approximation.

Lemma 2.5. *[12, 27, 54] If $\Delta t < \frac{1}{2L_n}, L_n = \max_{1\leq i\leq n} \| \boldsymbol{u}_h^i \|_{1,\infty}$, then for any function*

30

$v \in H^1(\Omega)$ and each time step n there is a constant C, such that

$$\| v(\boldsymbol{x}) - v(\check{\mathbf{x}}) \|_0^2 \leq C(\Delta t)^2 \| \nabla v \|_0^2 . \tag{2.21}$$

where $\check{\mathbf{x}} = \boldsymbol{x} - \Delta t \boldsymbol{u}_h^{n-1}$.

See the proof in page 12 of [54].

2.4.1   Error in velocity

Theorem 2.6. *(Error estimate of the velocity) Let $(\boldsymbol{u}^n, p^n)$ be the solution of (2.1), $\bar{\boldsymbol{\sigma}}^n \in (H^{k+1}(\Omega)^2)^2$ and $(\boldsymbol{u}_h^n, \bar{\boldsymbol{\sigma}}_h^n, p_h^n)$ be the solution of the CLDG scheme of (2.9). If $\Delta t < \frac{1}{2L_n}, L_n = \max_{1 \leq i \leq n} \| \boldsymbol{u}_h^i \|_{1,\infty}$, with the regularity of (2.20) such that for any integer $N = 1, 2, \cdots$, we have*

$$\begin{aligned} \| e_u^N \|_0^2 + \Delta t \sum_{n=1}^{N} \left| (e_u^n, \bar{e}_{\bar{\sigma}}^n, e_p^n) \right|_{\mathscr{A}}^2 + \sum_{n=1}^{N} \| e_u^n - \check{e}_u^{n-1} \|_0^2 \\ \leq C(\Delta t)^2 + \nu C h^{2k} + C h^{2k}, \end{aligned} \tag{2.22}$$

where $k \geq 1$, C is a generic constant.

Proof. The exact solution $(\boldsymbol{u}^n, \bar{\boldsymbol{\sigma}}^n, p^n)$ satisfies (2.6) because of the consistency of the scheme. We take $\boldsymbol{v} = \boldsymbol{\xi}_1^n, \bar{\boldsymbol{\tau}} = \bar{\boldsymbol{\eta}}_1^n, q = \zeta_1^n$ in (2.6) and (2.9), subtract (2.9) from (2.6) we have

$$\left(\partial_t \boldsymbol{u}^n + (\boldsymbol{u}^n \cdot \nabla) \boldsymbol{u}^n - \frac{\boldsymbol{u}_h^n - \check{\boldsymbol{u}}_h^{n-1}}{\Delta t}, \boldsymbol{\xi}_1^n \right) + \left| (\boldsymbol{\xi}_1^n, \bar{\boldsymbol{\eta}}_1^n, \zeta_1^n) \right|_{\mathscr{A}}^2$$

$$= \mathcal{A}(\boldsymbol{\xi}_2^n, \bar{\boldsymbol{\eta}}_2^n, \zeta_2^n; \boldsymbol{\xi}_1^n, \bar{\boldsymbol{\eta}}_1^n, \zeta_1^n)$$

$$= \mathrm{a}(\bar{\boldsymbol{\eta}}_2^n, \boldsymbol{\xi}_1^n) + \mathrm{b}(\zeta_2^n, \boldsymbol{\xi}_1^n) + \mathrm{c}(\boldsymbol{\xi}_2^n, \boldsymbol{\xi}_1^n) + (\bar{\boldsymbol{\eta}}_2^n, \bar{\boldsymbol{\eta}}_1^n) \tag{2.23}$$

$$- \mathrm{a}(\bar{\boldsymbol{\eta}}_1^n, \boldsymbol{\xi}_2^n) - \mathrm{b}(\zeta_1^n, \boldsymbol{\xi}_2^n) + \mathrm{d}(\zeta_2^n, \zeta_1^n)$$

$$= \sum_{i=1}^{7} \mathcal{I}_i,$$

31

where

$$\mathcal{I}_1 = \mathrm{a}(\bar{\boldsymbol{\eta}}_2^n, \boldsymbol{\xi}_1^n),$$
$$\mathcal{I}_2 = \mathrm{b}(\zeta_2^n, \boldsymbol{\xi}_1^n),$$
$$\mathcal{I}_3 = \mathrm{c}(\boldsymbol{\xi}_2^n, \boldsymbol{\xi}_1^n),$$
$$\mathcal{I}_4 = (\bar{\boldsymbol{\eta}}_2^n, \bar{\boldsymbol{\eta}}_1^n),$$
$$\mathcal{I}_5 = -\mathrm{a}(\bar{\boldsymbol{\eta}}_1^n, \boldsymbol{\xi}_2^n),$$
$$\mathcal{I}_6 = -\mathrm{b}(\zeta_1^n, \boldsymbol{\xi}_2^n),$$
$$\mathcal{I}_7 = \mathrm{d}(\zeta_2^n, \zeta_1^n).$$

Now we estimate each term $\mathcal{I}_i$, respectively. By the property of L^2-projection operator $\bar{\Pi}$, Hölder's inequality, and Lemma 1.7 we obtain

$$
\begin{aligned}
\mathcal{I}_1 &= (\bar{\boldsymbol{\eta}}_2^n, \sqrt{\nu}\nabla\boldsymbol{\xi}_1^n) - (\{\bar{\boldsymbol{\eta}}_2^n\}, \sqrt{\nu}[\boldsymbol{\xi}_1^n] \otimes \boldsymbol{n}_e)_{\mathscr{E}_h^B} \\
&\leq \sum_{e\in\mathscr{E}_h^B} \sqrt{\nu} \,\| \{\bar{\boldsymbol{\eta}}_2^n\} \,\|_{L^2(e)} \| \,[\boldsymbol{\xi}_1^n] \otimes \boldsymbol{n}_e \,\|_{L^2(e)} \\
&\leq C\Big(\sum_{e\in\mathscr{E}_h^B} \nu \,\| \{\bar{\boldsymbol{\eta}}_2^n\} \,\|^2_{L^2(e)} \Big)^{\frac{1}{2}} \Big(\sum_{e\in\mathscr{E}_h^B} \| \,[\boldsymbol{\xi}_1^n] \,\|^2_{L^2(e)} \Big)^{\frac{1}{2}} \\
&\leq \sqrt{\nu}Ch^{k+\frac{1}{2}}\big|(\boldsymbol{\xi}_1^n, \bar{\boldsymbol{\eta}}_1^n, \zeta_1^n)\big|_{\mathscr{A}}.
\end{aligned}
$$

Similarly, we deduce

$$
\begin{aligned}
\mathcal{I}_2 &= -(\zeta_2^n, \nabla \cdot \boldsymbol{\xi}_1^n) + (\{\zeta_2^n\}, [\boldsymbol{\xi}_1^n] \cdot \boldsymbol{n}_e)_{\mathscr{E}_h^B} \\
&\leq \Big(\sum_{e\in\mathscr{E}_h^B} \| \{\zeta_2^n\} \|^2_{L^2(e)} \Big)^{\frac{1}{2}} \Big(\sum_{e\in\mathscr{E}_h^B} \| \,[\boldsymbol{\xi}_1^n] \,\|^2_{L^2(e)} \Big)^{\frac{1}{2}} \\
&\leq Ch^{k+\frac{1}{2}}\big|(\boldsymbol{\xi}_1^n, \bar{\boldsymbol{\eta}}_1^n, \zeta_1^n)\big|_{\mathscr{A}},
\end{aligned}
$$

$$
\begin{aligned}
\mathcal{I}_3 &\leq \Big(\sum_{e\in\mathscr{E}_h^B} \| \,[\boldsymbol{\xi}_2^n] \,\|^2_{L^2(e)} \Big)^{\frac{1}{2}} \Big(\sum_{e\in\mathscr{E}_h^B} \| \,[\boldsymbol{\xi}_1^n] \,\|^2_{L^2(e)} \Big)^{\frac{1}{2}} \\
&\leq Ch^{k+\frac{1}{2}}\big|(\boldsymbol{\xi}_1^n, \bar{\boldsymbol{\eta}}_1^n, \zeta_1^n)\big|_{\mathscr{A}}.
\end{aligned}
$$

Note that $\mathcal{I}_4 = 0$ because of the property of L^2-projection operator $\bar{\Pi}$. By the property of L^2-projection operator $\boldsymbol{\Pi}$, Young's inequality, and trace inequality we imply

32

$$\mathcal{I}_5 = (\nabla \cdot \bar{\boldsymbol{\eta}}_1^n, \sqrt{\nu}\boldsymbol{\xi}_2^n) - ([\bar{\boldsymbol{\eta}}_1^n], \sqrt{\nu}\{\boldsymbol{\xi}_2^n\} \otimes \boldsymbol{n}_e)_{\mathscr{E}_h^i}$$

$$= -([\bar{\boldsymbol{\eta}}_1^n], \sqrt{\nu}\{\boldsymbol{\xi}_2^n\} \otimes \boldsymbol{n}_e)_{\mathscr{E}_h^i}$$

$$\leq \sum_{e \in \mathscr{E}_h^i} \sqrt{\nu} \parallel \{\boldsymbol{\xi}_2^n\} \otimes \boldsymbol{n}_e \parallel_{L^2(e)} \parallel [\bar{\boldsymbol{\eta}}_1^n] \parallel_{L^2(e)}$$

$$\leq \sum_{e \in \mathscr{E}_h^i} \sqrt{\nu} \parallel \{\boldsymbol{\xi}_2^n\} \otimes \boldsymbol{n}_e \parallel_{L^2(e)} \left(Ch_{E_1^e}^{-1/2} \parallel \bar{\boldsymbol{\eta}}_1^n \parallel_{L^2(E_1^e)} + Ch_{E_2^e}^{-1/2} \parallel \bar{\boldsymbol{\eta}}_1^n \parallel_{L^2(E_2^e)} \right)$$

$$\leq \sqrt{\nu}Ch^{-\frac{1}{2}} \left(\sum_{e \in \mathscr{E}_h^i} \parallel \{\boldsymbol{\xi}_2^n\} \parallel_{L^2(e)}^2 \right)^{\frac{1}{2}} \left(\sum_{e \in \mathscr{E}_h^i} \left(\parallel \bar{\boldsymbol{\eta}}_1^n \parallel_{L^2(E_1^e)} + \parallel \bar{\boldsymbol{\eta}}_1^n \parallel_{L^2(E_2^e)} \right)^2 \right)^{\frac{1}{2}}$$

$$\leq \sqrt{\nu}Ch^k \left| (\boldsymbol{\xi}_1^n, \bar{\boldsymbol{\eta}}_1^n, \zeta_1^n) \right|_{\mathscr{A}}.$$

From identity (2.7), with the same deduction there are

$$\mathcal{I}_6 = -(\nabla \zeta_1^n, \boldsymbol{\xi}_2^n) + ([\zeta_1^n], \{\boldsymbol{\xi}_2^n\} \cdot \boldsymbol{n}_e)_{\mathscr{E}_h^i}$$

$$= ([\zeta_1^n], \{\boldsymbol{\xi}_2^n\} \cdot \boldsymbol{n}_e)_{\mathscr{E}_h^i}$$

$$\leq C \left(\sum_{e \in \mathscr{E}_h^i} \parallel \{\boldsymbol{\xi}_2^n\} \cdot \boldsymbol{n}_e \parallel_{L^2(e)}^2 \right)^{\frac{1}{2}} \left(\sum_{e \in \mathscr{E}_h^i} \parallel [\zeta_1^n] \parallel_{L^2(e)}^2 \right)^{\frac{1}{2}}$$

$$\leq Ch^{k+\frac{1}{2}} \left| (\boldsymbol{\xi}_1^n, \bar{\boldsymbol{\eta}}_1^n, \zeta_1^n) \right|_{\mathscr{A}},$$

and

$$\mathcal{I}_7 = ([\zeta_2^n], [\zeta_1^n])_{\mathscr{E}_h^i}$$

$$= \sum_{e \mathscr{E}_h^i} ([\zeta_2^n], [\zeta_1^n])_e$$

$$\leq \sum_{e \in \mathscr{E}_h^i} \parallel [\zeta_2^n] \parallel_{L^2(e)} \parallel [\zeta_1^n] \parallel_{L^2(e)}$$

$$\leq \left(\sum_{e \in \mathscr{E}_h^i} \parallel [\zeta_2^n] \parallel_{L^2(e)}^2 \right)^{\frac{1}{2}} \left(\sum_{e \in \mathscr{E}_h^i} \parallel [\zeta_1^n] \parallel_{L^2(e)}^2 \right)^{\frac{1}{2}}$$

$$\leq Ch^{k+\frac{1}{2}} \left| (\boldsymbol{\xi}_1^n, \bar{\boldsymbol{\eta}}_1^n, \zeta_1^n) \right|_{\mathscr{A}}.$$

Now let us tackle the first term of the left side of equation (2.23). It is easy to obtain

33

$$\left(\partial_t \boldsymbol{u}^n + (\boldsymbol{u}^n \cdot \nabla)\boldsymbol{u}^n - \frac{\boldsymbol{u}_h^n - \check{\boldsymbol{u}}_h^{n-1}}{\Delta t}, \boldsymbol{\xi}_1^n\right)$$

$$= \left(\partial_t \boldsymbol{u}^n + (\boldsymbol{u}^n \cdot \nabla)\boldsymbol{u}^n - \frac{\boldsymbol{u}^n - \dot{\boldsymbol{u}}^{n-1}}{\Delta t}, \boldsymbol{\xi}_1^n\right) + \left(\frac{\check{\boldsymbol{u}}^{n-1} - \dot{\boldsymbol{u}}^{n-1}}{\Delta t}, \boldsymbol{\xi}_1^n\right) \qquad (2.24)$$

$$+ \left(\frac{\boldsymbol{\xi}_1^n - \check{\boldsymbol{\xi}}_1^{n-1}}{\Delta t}, \boldsymbol{\xi}_1^n\right) - \left(\frac{\boldsymbol{\xi}_2^n - \check{\boldsymbol{\xi}}_2^{n-1}}{\Delta t}, \boldsymbol{\xi}_1^n\right) = \sum_{i=1}^4 \mathcal{B}_i.$$

From Lemma 2.1 and Hölder's inequality, there is

$$\left|\mathcal{B}_1\right| = \left|\left(\partial_t \boldsymbol{u}^n + (\boldsymbol{u}^n \cdot \nabla)\boldsymbol{u}^n - \frac{\boldsymbol{u}^n - \dot{\boldsymbol{u}}^{n-1}}{\Delta t}, \boldsymbol{\xi}_1^n\right)\right|$$

$$\leq C\Delta t \parallel \boldsymbol{\xi}_1^n \parallel_0 \leq C(\Delta t)^2 + C \parallel \boldsymbol{\xi}_1^n \parallel_0^2.$$

By the definitions of $\check{\mathbf{x}}$ and $\dot{\mathbf{x}}$,

$$\check{\mathbf{x}} - \dot{\mathbf{x}} = \Delta t(\boldsymbol{u}_h^{n-1} - \boldsymbol{u}^{n-1}).$$

Using the Taylor formula, we have

$$|\check{\boldsymbol{u}}^{n-1} - \dot{\boldsymbol{u}}^{n-1}| = |\boldsymbol{u}^{n-1}(\check{\mathbf{x}}) - \boldsymbol{u}^{n-1}(\dot{\mathbf{x}})|$$

$$\leq \Delta t \parallel \nabla \boldsymbol{u}^{n-1} \parallel_\infty |\boldsymbol{u}_h^{n-1} - \boldsymbol{u}^{n-1}|$$

$$\leq C\Delta t \parallel \nabla \boldsymbol{u}^{n-1} \parallel_\infty (|\boldsymbol{\xi}_1^{n-1}| + |\boldsymbol{\xi}_2^{n-1}|).$$

Therefore,

$$\parallel \check{\boldsymbol{u}}^{n-1} - \dot{\boldsymbol{u}}^{n-1} \parallel_0$$

$$\leq C\Delta t \parallel \nabla \boldsymbol{u}^{n-1} \parallel_{L^\infty(\Omega)} (\parallel \boldsymbol{\xi}_1^{n-1} \parallel_0 + \parallel \boldsymbol{\xi}_2^{n-1} \parallel_0) \qquad (2.25)$$

$$\leq C\Delta t(h^{k+1} + \parallel \boldsymbol{\xi}_1^{n-1} \parallel_0).$$

From inequality (2.25) we deduce

$$\left|\mathcal{B}_2\right| = \left|\left(\frac{\check{\boldsymbol{u}}^{n-1} - \dot{\boldsymbol{u}}^{n-1}}{\Delta t}, \boldsymbol{\xi}_1^n\right)\right|$$

$$\leq \frac{1}{\Delta t} \parallel \check{\boldsymbol{u}}^{n-1} - \dot{\boldsymbol{u}}^{n-1} \parallel_0 \parallel \boldsymbol{\xi}_1^n \parallel_0$$

$$\leq Ch^{2k+2} + C \parallel \boldsymbol{\xi}_1^{n-1} \parallel_0^2 + C \parallel \boldsymbol{\xi}_1^n \parallel_0^2.$$

34

By Lemma 3.1 there is

$$
\begin{aligned}
\mathcal{B}_3 &= \Big(\frac{\boldsymbol{\xi}_1^n - \check{\boldsymbol{\xi}}_1^{n-1}}{\Delta t}, \boldsymbol{\xi}_1^n\Big) \\
&= \frac{1}{2\Delta t}\big(\,\|\,\boldsymbol{\xi}_1^n\,\|_0^2 - \|\,\check{\boldsymbol{\xi}}_1^{n-1}\,\|_0^2\,\big) + \frac{1}{2\Delta t}\,\|\,\boldsymbol{\xi}_1^n - \check{\boldsymbol{\xi}}_1^{n-1}\,\|_0^2 \\
&\geq \frac{1}{2\Delta t}\big(\,\|\,\boldsymbol{\xi}_1^n\,\|_0^2 - \|\,\boldsymbol{\xi}_1^{n-1}\,\|_0^2\,\big) - C\,\|\,\boldsymbol{\xi}_1^{n-1}\,\|_0^2 + \frac{1}{2\Delta t}\,\|\,\boldsymbol{\xi}_1^n - \check{\boldsymbol{\xi}}_1^{n-1}\,\|_0^2 .
\end{aligned}
$$

From the definition, we can get

$$
\begin{aligned}
\mathcal{B}_4 &= -\Big(\frac{\boldsymbol{\xi}_2^n - \check{\boldsymbol{\xi}}_2^{n-1}}{\Delta t}, \boldsymbol{\xi}_1^n\Big) \\
&= -\Big(\frac{\boldsymbol{\xi}_2^n - \boldsymbol{\xi}_2^{n-1}}{\Delta t}, \boldsymbol{\xi}_1^n\Big) - \Big(\frac{\boldsymbol{\xi}_2^{n-1} - \check{\boldsymbol{\xi}}_2^{n-1}}{\Delta t}, \boldsymbol{\xi}_1^n\Big).
\end{aligned}
$$

Consequently, from Taylor formula and Hölder's inequality, it follows that

$$
\Big|\Big(\frac{\boldsymbol{\xi}_2^n - \boldsymbol{\xi}_2^{n-1}}{\Delta t}, \boldsymbol{\xi}_1^n\Big)\Big| \leq C\big(\,\|\,\boldsymbol{\xi}_1^n\,\|_0^2 + \frac{1}{\Delta t}\,\|\,\partial_t \boldsymbol{\xi}_2\,\|_{L^2(J^n;\Omega)}^2\,\big).
$$

Using the Hölder's inequality, Young's inequality and Lemma 2.5, we have

$$
\Big|\Big(\frac{\boldsymbol{\xi}_2^{n-1} - \check{\boldsymbol{\xi}}_2^{n-1}}{\Delta t}, \boldsymbol{\xi}_1^n\Big)\Big| \leq C\big(\,\|\,\boldsymbol{\xi}_1^n\,\|_0^2 + \|\,\nabla\boldsymbol{\xi}_2^{n-1}\,\|_0^2\,\big).
$$

Combining $\mathcal{B}_i, i = 1, \cdots, 4$, there is

$$
\begin{aligned}
&\Big(\partial_t \boldsymbol{u}^n + (\boldsymbol{u}^n \cdot \nabla)\boldsymbol{u}^n - \frac{\boldsymbol{u}_h^n - \check{\boldsymbol{u}}_h^{n-1}}{\Delta t}, \boldsymbol{\xi}_1^n\Big) \\
&\geq \frac{1}{2\Delta t}\big(\,\|\,\boldsymbol{\xi}_1^n\,\|_0^2 - \|\,\boldsymbol{\xi}_1^{n-1}\,\|_0^2\,\big) - C\,\|\,\boldsymbol{\xi}_1^{n-1}\,\|_0^2 \\
&\quad + \frac{1}{2\Delta t}\,\|\,\boldsymbol{\xi}_1^n - \check{\boldsymbol{\xi}}_1^{n-1}\,\|_0^2 - C\,\|\,\boldsymbol{\xi}_1^n\,\|_0^2 - \frac{C}{\Delta t}\,\|\,\partial_t \boldsymbol{\xi}_2\,\|_{L^2(J^n;\Omega)}^2 \\
&\quad - C\,\|\,\nabla\boldsymbol{\xi}_2^{n-1}\,\|_0^2 - Ch^{2k+2} - C(\Delta t)^2.
\end{aligned} \tag{2.26}
$$

Substituting $\mathcal{I}_i, i = 1, \cdots, 7$ and inequality (2.26) into (2.23). Equality (2.23) becomes

$$
\begin{aligned}
&\frac{1}{2\Delta t}\big(\,\|\,\boldsymbol{\xi}_1^n\,\|_0^2 - \|\,\boldsymbol{\xi}_1^{n-1}\,\|_0^2\,\big) + \frac{1}{2}\big|(\boldsymbol{\xi}_1^n, \bar{\boldsymbol{\eta}}_1^n, \zeta_1^n)\big|_{\mathscr{A}}^2 + \frac{1}{2\Delta t}\,\|\,\boldsymbol{\xi}_1^n - \check{\boldsymbol{\xi}}_1^{n-1}\,\|_0^2 \\
&\leq C\,\|\,\boldsymbol{\xi}_1^{n-1}\,\|_0^2 + C\,\|\,\boldsymbol{\xi}_1^n\,\|_0^2 + \frac{C}{\Delta t}\,\|\,\partial_t \boldsymbol{\xi}_2\,\|_{L^2(J^n;\Omega)}^2 \\
&\quad + C\,\|\,\nabla\boldsymbol{\xi}_2^{n-1}\,\|_0^2 + C(\Delta t)^2 + Ch^{2k+1} + \nu Ch^{2k}.
\end{aligned} \tag{2.27}
$$

Summing over n from 1 to N and multiplying $2\Delta t$ from the both sides of (2.27), using

35

discrete Gronwall inequality we finally obtain

$$
\begin{aligned}
\| \boldsymbol{\xi}_1^N \|_0^2 &+\Delta t \sum_{n=1}^N |(\boldsymbol{\xi}_1^n, \bar{\boldsymbol{\eta}}_1^n, \zeta_1^n)|_{\mathscr{A}}^2 + \sum_{n=1}^N \| \boldsymbol{\xi}_1^n - \check{\boldsymbol{\xi}}_1^{n-1} \|_0^2 \\
&\le C \sum_{n=1}^N \| \partial_t \boldsymbol{\xi}_2 \|_{L^2(J^n;\Omega)}^2 + C\Delta t \sum_{n=1}^N \| \nabla \boldsymbol{\xi}_2^{n-1} \|_0^2 \\
&+ C(\Delta t)^2 + Ch^{2k+1} + \nu Ch^{2k}.
\end{aligned}
\tag{2.28}
$$

By the triangular inequality, the desired error bound of (2.22) is obtained. $\qquad\square$

Remark 2.2. From (2.28) for any integer $N = 1, 2, \cdots$, we have

$$
\| \boldsymbol{\xi}_1^N \|_0^2 \le C((\Delta t)^2 + h^{2k}), \quad \sum_{n=1}^N \| \boldsymbol{\xi}_1^n - \check{\boldsymbol{\xi}}_1^{n-1} \|_0^2 \le C((\Delta t)^2 + h^{2k}).
$$

2.4.2 Error in pressure

Lemma 2.7. *(Div-grad relation) [44] If $\boldsymbol{v} \in H_0^1(\Omega)^2$, then*

$$
\| \nabla \cdot \boldsymbol{v} \|_0 \le \| \nabla \boldsymbol{v} \|_0 .
\tag{2.29}
$$

Lemma 2.8. *[12, 27, 54] If $v \in L^2(\Omega)$ and $\Delta t < \frac{1}{2L_n}, L_n = \max_{1 \le i \le n} \| \boldsymbol{u}_h^i \|_{1,\infty}$, such that for any time step n there exists a constant C*

$$
\| v(\boldsymbol{x}) - v(\check{\mathbf{x}}) \|_{-1} \le C\Delta t \| v \|_0,
\tag{2.30}
$$

where $\check{\mathbf{x}} = \boldsymbol{x} - \Delta t \boldsymbol{u}_h^{n-1}$.

The proof can be found in [12, 27, 54].

To obtain the error estimate in the pressure, we shall recall the continuous inf-sup condition for the spaces $H_0^1(\Omega)^2$ and $L_0^2(\Omega)$.

Lemma 2.9. *[15, 30, 50] There exists a positive constant β, such that*

$$
\inf_{q \in L_0^2(\Omega)} \sup_{\boldsymbol{v} \in H_0^1(\Omega)^2} \frac{(\nabla \cdot \boldsymbol{v}, q)}{\| q \|_0 \| \nabla \boldsymbol{v} \|_0} \ge \beta.
\tag{2.31}
$$

Equivalently, such that for any $q \in L_0^2(\Omega)$ there is a function $\tilde{\boldsymbol{v}} \in H_0^1(\Omega)^2$

$$
-\int_\Omega q\nabla \cdot \tilde{\boldsymbol{v}} \ge \beta_1 \| q \|_0^2, \quad \| \tilde{\boldsymbol{v}} \|_1 \le \beta_2 \| q \|_0,
\tag{2.32}
$$

where $\beta_1 > 0, \beta_2 > 0$ *are positive constants independent of* $h, \Delta t, q$ *and* $\tilde{\boldsymbol{v}}$.

Lemma 2.10. *For any functions* $(\boldsymbol{v}, \bar{\boldsymbol{\tau}}, q) \in \mathbb{V}_h \times \mathbb{V}_h^2 \times \mathbb{Q}_h$, *there exist a function* $\tilde{\boldsymbol{v}} \in H_0^1(\Omega)^2$ *and two positive constants* K_1 *and* K_2 *independent of* $h, \Delta t$ *and* q,

$$K_1 \parallel q \parallel_0^2 \leq \mathcal{A}(\boldsymbol{v}, \bar{\boldsymbol{\tau}}, q; \boldsymbol{\Pi}\tilde{\boldsymbol{v}}, \bar{\boldsymbol{0}}, 0) + K_2 \big|(\boldsymbol{v}, \bar{\boldsymbol{\tau}}, q)\big|_{\mathscr{A}}^2, \quad \parallel \boldsymbol{\Pi}\tilde{\boldsymbol{v}} \parallel_1 \leq C \parallel q \parallel_0, \qquad (2.33)$$

where $\boldsymbol{\Pi}\tilde{\boldsymbol{v}}$ *is the* L^2-*projection of* $\tilde{\boldsymbol{v}}$ *onto the finite element space* $\mathbb{V}_h$, *C is a generic constant.*

Proof. With similar deduction as [15], we fix $q \in \mathbb{Q}_h \subset L_0^2(\Omega)$. From Lemma 2.9, for $(\boldsymbol{v}, \bar{\boldsymbol{\tau}}, q) \in \mathbb{V}_h \times \mathbb{V}_h^2 \times \mathbb{Q}_h$ there is a function $\tilde{\boldsymbol{v}} \in H_0^1(\Omega)^2$ satisfying (2.32). From equality (2.11) we have

$$\begin{aligned}
&\mathcal{A}(\boldsymbol{v}, \bar{\boldsymbol{\tau}}, q; \boldsymbol{\Pi}\tilde{\boldsymbol{v}}, \bar{\boldsymbol{0}}, 0) \\
&= \mathrm{a}(\bar{\boldsymbol{\tau}}, \boldsymbol{\Pi}\tilde{\boldsymbol{v}}) + \mathrm{b}(q, \boldsymbol{\Pi}\tilde{\boldsymbol{v}}) + \mathrm{c}(\boldsymbol{v}, \boldsymbol{\Pi}\tilde{\boldsymbol{v}}) \\
&= \mathcal{T}_1 + \mathcal{T}_2 + \mathcal{T}_3.
\end{aligned} \qquad (2.34)$$

Now we shall estimate $\mathcal{T}_i$ as follow

$$\begin{aligned}
\big|\mathcal{T}_1\big| &= \big|\mathrm{a}(\bar{\boldsymbol{\tau}}, \boldsymbol{\Pi}\tilde{\boldsymbol{v}})\big| \leq \big|\mathrm{a}(\bar{\boldsymbol{\tau}}, \boldsymbol{\Pi}\tilde{\boldsymbol{v}} - \tilde{\boldsymbol{v}})\big| + \big|\mathrm{a}(\bar{\boldsymbol{\tau}}, \tilde{\boldsymbol{v}})\big| \\
&= \big| - (\nabla \cdot \bar{\boldsymbol{\tau}}, \sqrt{\nu}(\boldsymbol{\Pi}\tilde{\boldsymbol{v}} - \tilde{\boldsymbol{v}})) + ([\bar{\boldsymbol{\tau}}], \sqrt{\nu}\{\boldsymbol{\Pi}\tilde{\boldsymbol{v}} - \tilde{\boldsymbol{v}}\} \otimes \boldsymbol{n}_e)_{\mathscr{E}_h^i}\big| + \big|(\bar{\boldsymbol{\tau}}, \sqrt{\nu}\nabla\tilde{\boldsymbol{v}})\big| \\
&= \big|([\bar{\boldsymbol{\tau}}], \sqrt{\nu}\{\boldsymbol{\Pi}\tilde{\boldsymbol{v}} - \tilde{\boldsymbol{v}}\} \otimes \boldsymbol{n}_e)_{\mathscr{E}_h^i}\big| + \big|(\bar{\boldsymbol{\tau}}, \sqrt{\nu}\nabla\tilde{\boldsymbol{v}})\big| \\
&\leq C\sqrt{\nu}\Big(\sum_{e \in \mathscr{E}_h^i} \parallel [\bar{\boldsymbol{\tau}}] \parallel_{L^2(e)}^2\Big)^{\frac{1}{2}}\Big(\sum_{e \in \mathscr{E}_h^i} \parallel \{\boldsymbol{\Pi}\tilde{\boldsymbol{v}} - \tilde{\boldsymbol{v}}\} \otimes \boldsymbol{n}_e \parallel_{L^2(e)}^2\Big)^{\frac{1}{2}} + C\sqrt{\nu} \parallel \bar{\boldsymbol{\tau}} \parallel_0 \parallel \tilde{\boldsymbol{v}} \parallel_1 \\
&\leq C\sqrt{\nu}h^{\frac{1}{2}}\Big(\sum_{e \in \mathscr{E}_h^i} \parallel [\bar{\boldsymbol{\tau}}] \parallel_{L^2(e)}^2\Big)^{\frac{1}{2}} \parallel \tilde{\boldsymbol{v}} \parallel_1 + C\sqrt{\nu} \parallel \bar{\boldsymbol{\tau}} \parallel_0 \parallel \tilde{\boldsymbol{v}} \parallel_1 \\
&\leq C\sqrt{\nu} \parallel \bar{\boldsymbol{\tau}} \parallel_0 \parallel \tilde{\boldsymbol{v}} \parallel_1 \\
&\leq C\sqrt{\nu}\big|(\boldsymbol{v}, \bar{\boldsymbol{\tau}}, q)\big|_{\mathscr{A}} \parallel q \parallel_0 .
\end{aligned}$$

Then, we have

$$\mathcal{T}_1 \geq -\nu C\epsilon_1 \parallel q \parallel_0^2 - C\epsilon_1^{-1}\big|(\boldsymbol{v}, \bar{\boldsymbol{\tau}}, q)\big|_{\mathscr{A}}^2. \qquad (2.35)$$

By the definition of $\mathcal{T}_2$ we obtain

$$\mathcal{T}_2 = \mathrm{b}(q, \boldsymbol{\Pi}\tilde{\boldsymbol{v}}) = \mathrm{b}(q, \boldsymbol{\Pi}\tilde{\boldsymbol{v}} - \tilde{\boldsymbol{v}}) + \mathrm{b}(q, \tilde{\boldsymbol{v}}).$$

Since

$$\left| \mathbb{b}(q, \boldsymbol{\Pi}\tilde{\boldsymbol{v}} - \tilde{\boldsymbol{v}}) \right| = \left| ([q], \{\boldsymbol{\Pi}\tilde{\boldsymbol{v}} - \tilde{\boldsymbol{v}}\} \cdot \boldsymbol{n}_e)_{\mathscr{E}_h^i} \right|$$

$$\leq \Big(\sum_{e \in \mathscr{E}_h^i} \| [q] \|_{L^2(e)}^2 \Big)^{\frac{1}{2}} \Big(\sum_{e \in \mathscr{E}_h^i} \| \{\boldsymbol{\Pi}\tilde{\boldsymbol{v}} - \tilde{\boldsymbol{v}}\} \cdot \boldsymbol{n}_e \|_{L^2(e)}^2 \Big)^{\frac{1}{2}} \tag{2.36}$$

$$\leq Ch^{\frac{1}{2}} \left| (\boldsymbol{v}, \bar{\boldsymbol{\tau}}, q) \right|_{\mathscr{A}} \| \tilde{\boldsymbol{v}} \|_1$$

$$\leq Ch^{\frac{1}{2}} \left| (\boldsymbol{v}, \bar{\boldsymbol{\tau}}, q) \right|_{\mathscr{A}} \| q \|_0,$$

and

$$\mathbb{b}(q, \tilde{\boldsymbol{v}}) = -(q, \nabla \cdot \tilde{\boldsymbol{v}}) \geq \beta_1 \| q \|_0^2 . \tag{2.37}$$

Combining (2.36) and (2.37) gives

$$\mathcal{T}_2 \geq \beta_1 \| q \|_0^2 - Ch\epsilon_2 \| q \|_0^2 - C\epsilon_2^{-1} \left| (\boldsymbol{v}, \bar{\boldsymbol{\tau}}, q) \right|_{\mathscr{A}}^2 . \tag{2.38}$$

Observe that

$$\mathcal{T}_3 = \mathbb{c}(\boldsymbol{v}, \boldsymbol{\Pi}\tilde{\boldsymbol{v}} - \tilde{\boldsymbol{v}})$$

$$\leq \Big(\sum_{e \in \mathscr{E}_h^B} \| [\boldsymbol{v}] \|_{L^2(e)}^2 \Big)^{\frac{1}{2}} \Big(\sum_{e \in \mathscr{E}_h^B} \| [\boldsymbol{\Pi}\tilde{\boldsymbol{v}} - \tilde{\boldsymbol{v}}] \|_{L^2(e)}^2 \Big)^{\frac{1}{2}}$$

$$\leq Ch^{\frac{1}{2}} \left| (\boldsymbol{v}, \bar{\boldsymbol{\tau}}, q) \right|_{\mathscr{A}} \| \tilde{\boldsymbol{v}} \|_1$$

$$\leq Ch^{\frac{1}{2}} \left| (\boldsymbol{v}, \bar{\boldsymbol{\tau}}, q) \right|_{\mathscr{A}} \| q \|_0 .$$

Hence

$$\mathcal{T}_3 \geq -Ch\epsilon_3 \| q \|_0^2 - C\epsilon_3^{-1} \left| (\boldsymbol{v}, \bar{\boldsymbol{\tau}}, q) \right|_{\mathscr{A}}^2 . \tag{2.39}$$

Substituting $\mathcal{T}_1, \mathcal{T}_2, \mathcal{T}_3$ into (2.34), we deduce

$$\mathcal{A}(\boldsymbol{v}, \bar{\boldsymbol{\tau}}, q; \boldsymbol{\Pi}\tilde{\boldsymbol{v}}, \bar{\boldsymbol{0}}, 0)$$

$$\geq (\beta_1 - \nu C\epsilon_1 - Ch\epsilon_2 - Ch\epsilon_3) \| q \|_0^2 - (C\epsilon_1^{-1} + C\epsilon_2^{-1} + C\epsilon_3^{-1}) \left| (\boldsymbol{v}, \bar{\boldsymbol{\tau}}, q) \right|_{\mathscr{A}}^2 , \tag{2.40}$$

where $\epsilon_1, \epsilon_2, \epsilon_3$ are chosen such that $K_1 = \beta_1 - \nu C\epsilon_1 - Ch\epsilon_2 - Ch\epsilon_3 > 0$ and $K_2 = C\epsilon_1^{-1} + C\epsilon_2^{-1} + C\epsilon_3^{-1} > 0$, and K_1, K_2 are positive constants independent of h.

Furthermore, from Lemma 1.6 we have

$$\| \ \boldsymbol{\Pi}\tilde{\boldsymbol{v}} \ \|_1 \leq \| \ \boldsymbol{\Pi}\tilde{\boldsymbol{v}} - \tilde{\boldsymbol{v}} \ \|_1 + \| \ \tilde{\boldsymbol{v}} \ \|_1 \leq C \| \ \tilde{\boldsymbol{v}} \ \|_1 \leq C \| \ q \ \|_0 \ . \tag{2.41}$$

$\square$

Theorem 2.11. *(Error estimate of the pressure) Let $(\boldsymbol{u}^n, p^n)$ be the solution of (2.1), $\bar{\boldsymbol{\sigma}}^n \in (H^{k+1}(\Omega)^2)^2$, and $(\boldsymbol{u}_h^n, \bar{\boldsymbol{\sigma}}_h^n, p_h^n)$ be the solution of the CLDG scheme of (2.9). If $\Delta t < \frac{1}{2L_n}, L_n = \max_{1 \leq i \leq n} \| \ \boldsymbol{u}_h^i \ \|_{1,\infty}$, with the regularity of (2.20) such that for any integer $N = 1, 2, \cdots$, the following holds*

$$\Delta t \sum_{n=1}^{N} \| \ e_p^n \ \|_0^2 \leq C(\Delta t + h^{2k}/\Delta t). \tag{2.42}$$

Proof. From Lemma 2.9 and Lemma 2.10, for $\zeta_1^n \in \mathbb{Q}_h$ there exists a function $\boldsymbol{w} \in H_0^1(\Omega)^2$ with its L^2-projection $\boldsymbol{\Pi}\boldsymbol{w}$ satisfying equation (2.33), i.e.

$$K_1 \| \ \zeta_1^n \ \|_0^2 \leq \mathcal{A}(\boldsymbol{\xi}_1^n, \bar{\boldsymbol{\eta}}_1^n, \zeta_1^n; \boldsymbol{\Pi}\boldsymbol{w}, \bar{\boldsymbol{0}}, 0) + K_2 \big|(\boldsymbol{\xi}_1^n, \bar{\boldsymbol{\eta}}_1^n, \zeta_1^n)\big|_{\mathscr{A}}^2, \quad \| \ \boldsymbol{\Pi}\boldsymbol{w} \ \|_1 \leq C \| \ \zeta_1^n \ \|_0 \ .$$

From the first equation of (2.6) and the first equation of (2.10), we have

$$\left(\partial_t \boldsymbol{u}^n + (\boldsymbol{u}^n \cdot \nabla)\boldsymbol{u}^n - \frac{\boldsymbol{u}_h^n - \check{\boldsymbol{u}}_h^{n-1}}{\Delta t}, \boldsymbol{\Pi}\boldsymbol{w}\right) + \mathcal{A}(\boldsymbol{\xi}_1^n, \bar{\boldsymbol{\eta}}_1^n, \zeta_1^n; \boldsymbol{\Pi}\boldsymbol{w}, \bar{\boldsymbol{0}}, 0) \\ = \mathcal{A}(\boldsymbol{\xi}_2^n, \bar{\boldsymbol{\eta}}_2^n, \zeta_2^n; \boldsymbol{\Pi}\boldsymbol{w}, \bar{\boldsymbol{0}}, 0). \tag{2.43}$$

By Lemma 2.10 and rearranging the identity (2.43),

$$\begin{aligned} K_1 \| \ \zeta_1^n \ \|_0^2 &\leq \mathcal{A}(\boldsymbol{\xi}_1^n, \bar{\boldsymbol{\eta}}_1^n, \zeta_1^n; \boldsymbol{\Pi}\boldsymbol{w}, \bar{\boldsymbol{0}}, 0) + K_2 \big|(\boldsymbol{\xi}_1^n, \bar{\boldsymbol{\eta}}_1^n, \zeta_1^n)\big|_{\mathscr{A}}^2 \\ &\leq \left|\left(\partial_t \boldsymbol{u}^n + (\boldsymbol{u}^n \cdot \nabla)\boldsymbol{u}^n - \frac{\boldsymbol{u}_h^n - \check{\boldsymbol{u}}_h^{n-1}}{\Delta t}, \boldsymbol{\Pi}\boldsymbol{w}\right)\right| \\ &\quad + \big|\mathcal{A}(\boldsymbol{\xi}_2^n, \bar{\boldsymbol{\eta}}_2^n, \zeta_2^n; \boldsymbol{\Pi}\boldsymbol{w}, \bar{\boldsymbol{0}}, 0)\big| + C_2 \big|(\boldsymbol{\xi}_1^n, \bar{\boldsymbol{\eta}}_1^n, \zeta_1^n)\big|_{\mathscr{A}}^2. \end{aligned} \tag{2.44}$$

With the same deduction of $\mathcal{I}_1, \mathcal{I}_2, \mathcal{I}_3$, there is

$$\begin{aligned} &\big|\mathscr{A}(\boldsymbol{\xi}_2^n, \bar{\boldsymbol{\eta}}_2^n, \zeta_2^n; \boldsymbol{\Pi}\boldsymbol{w}, \bar{\boldsymbol{0}}, 0)\big| \\ &\leq Ch^{k+\frac{1}{2}} \big|(\boldsymbol{\Pi}\boldsymbol{w}, \bar{\boldsymbol{0}}, 0)\big|_{\mathscr{A}} \\ &\leq Ch^k \| \ \boldsymbol{\Pi}\boldsymbol{w} \ \|_0 \\ &\leq Ch^k \| \ \zeta_1^n \ \|_0 \ . \end{aligned} \tag{2.45}$$

According to the deduction of the bound of the characteristic term, we obtain

$$
\left| \left(\partial_t \boldsymbol{u}^n + (\boldsymbol{u}^n \cdot \nabla) \boldsymbol{u}^n - \frac{\boldsymbol{u}_h^n - \check{\boldsymbol{u}}_h^{n-1}}{\Delta t}, \boldsymbol{\Pi}\boldsymbol{w} \right) \right|
$$

$$
\leq C\Delta t \parallel \boldsymbol{\Pi}\boldsymbol{w} \parallel_0 + \frac{1}{\Delta t} \parallel \check{\boldsymbol{u}}^{n-1} - \dot{\boldsymbol{u}}^{n-1} \parallel_0 \parallel \boldsymbol{\Pi}\boldsymbol{w} \parallel_0
$$

$$
+ \frac{1}{\Delta t} |(\boldsymbol{\xi}_1^n - \check{\boldsymbol{\xi}}_1^{n-1}, \boldsymbol{\Pi}\boldsymbol{w})| + \frac{1}{\Delta t} |(\boldsymbol{\xi}_2^n - \check{\boldsymbol{\xi}}_2^{n-1}, \boldsymbol{\Pi}\boldsymbol{w})|
$$

$$
\leq C(\Delta t + h^{k+1} + \parallel \boldsymbol{\xi}_1^{n-1} \parallel_0) \parallel \boldsymbol{\Pi}\boldsymbol{w} \parallel_1 + \frac{1}{\Delta t} \parallel \boldsymbol{\xi}_1^n - \check{\boldsymbol{\xi}}_1^{n-1} \parallel_0 \parallel \boldsymbol{\Pi}\boldsymbol{w} \parallel_0
$$

$$
+ \frac{1}{\Delta t} \parallel \boldsymbol{\xi}_2^n - \boldsymbol{\xi}_2^{n-1} \parallel_0 \parallel \boldsymbol{\Pi}\boldsymbol{w} \parallel_0 + \frac{1}{\Delta t} \parallel \boldsymbol{\xi}_2^{n-1} - \check{\boldsymbol{\xi}}_2^{n-1} \parallel_{-1} \parallel \boldsymbol{\Pi}\boldsymbol{w} \parallel_1
$$

$$
\leq C\big(\Delta t + h^k + \frac{1}{\Delta t} \parallel \boldsymbol{\xi}_1^n - \check{\boldsymbol{\xi}}_1^{n-1} \parallel_0 \big) \parallel \boldsymbol{\Pi}\boldsymbol{w} \parallel_1
$$

$$
+ \big(\frac{1}{\sqrt{\Delta t}} \parallel \partial_t \boldsymbol{\xi}_2 \parallel_{L^2(J^n;\Omega)} + \parallel \boldsymbol{\xi}_2^{n-1} \parallel_0 \big) \parallel \boldsymbol{\Pi}\boldsymbol{w} \parallel_1
$$

$$
\leq C\big(\Delta t + h^k + \frac{1}{\Delta t} \parallel \boldsymbol{\xi}_1^n - \check{\boldsymbol{\xi}}_1^{n-1} \parallel_0 \big) \parallel \zeta_1^n \parallel_0 .
$$

From (2.44) and Young's inequality, it follows that

$$
\begin{aligned}
K_1 \parallel \zeta_1^n \parallel_0^2 &\leq C(\Delta t + h^k + \frac{1}{\Delta t} \parallel \boldsymbol{\xi}_1^n - \check{\boldsymbol{\xi}}_1^{n-1} \parallel_0) \parallel \zeta_1^n \parallel_0 \\
&\quad + Ch^k \parallel \zeta_1^n \parallel_0 + K_2 \big| (\boldsymbol{\xi}_1^n, \bar{\boldsymbol{\eta}}_1^n, \zeta_1^n) \big|_{\mathscr{A}}^2 \\
&\leq C/K_1((\Delta t)^2 + h^{2k} + \frac{1}{\Delta t} \parallel \boldsymbol{\xi}_1^n - \check{\boldsymbol{\xi}}_1^{n-1} \parallel_0^2) \\
&\quad + \frac{K_1}{2} \parallel \zeta_1^n \parallel_0^2 + K_2 \big| (\boldsymbol{\xi}_1^n, \bar{\boldsymbol{\eta}}_1^n, \zeta_1^n) \big|_{\mathscr{A}}^2.
\end{aligned}
\tag{2.46}
$$

Rearranging above inequality, multiplying $2\Delta t$ for both sides, and summing n from 1 to N, using Remark 2.2 we have

$$
\begin{aligned}
\Delta t \sum_{n=1}^{N} \parallel \zeta_1^n \parallel_0^2 &\leq C((\Delta t)^2 + h^{2k}) + C\Delta t \sum_{n=1}^{N} \big| (\boldsymbol{\xi}_1^n, \bar{\boldsymbol{\eta}}_1^n, \zeta_1^n) \big|_{\mathscr{A}}^2 + \Delta t \sum_{n=1}^{N} \parallel \frac{\boldsymbol{\xi}_1^n - \check{\boldsymbol{\xi}}_1^{n-1}}{\Delta t} \parallel_0^2 \\
&\leq C((\Delta t)^2 + h^{2k}) + \frac{C}{\Delta t} \sum_{n=1}^{N} \parallel \boldsymbol{\xi}_1^n - \check{\boldsymbol{\xi}}_1^{n-1} \parallel_0^2 \\
&\leq C(\Delta t + h^{2k}/\Delta t).
\end{aligned}
$$

Using triangular inequality, we complete the proof. □

2.5 Numerical experiments

In this section, we give four test examples to verify our theoretical error estimates. Initially, we employ uniform triangular meshes. For numerical computation, the characteristic part is calculated by the high-order accurate Gauss quadrature points, for example, we choose the Gauss quadrature rule with 3 nodes when $k = 1$ and the Gauss quadrature rule with 7 nodes when $k = 2$. The CLDG scheme is performed with $(\mathbb{P}^k, \mathbb{P}^k, \mathbb{P}^k)$ finite element pair $(k \geq 1)$. The time stepsize is taken as $\Delta t = \mathcal{O}(h)$ for the local $\mathbb{P}^1$-DG scheme and $\Delta t = \mathcal{O}(h^2)$ for the local $\mathbb{P}^2$-DG scheme. In Tabels 2.1-2.6 the k denotes the degree of approximation polynomials. Comparing the numerical solutions with the constructed analytical ones, we show that the suboptimal convergence rates are obtained for the presented numerical scheme with a wide range of Reynolds numbers, such as $Re = 10, 10^2, 10^3, 10^4, 10^6, 10^8, 10^{12}, 10^{15}, 10^{16}$. One of the striking benefits of the proposed numerical scheme is that with the refining of the meshes the conditional number of the matrix A of the equation $Ax = b$ corresponding to the numerical scheme almost does not increase.

In Figures 2.1-2.4, we numerically display one of the striking benefits of the proposed scheme: the condition number of the corresponding matrix equation almost does not increase with the refining of the meshes for different Reynolds numbers. Here the nodal discontinuous Galerkin methods [33] are used to simulate the numerical examples.

Fig. 2.1: Condition number of the corresponding matrix for the CLDG scheme for (2.9) vs the reciprocal of spatial step h with $\Delta t = 10^{-3}, Re = 10^6$.

Fig. 2.2: Condition number of the corresponding matrix for the CLDG scheme for (2.9) vs the reciprocal of spatial step h with $\Delta t = 10^{-3}, Re = 10^{12}$.

Fig. 2.3: Condition number of the corresponding matrix for the CLDG scheme for (2.9) vs the reciprocal of spatial step h with $\Delta t = 10^{-2}, Re = 10^{8}$.
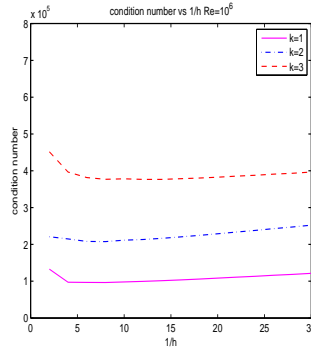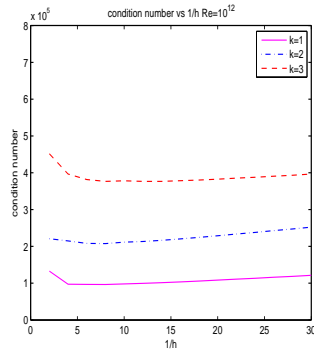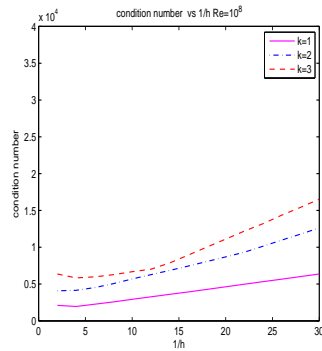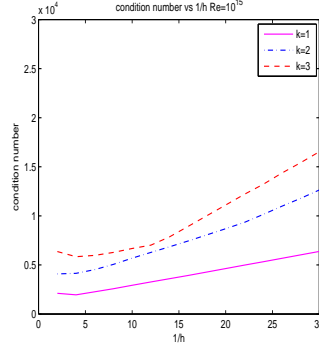
Fig. 2.4: Condition number of the corresponding matrix for the CLDG scheme for (2.9) vs the reciprocal of spatial step h with $\Delta t = 10^{-2}, Re = 10^{15}$.

Example 2.1. Consider the time-dependent incompressible Navier-Stokes equations in a square domain $\Omega = [-1, 1]^2$. We choose the initial data so that the exact solution is specified as

$$\begin{cases} u_1(\boldsymbol{x}, t) = \frac{1}{4} e^{\nu t} y(y^2 - 1)(x^2 - 1)^2, \\ u_2(\boldsymbol{x}, t) = -\frac{1}{4} e^{\nu t} x(x^2 - 1)(y^2 - 1)^2, \\ p(\boldsymbol{x}, t) = e^{\nu t}(x^2 - 1)(y^2 - 1). \end{cases} \tag{2.47}$$

Then the exact solution has homogenous boundary value and the forcing term $\boldsymbol{f}$ can be determined for any given ν. Tables 2.1-2.3 display the L^2-norm errors and convergence rates of velocity and pressure for Example 2.1 at time $T = 0.25$ with different choices of Reynolds numbers, such as $Re = 10^3, 10^6, 10^{12}$.

h	$k = 1$		$k = 2$		$k = 1$		$k = 2$	
	$\| \boldsymbol{e_u} \|_0$	$rate$	$\| \boldsymbol{e_u} \|_0$	$rate$	$\| e_p \|_0$	$rate$	$\| e_p \|_0$	$rate$
1/2	7.33e-02	–	2.18e-02	–	7.44e-01	–	9.23e-02	–
1/4	3.01e-02	1.3	6.17e-03	1.8	1.71e-01	2.1	7.60e-03	3.6
1/8	1.17e-02	1.4	8.07e-04	2.9	3.96e-02	2.1	9.11e-04	3.1
1/16	3.27e-03	1.8	1.11e-04	2.9	9.10e-03	2.1	1.17e-04	3.0
1/32	8.49e-04	2.0	1.42e-05	3.0	2.14e-03	2.1	1.50e-05	3.0

Tab. 2.1: The L^2-norm errors and convergence rates of velocity and pressure for Example 2.1 with $T = 0.25$, $Re = 10^3$.

43

h	$k=1$		$k=2$		$k=1$		$k=2$	
	$\parallel \boldsymbol{e_u} \parallel_0$	$rate$	$\parallel \boldsymbol{e_u} \parallel_0$	$rate$	$\parallel e_p \parallel_0$	$rate$	$\parallel e_p \parallel_0$	$rate$
1/2	7.34e-02	–	2.18e-02	–	7.44e-01	–	9.23e-02	–
1/4	3.02e-02	1.3	6.24e-03	1.8	1.71e-01	2.1	7.60e-03	3.6
1/8	1.18e-02	1.4	8.38e-04	2.9	3.97e-02	2.1	9.11e-04	3.1
1/16	3.38e-03	1.8	1.25e-04	2.7	9.13e-03	2.1	1.16e-04	3.0
1/32	9.05e-04	1.9	2.06e-05	2.6	2.15e-03	2.1	1.48e-05	2.0

Tab. 2.2: The L^2-norm errors and convergence rates of velocity and pressure for Example 2.1 with $T = 0.25$, $Re = 10^6$.

h	$k=1$		$k=2$		$k=1$		$k=2$	
	$\parallel \boldsymbol{e_u} \parallel_0$	$rate$	$\parallel \boldsymbol{e_u} \parallel_0$	$rate$	$\parallel e_p \parallel_0$	$rate$	$\parallel e_p \parallel_0$	$rate$
1/2	7.34e-02	–	2.18e-02	–	7.44e-01	–	9.23e-02	–
1/4	3.02e-02	1.3	6.24e-03	1.8	1.71e-01	2.1	7.60e-03	3.6
1/8	1.18e-02	1.4	8.38e-04	2.9	3.97e-02	2.1	9.11e-04	3.1
1/16	3.38e-03	1.8	1.25e-04	2.7	9.13e-03	2.1	1.16e-04	3.0
1/32	9.05e-04	1.9	2.06e-05	2.6	2.15e-03	2.1	1.48e-05	3.0

Tab. 2.3: The L^2-norm errors and convergence rates of velocity and pressure for Example 2.1 with $T = 0.25$, $Re = 10^{12}$.

Figures 2.5-2.10 display the contour figures of exact and numerical solutions. We observe that the numerical solutions have efficient simulations with high Reynolds's number $Re = 10^{12}$.

Fig. 2.5: The contour of exact solution $u_1(t = 0.25)$ of Example 2.1, $Re = 10^{12}$.

Fig. 2.6: The contour of numerical solution $u_{1h}(t = 0.25)$ of Example 2.1, $Re = 10^{12}$.

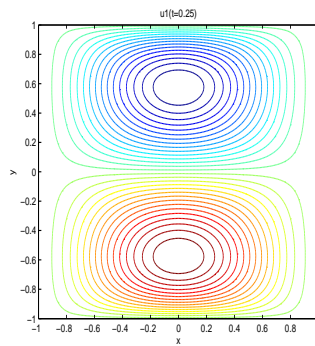

Fig. 2.7: The contour of exact solution $u_2(t = 0.25)$ of Example 2.1, $Re = 10^{12}$.
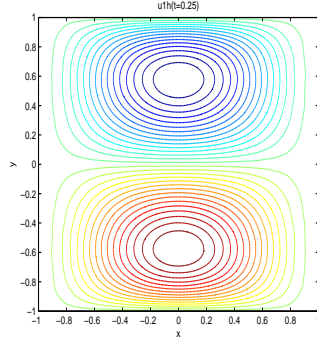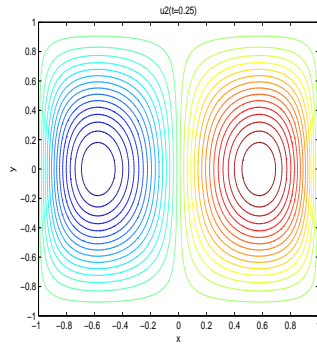

Fig. 2.8: The contour of numerical solution $u_{2h}(t = 0.25)$ of Example 2.1, $Re = 10^{12}$.

Fig. 2.9: The contour of exact solution $p(t = 0.25)$ of Example 2.1, $Re = 10^{12}$.

Fig. 2.10: The contour of numerical solution $p_h(t = 0.25)$ of Example 2.1, $Re = 10^{12}$.

Example 2.2. We further verify theoretical results of the CLDG scheme (2.9) in the domain $\Omega = [0, 1]^2$ for the exact solution defined by

$$\begin{cases} u_1(\boldsymbol{x}, t) = cos(\nu t)sin^2(\pi x)sin(2\pi y), \\ u_2(\boldsymbol{x}, t) = -cos(\nu t)sin(2\pi x)sin^2(\pi y), \\ \quad p(\boldsymbol{x}, t) = cos(\nu t)sin(2\pi x)sin(2\pi y). \end{cases} \qquad (2.48)$$

The forcing term $\boldsymbol{f}$ can be determined for any given ν. In Tables 2.4-2.6, we choose big Reynolds numbers to demonstrate the efficiency of the presented scheme, such as $Re = 10^3, 10^8, 10^{15}$. Note that errors and convergence rates for both velocity and pressure almost do not change with $Re = 10^8, Re = 10^{15}$, since $cos(\nu t)$ does not change when ν is small enough (corresponding Re big enough). Comparing with the errors and convergence rates for Example 2.1, even the errors and the convergence rates are

46

not as good as Example 2.1, they still coincide with theoretical results. In order to further observe the simulations of numerical solutions, we compare the figures of exact and numerical solutions with $Re = 10^{15}$ in Figures 2.11-2.16.

h	$k = 1$		$k = 2$		$k = 1$		$k = 2$	
	$\| e_u \|_0$	$rate$	$\| e_u \|_0$	$rate$	$\| e_p \|_0$	$rate$	$\| e_p \|_0$	$rate$
1/4	8.15e-02	–	4.63e-02	–	2.11e-01	–	3.26e-02	–
1/8	3.88e-02	1.1	4.51e-03	3.4	4.17e-02	2.3	6.10e-03	2.4
1/16	1.35e-02	1.5	5.67e-04	3.0	9.89e-02	2.1	1.05e-03	2.5
1/32	5.45e-03	1.3	1.01e-04	2.5	4.37e-03	1.2	2.34e-04	2.2

Tab. 2.4: The L^2-norm errors and convergence rates of velocity and pressure for Example 2.2 with $T = 0.5$, $Re = 10^2$.

h	$k = 1$		$k = 2$		$k = 1$		$k = 2$	
	$\| e_u \|_0$	$rate$	$\| e_u \|_0$	$rate$	$\| e_p \|_0$	$rate$	$\| e_p \|_0$	$rate$
1/4	1.08e-01	–	1.13e-01	–	2.10e-01	–	4.91e-02	–
1/8	7.65e-02	0.5	1.72e-02	2.7	4.02e-02	2.4	1.29e-02	1.9
1/16	2.95e-02	1.4	2.93e-03	2.6	1.79e-02	1.2	3.17e-03	2.0
1/32	1.33e-02	1.1	1.01e-03	1.5	1.10e-02	0.7	7.38e-04	2.1

Tab. 2.5: The L^2-norm errors and convergence rates of velocity and pressure for Example 2.2 with $T = 0.5$, $Re = 10^8$.

h	$k = 1$		$k = 2$		$k = 1$		$k = 2$	
	$\| e_u \|_0$	$rate$	$\| e_u \|_0$	$rate$	$\| e_p \|_0$	$rate$	$\| e_p \|_0$	$rate$
1/4	1.08e-01	–	1.13e-01	–	2.10e-01	–	4.91e-02	–
1/8	7.65e-02	0.5	1.72e-02	2.7	4.02e-02	2.4	1.29e-02	1.9
1/16	2.91e-02	1.4	2.93e-03	2.6	1.80e-02	1.2	3.17e-03	2.0
1/32	1.33e-02	1.1	1.01e-03	1.5	1.10e-02	0.7	7.38e-04	2.1

Tab. 2.6: The L^2-norm errors and convergence rates of velocity and pressure for Example 2.2 with $T = 0.5$, $Re = 10^{15}$.

Fig. 2.11: Exact solution $u_1(t = 1)$ of Example 2.2, $Re = 10^{15}$.

Fig. 2.12: Numerical solution $u_{1h}(t = 1)$ of Example 2.2, $Re = 10^{15}$.

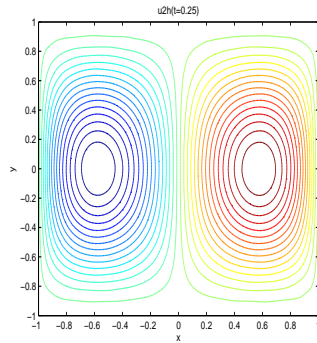Fig. 2.13: Exact solution $u_2(t = 1)$ of Example 2.2, $Re = 10^{15}$.

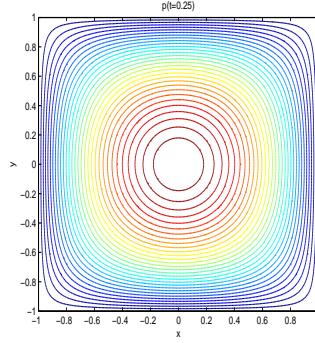Fig. 2.14: Numerical solution $u_{2h}(t = 1)$ of Example 2.2, $Re = 10^{15}$.

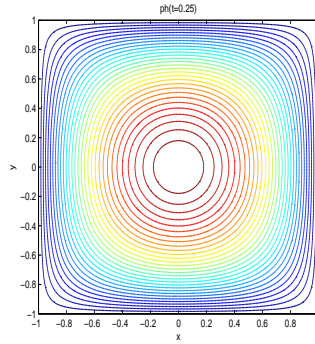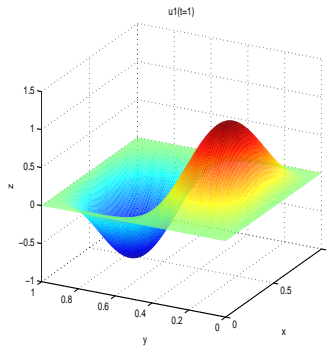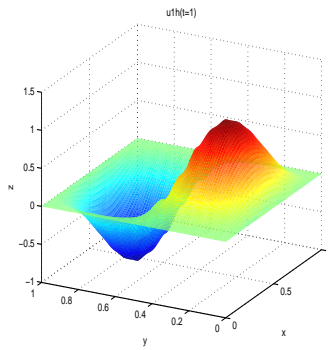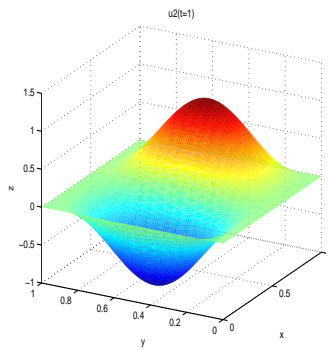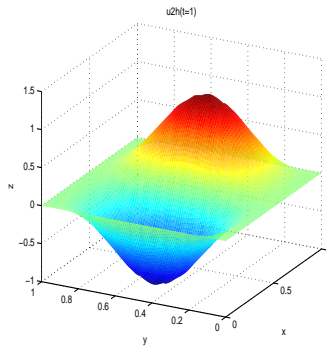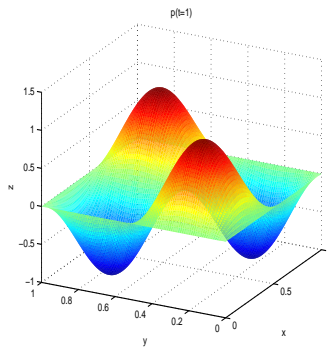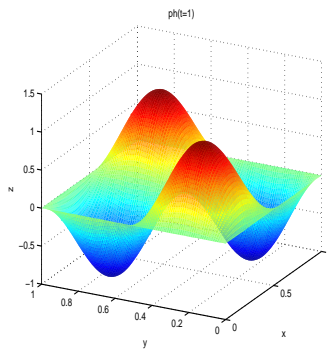Fig. 2.15: Exact solution $p(t = 1)$ of Example 2.2, $Re = 10^{15}$.

Fig. 2.16: Numerical solution $p_h(t = 1)$ of Example 2.2, $Re = 10^{15}$.

49

Example 2.3. In this example we consider the exact solution with nonsymmetric formulas in the domain $[0,1]^2$. The exact solution is specified as

$$\begin{cases} u_1(\boldsymbol{x},t) = \omega(t)\sin^2(\pi x)(2y - 6y^2 + 4y^3), \\ u_2(\boldsymbol{x},t) = -\omega(t)\pi\sin(2\pi x)(y^2 - 2y^3 + y^4), \\ p(\boldsymbol{x},t) = \frac{\partial_t\omega(t)}{2\pi\nu}y\cos(\frac{\pi y}{2})(x-1)^3(e^x - 1), \end{cases} \tag{2.49}$$

where $\omega(t) = 1 + \sin(2\pi\nu t)$.

In Tables 2.7-2.9, we choose the exact solution of problem (2.1) with nonsymmetric formulas for both velocity and pressure because in above two examples the exact solutions have symmetric formulas with respect to variables x and y. In simulations, we use more general triangular meshes (i.e. not the meshes with uniform triangulation of squares). Note that the errors and rates change when $Re = 10, 10^4, 10^{16}$ at time $T = 1$, but they still have some good results.

h	$k=1$		$k=2$		$k=1$		$k=2$	
	$\| \boldsymbol{e_u} \|_0$	$rate$	$\| \boldsymbol{e_u} \|_0$	$rate$	$\| e_p \|_0$	$rate$	$\| e_p \|_0$	$rate$
1/5	1.12e-02	–	1.84e-03	–	6.01e-03	–	1.04e-03	–
1/10	2.78e-03	2.0	1.70e-04	3.4	1.41e-03	2.1	9.98e-05	3.4
1/20	7.01e-04	2.0	2.19e-05	3.0	3.33e-04	2.1	1.52e-05	2.7
1/40	2.00e-04	1.8	3.82e-06	2.5	8.83e-05	1.9	4.00e-06	1.9

Tab. 2.7: The L^2-norm errors and convergence rates of velocity and pressure for Example 2.3 with $T = 0.5$, $Re = 10^2$.

h	$k=1$		$k=2$		$k=1$		$k=2$	
	$\| \boldsymbol{e_u} \|_0$	$rate$	$\| \boldsymbol{e_u} \|_0$	$rate$	$\| e_p \|_0$	$rate$	$\| e_p \|_0$	$rate$
1/5	1.05e-02	–	2.76e-03	–	5.37e-03	–	8.87e-04	–
1/10	2.81e-03	1.9	5.15e-04	2.4	1.05e-03	2.4	8.84e-05	3.3
1/20	6.99e-04	2.0	1.02e-04	2.3	2.18e-04	2.3	1.74e-05	2.3
1/40	2.17e-04	1.7	2.08e-05	2.3	4.86e-05	2.2	5.90e-06	1.6

Tab. 2.8: The L^2-norm errors and convergence rates of velocity and pressure for Example 2.3 with $T = 0.5$, $Re = 10^8$.

h	$k=1$		$k=2$		$k=1$		$k=2$	
	$\parallel \boldsymbol{e_u} \parallel_0$	$rate$	$\parallel \boldsymbol{e_u} \parallel_0$	$rate$	$\parallel e_p \parallel_0$	$rate$	$\parallel e_p \parallel_0$	$rate$
$1/5$	1.05e-02	$-$	2.76e-03	$-$	5.37e-03	$-$	8.87e-04	$-$
$1/10$	2.81e-03	1.9	5.15e-04	2.4	1.05e-03	2.4	8.84e-05	3.3
$1/20$	6.99e-04	2.0	1.02e-04	2.3	2.18e-04	2.3	1.74e-05	2.3
$1/40$	2.17e-04	1.7	2.08e-05	2.3	4.86e-05	2.2	5.90e-06	1.6

Tab. 2.9: The L^2-norm errors and convergence rates of velocity and pressure for Example 2.3 with $T = 0.5$, $Re = 10^{15}$.
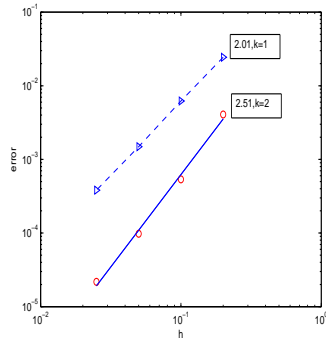
Fig. 2.17: Error and rate of velocity in Example 2.3, $Re = 10$.
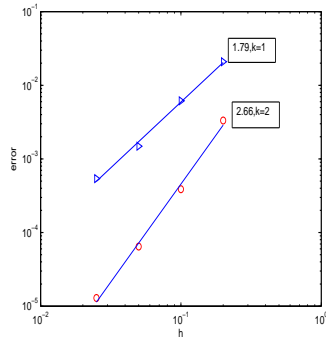
Fig. 2.18: Error and rate of pressure in Example 2.3, $Re = 10$.
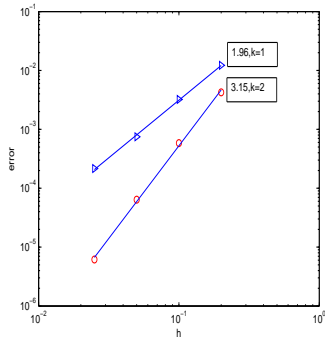
Fig. 2.19: Error and rate of velocity in Example 2.3, $Re = 10^4$.
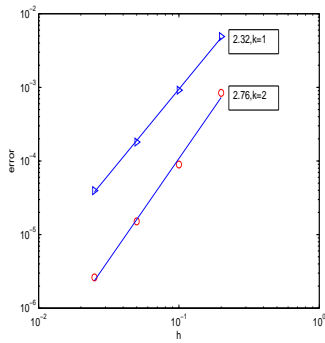
Fig. 2.20: Error and rate of pressure in Example 2.3, $Re = 10^4$.
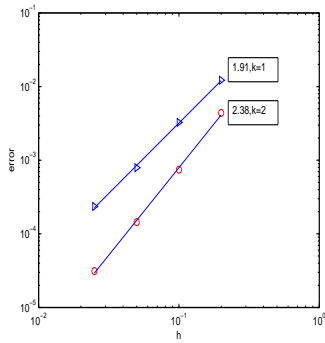
Fig. 2.21: Error and rate of velocity in Example 2.3, $Re = 10^{16}$.
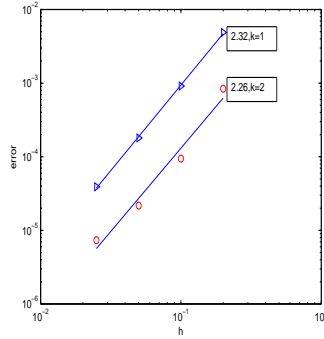
Fig. 2.22: Error and rate of pressure in Example 2.3, $Re = 10^{16}$.

Example 2.4. In this example we will consider discontinuous solution in the domain $[-1, 1]^2$. The exact solution is specified as

$$u_1(\boldsymbol{x}, t) = \begin{cases} -e^{-4\pi^2\nu t}\sin(2\pi y), & \text{if } |x| < 0.5, |y| < 0.5, \\ 0, & \text{else}, \end{cases}$$

$$u_2(\boldsymbol{x}, t) = \begin{cases} e^{-4\pi^2\nu t}\sin(2\pi x), & \text{if } |x| < 0.5, |y| < 0.5, \\ 0, & \text{else}, \end{cases}$$

$$p(\boldsymbol{x}, t) = \begin{cases} e^{-8\pi^2\nu t}\sin(2\pi x)\sin(2\pi y), & \text{if } |x| < 0.5, |y| < 0.5, \\ 0, & \text{else}. \end{cases}$$

The force function f can be determined by any ν according to the above solution.

In this example, we choose the discontinuous solution to show the advantage of discontinuous Galerkin method comparing with continuous finite element method that discontinuous Galerkin method can simulate the discontinuous solutions very well. From the Figures 2.17-2.22, we give the figures of exact and numerical ones to compare. Note that the simulations can display the discontinuous parts and separate different values clearly. Even for the pressure p, it still has a good approximation. Figures 2.23-2.25, display the contour figures of numerical solutions to validate the efficiency of the CLDG scheme we proposed.

h	$k = 1$	$k = 2$	$k = 1$	$k = 2$
	$\parallel \boldsymbol{e_u} \parallel_0$	$\parallel \boldsymbol{e_u} \parallel_0$	$\parallel e_p \parallel_0$	$\parallel e_p \parallel_0$
1/4	2.93e-01	3.65e-01	6.08e-01	5.06e-01
1/8	3.37e-01	3.69e-01	5.11e-01	4.50e-01
1/16	3.59e-01	3.73e-01	4.73e-01	4.23e-01
1/32	3.68e-01	3.74e-01	4.60e-01	4.11e-01

Tab. 2.10: The L^2-norm errors and convergence rates of velocity and pressure for Example 2.4 with $T = 0.05$, $Re = 10^2$.

h	$k = 1$	$k = 2$	$k = 1$	$k = 2$
	$\parallel \boldsymbol{e_u} \parallel_0$	$\parallel \boldsymbol{e_u} \parallel_0$	$\parallel e_p \parallel_0$	$\parallel e_p \parallel_0$
1/4	2.99e-01	3.71e-01	6.31e-01	5.25e-01
1/8	3.42e-01	3.77e-01	5.33e-01	4.70e-01
1/16	3.66e-01	3.80e-01	4.89e-01	4.43e-01
1/32	3.75e-01	3.81e-01	4.60e-01	4.30e-01

Tab. 2.11: The L^2-norm errors of velocity and pressure for Example 2.4 with $T = 0.05$, $Re = 10^8$.
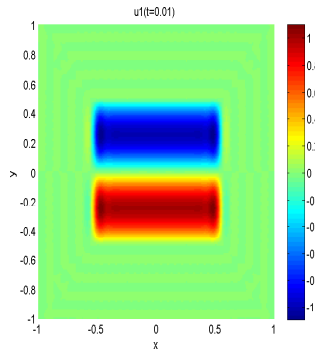
Fig. 2.23: Exact solution $u_1(t = 0.01)$ of Example 2.4, $Re = 10^8$.
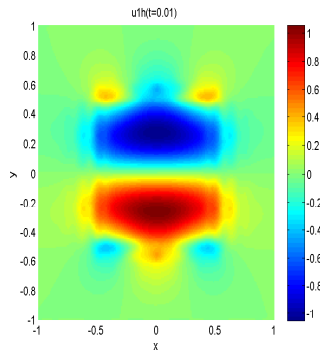
Fig. 2.24: Numerical solution $u_{1h}(t = 0.01)$ of Example 2.4, $Re = 10^8$.
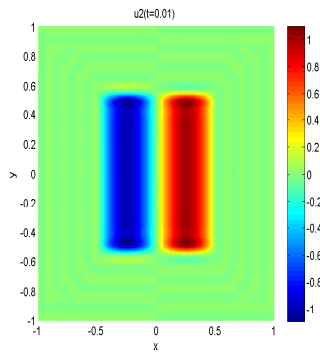
Fig. 2.25: Exact solution $u_2(t = 0.01)$ of Example 2.4, $Re = 10^8$.
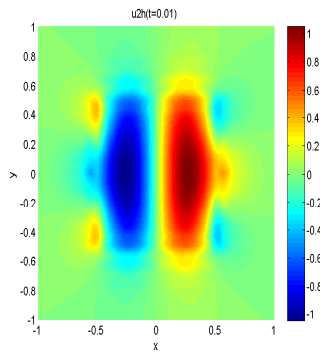
Fig. 2.26: Numerical solution $u_{2h}(t = 0.01)$ of Example 2.4, $Re = 10^8$.
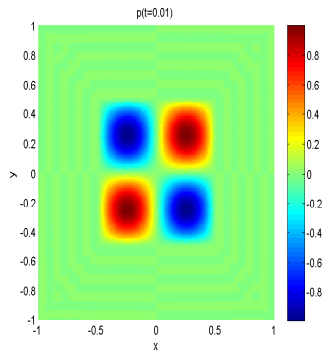
Fig. 2.27: Exact solution $p(t = 0.01)$ of Example 2.4, $Re = 10^8$.
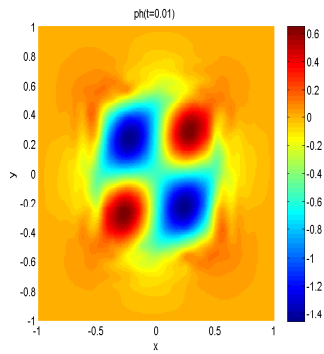
Fig. 2.28: Numerical solution $p_h(t = 0.01)$ of Example 2.4, $Re = 10^8$.
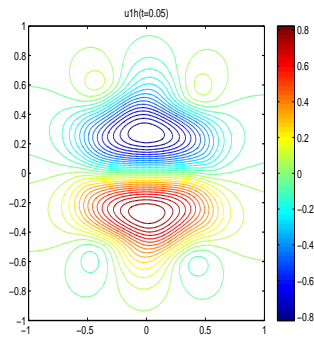
Fig. 2.29: The contour of numerical solution $u_{1h}(t = 0.05)$ of Example 2.4, $Re = 10$.
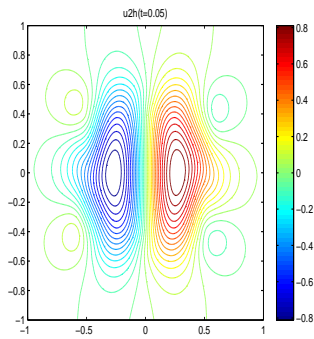
Fig. 2.30: The contour of numerical solution $u_{2h}(t = 0.05)$ of Example 2.4, $Re = 10$.
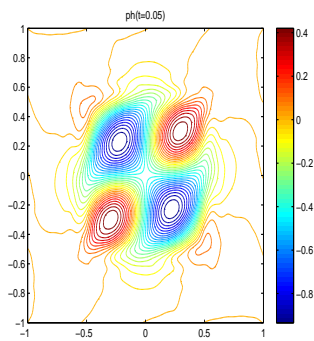
Fig. 2.31: The contour of numerical solution $p_h(t = 0.05)$ of Example 2.4, $Re = 10$.

Chapter 3

HDG method for fractional convection-diffusion equations

3.1 Fractional convection-diffusion problem

Here, we shall consider time-dependent space-fractional convection-diffusion problem for u in the form:

$$\begin{cases} \partial_t u + \boldsymbol{b} \cdot \nabla u - c_1 \frac{\partial^\alpha u}{\partial x^\alpha} - c_2 \frac{\partial^\beta u}{\partial y^\beta} = f, & (\boldsymbol{x}, t) \in \Omega \times J, \\ u(\boldsymbol{x}, t) = 0, & (\boldsymbol{x}, t) \in \partial\Omega \times J, \\ u(\boldsymbol{x}, 0) = u_0(\boldsymbol{x}), & \boldsymbol{x} \in \Omega, \end{cases} \qquad (3.1)$$

where $\Omega = (a, b) \times (c, d)$ and $J = [0, T]$ with the superdiffusion operators defined by operators $\frac{\partial^\alpha u}{\partial x^\alpha}$ and $\frac{\partial^\beta u}{\partial y^\beta}, 1 < \alpha, \beta \le 2$. The function $f(\boldsymbol{x}, t) \in L^2(J; L^2(\Omega))$ is a source term, the diffusion coefficients c_1 and c_2 are supposed to be positive constants, the convection coefficient $\boldsymbol{b}(\boldsymbol{x}, t)$ is bounded vector function, and the solution u is also supposed to satisfy $u \in L^\infty(J; H^2(\Omega)), \partial_t u \in L^2(J; H^1(\Omega)), \partial_{tt} u \in L^2(J; L^2(\Omega)), u_0 \in L^2(\Omega)$.

3.2 Fractional norms in variational norms

Lemma 3.1. *[26, 59] Suppose that $u(x)$ is a function defined in the interval (a, b). If $u^{(k)}(x) = 0$, when $x = a$ or $x = b$, $\forall\, 0 \le k \le n - 1$, then for $n - 1 < \nu < n, n \in N^+$, the*

58

following hold

$$_aD_x^\nu u(x) = D^n {}_a\mathcal{I}_x^{n-\nu} u(x) = {}_a\mathcal{I}_x^{n-\nu}\big(D^n u(x)\big),$$

$$_xD_b^\nu u(x) = (-D)^n {}_x\mathcal{I}_b^{n-\nu} u(x) = {}_x\mathcal{I}_b^{n-\nu}\big((-D)^n u(x)\big).$$

Note that, from Definition 1.2, Definition 1.3 and Lemma 3.1 if the solution u of (3.1) satisfies $u^{(k)}(x,y) = 0, k = 0, 1$ when $x = a$ or $y = c$, then for any $1 < \alpha, \beta \leq 2$, the fractional derivatives of function $u(x,y)$ on $\Omega = (a,b) \times (c,d)$ can be rewritten as (see [47, 59]):

$$\frac{\partial^\alpha u}{\partial x^\alpha} = \frac{\partial^2}{\partial x^2}\mathcal{I}_x^{2-\alpha}u(x,y) = \frac{\partial}{\partial x}{}_a\mathcal{I}_x^{2-\alpha}\big(\frac{\partial}{\partial x}u(x,y)\big) = {}_a\mathcal{I}_x^{2-\alpha}\big(\frac{\partial^2}{\partial x^2}u(x,y)\big), \qquad (3.2)$$

$$\frac{\partial^\beta u}{\partial y^\beta} = \frac{\partial^2}{\partial y^2}\mathcal{I}_y^{2-\beta}u(x,y) = \frac{-\partial}{\partial y}{}_c\mathcal{I}_y^{2-\beta}\big(\frac{-\partial}{\partial y}u(x,y)\big) = {}_c\mathcal{I}_y^{2-\beta}\big(\frac{\partial^2}{\partial y^2}u(x,y)\big). \qquad (3.3)$$

Definition 3.1. [26] (The left and right fractional spaces) For $0 < \mu < 1$, extend $u(x)$ outside of $\mathfrak{I} := (a,b)$ by zero. Then define the norm

$$\| u \|_{J_L^{-\mu}(\mathbb{R})} := \|_{-\infty}\mathcal{I}_x^\mu u \|_{L^2(\mathbb{R})}, \qquad (3.4)$$

$$\| u \|_{J_R^{-\mu}(\mathbb{R})} := \|_x\mathcal{I}_\infty^\mu u \|_{L^2(\mathbb{R})} . \qquad (3.5)$$

Let the two spaces $J_L^{-\mu}(\mathbb{R})$ and $J_R^{-\mu}(\mathbb{R})$ denote the closures of $C_0^\infty(\mathbb{R})$ with respect to $\| \cdot \|_{J_L^{-\mu}}$ and $\| \cdot \|_{J_R^{-\mu}}$, respectively.

Lemma 3.2. *[26, 28, 59] For $\mu > 0$, assume that $u(x)$ is a real function. Then*

$$(_{-\infty}\mathcal{I}_x^\mu u, {}_x\mathcal{I}_\infty^\mu) = cos(\mu\pi) \| u \|_{J_L^{-\mu}(\mathbb{R})}^2 = cos(\mu\pi) \| u \|_{J_R^{-\mu}(\mathbb{R})}^2 . \qquad (3.6)$$

Generally, we consider the case in which the problem in a bounded domain instead of $\mathbb{R}$. Then, we restrict the definitions to $\mathfrak{I} = (a,b)$.

Definition 3.2. [26, 59] Define the spaces $J_{L,0}^{-\mu}(\mathfrak{I})$ and $J_{R,0}^{-\mu}(\mathfrak{I})$ as the closures of $C_0^\infty(\mathfrak{I})$ under their norms.

Theorem 3.3. *[26, 59] If $-\mu_2 < -\mu_1 < 0$, then $J_{L,0}^{-\mu_1}(\mathfrak{I})$ and $J_{R,0}^{-\mu_1}(\mathfrak{I})$ are embedded into $J_{L,0}^{-\mu_2}(\mathfrak{I})$ and $J_{R,0}^{-\mu_2}(\mathfrak{I})$, respectively. Furthermore, $L^2(\mathfrak{I})$ is embedded into both of*

them.

Definition 3.3. [26, 59] By Lemma 1, Lemma 3.2, Definition 3.1 and Definition 3.2, there are

$$\int_c^d ({}_a\mathcal{I}_x^{2-\alpha}u(\cdot,y),u(\cdot,y))_{L^2(a,b)}dy = cos(\alpha_1\pi)\int_c^d \|u(\cdot,y)\|^2_{J_{R,0}^{-\alpha_1}(a,b)}dy, \qquad (3.7)$$

$$\int_a^b ({}_c\mathcal{I}_y^{2-\beta}u(x,\cdot),u(x,\cdot))_{L^2(c,d)}dx = cos(\beta_1\pi)\int_a^b \|u(x,\cdot)\|^2_{J_{R,0}^{-\beta_1}(c,d)}dx, \qquad (3.8)$$

where the spaces $J_{R,0}^{-\alpha_1}(a,b)$ and $J_{R,0}^{-\beta_1}(c,d)$ are the closures of $\mathcal{C}_0^\infty(a,b)$ and $\mathcal{C}_0^\infty(c,d)$ under their norms, respectively, and $\alpha_1 = 1 - \frac{\alpha}{2}, \beta_1 = 1 - \frac{\beta}{2}, 0 \le \alpha_1,\beta_1 < \frac{1}{2}$.

Remark 3.1. It follows from Theorem 3.3 that

$$\int_c^d \|u(\cdot,y)\|^2_{J_{R,0}^{-(2-\alpha)}(a,b)}dy \le C\int_c^d \|u(\cdot,y)\|^2_{J_{R,0}^{-\alpha_1}(a,b)}dy,$$

$$\int_a^b \|u(x,\cdot)\|^2_{J_{R,0}^{-(2-\beta)}(c,d)}dx \le C\int_a^b \|u(x,\cdot)\|^2_{J_{R,0}^{-\beta_1}(c,d)}dx,$$

where C is a generic constant.

3.3 Derivation of numerical scheme

We focus on deriving the fully discrete numerical scheme of two dimensional (2D) space-fractional convection-diffusion equations.

As Ref. [11], let $\psi(\boldsymbol{x},t) = (1 + |\boldsymbol{b}(\boldsymbol{x},t)|^2)^{\frac{1}{2}}$, where $|\boldsymbol{b}(\boldsymbol{x},t)|^2 = b_1^2 + b_2^2$. Hence, the characteristic direction associated with $\partial_t u + \boldsymbol{b} \cdot \nabla u$ is denoted by $\partial_\tau = \frac{\partial_t}{\psi} + \frac{\boldsymbol{b}\cdot\nabla}{\psi}$. Then the original equation of (3.1) can be rewritten as a mixed form [21, 26, 59]:

$$\begin{cases} \psi\partial_\tau u - \nabla \cdot \boldsymbol{\sigma} = f(\boldsymbol{x},t), & (\boldsymbol{x},t) \in \Omega \times J, \\ \boldsymbol{\sigma} - (c_1{}_a\mathcal{I}_x^{2-\alpha}p_x, c_2{}_c\mathcal{I}_y^{2-\beta}p_y) = 0, & (\boldsymbol{x},t) \in \Omega \times J, \\ \boldsymbol{p} - \nabla u = 0, & (\boldsymbol{x},t) \in \Omega \times J, \\ u(\boldsymbol{x},t) = 0, & (\boldsymbol{x},t) \in \partial\Omega \times J, \\ u(\boldsymbol{x},0) = u_0(\boldsymbol{x}), & \boldsymbol{x} \in \Omega, \end{cases} \qquad (3.9)$$

where $_a\mathcal{I}_x^{2-\alpha}$ and $_c\mathcal{I}_y^{2-\beta}$ are fractional operators of Definition 1.1.

For an arbitrary subset $E \in \mathcal{E}_h$, we multiply the first, second, and the third equation of (3.9) by the smooth test functions $(v, \boldsymbol{\tau}, \boldsymbol{q})$, respectively. In order to obtain a symmetric weak variational formulation, we only integrate the first equation of (3.9) by parts, and obtain

$$
\begin{cases}
\int_E \psi \partial_\tau u v d\boldsymbol{x} + \int_E \boldsymbol{\sigma} \cdot \nabla v d\boldsymbol{x} - \int_{\partial E} \boldsymbol{\sigma} \cdot \boldsymbol{n}_E v ds = \int_E f v d\boldsymbol{x}, \\[3mm]
\int_E \boldsymbol{\sigma} \cdot \boldsymbol{\tau} d\boldsymbol{x} - \int_E (c_1 {_a\mathcal{I}_x^{2-\alpha}} p_x, c_2 {_c\mathcal{I}_y^{2-\beta}} p_y) \cdot \boldsymbol{\tau} d\boldsymbol{x} = 0, \\[3mm]
\int_E \boldsymbol{p} \cdot \boldsymbol{q} d\boldsymbol{x} - \int_E \nabla u \cdot \boldsymbol{q} d\boldsymbol{x} = 0,
\end{cases}
\tag{3.10}
$$

where $\boldsymbol{n}_E$ is the outward unit normal to ∂E. Note that the above equations are well defined by any functions $(u, \boldsymbol{\sigma}, \boldsymbol{p})$ and $(v, \boldsymbol{\tau}, \boldsymbol{q})$ in $V \times \mathbf{Q} \times \mathbf{Q}$, where

$$
\begin{aligned}
V &= \Big\{ u \in L^2(\Omega) : u|_E \in H^1(E), \ \forall E \in \mathcal{E}_h \Big\}, \\
\mathbf{Q} &= \Big\{ \boldsymbol{p} \in (L^2(\Omega))^2 : \boldsymbol{p}|_E \in (H^1(E))^2, \ \forall E \in \mathcal{E}_h \Big\}.
\end{aligned}
$$

Next we will approximate the exact solution $(u, \boldsymbol{\sigma}, \boldsymbol{p})$ with the functions $(u_h, \boldsymbol{\sigma}_h, \boldsymbol{p}_h)$ in the finite element spaces $V_h \times \mathbf{Q}_h \times \mathbf{Q}_h \subset V \times \mathbf{Q} \times \mathbf{Q}$, where

$$
\begin{aligned}
V_h &= \Big\{ u_h \in L^2(\Omega) : u_h|_E \in \mathbb{P}^k(E), \ \ \forall E \in \mathcal{E}_h \Big\}, \\
\mathbf{Q}_h &= \Big\{ \boldsymbol{p}_h \in (L^2(\Omega))^2 : \boldsymbol{p}_h|_E \in (\mathbb{P}^k(E))^2, \ \ \forall E \in \mathcal{E}_h \Big\},
\end{aligned}
$$

where the finite element space $\mathbb{P}^k(E)$ denotes the set of polynomials of degree less than or equal to $k \geq 0$.

Thus, the approximate solution $(u_h, \boldsymbol{\sigma}_h, \boldsymbol{p}_h)$ satisfies the weak formulation, for all $(v, \boldsymbol{\tau}, \boldsymbol{q}) \in V_h \times \mathbf{Q}_h \times \mathbf{Q}_h$ such that

$$
\begin{cases}
\int_E \psi \partial_\tau u_h v d\boldsymbol{x} + \int_E \boldsymbol{\sigma}_h \cdot \nabla v d\boldsymbol{x} - \int_{\partial E} \boldsymbol{\sigma}_h^\star \cdot \boldsymbol{n}_E v ds = \int_E f v d\boldsymbol{x}, \\[3mm]
\int_E \boldsymbol{\sigma}_h \cdot \boldsymbol{\tau} d\boldsymbol{x} - \int_E (c_1 {_a\mathcal{I}_x^{2-\alpha}} p_{xh}, c_2 {_c\mathcal{I}_y^{2-\beta}} p_{yh}) \cdot \boldsymbol{\tau} d\boldsymbol{x} = 0, \\[3mm]
\int_E \boldsymbol{p}_h \cdot \boldsymbol{q} d\boldsymbol{x} - \int_E \nabla u_h \cdot \boldsymbol{q} d\boldsymbol{x} = 0,
\end{cases}
\tag{3.11}
$$

61

where the numerical fluxes are well chosen as $\boldsymbol{\sigma}_h^\star = \{\boldsymbol{\sigma}_h\}$, $\forall e \in \mathscr{E}_h^B$ in order to ensure the stability of the scheme and its accuracy.

It is well known that the fluxes $\boldsymbol{\sigma}_h^\star = \{\boldsymbol{\sigma}_h\}$ are consistent. By inspiration in penalty Galerkin methods [50], we naturally consider a fact that $[u]\big|_e = 0, \forall e \in \mathscr{E}_h^B$ and $[\boldsymbol{\sigma}] = 0, \forall e \in \mathscr{E}_h^i$. Therefore, a symmetric and stable DG scheme is obtained as following.

Substituting the flux $\boldsymbol{\sigma}_h^\star = \{\boldsymbol{\sigma}_h\}$ into equation (3.11), summing over all the elements, and adding the penalty terms, we observe that for $(u_h, \boldsymbol{\sigma}_h, \boldsymbol{p}_h) \in V_h \times \mathbf{Q}_h \times \mathbf{Q}_h$, the semi-discrete variational formulation is given by

$$
\begin{cases}
\left(\psi \partial_\tau u_h, v\right) + (\boldsymbol{\sigma}_h, \nabla v) - (\{\boldsymbol{\sigma}_h\} \cdot \boldsymbol{n}_e, [v])_{\mathscr{E}_h^B} + \epsilon_1([u_h], [v])_{\mathscr{E}_h^B} = (f, v), \\[2ex]
(\boldsymbol{\sigma}_h, \boldsymbol{\tau}) - \left((c_1 \mathcal{I}_x^{2-\alpha} p_{xh}, c_2 \mathcal{I}_y^{2-\beta} p_{yh}), \boldsymbol{\tau}\right) = 0, \\[2ex]
(\boldsymbol{p}_h, \boldsymbol{q}) - (\nabla u_h, \boldsymbol{q}) + ([u_h], \{\boldsymbol{q}\} \cdot \boldsymbol{n}_e)_{\mathscr{E}_h^B} + \epsilon_2([\boldsymbol{\sigma}_h], [\boldsymbol{q}])_{\mathscr{E}_h^i} = 0.
\end{cases}
\tag{3.12}
$$

For any $(v, \boldsymbol{\tau}, \boldsymbol{q}) \in V_h \times \mathbf{Q}_h \times \mathbf{Q}_h$, the exact solution of (3.1) is expected to be at least continuous and differentiable, which keeps the consistency of the scheme. The term $([u], \{\boldsymbol{q}\} \cdot \boldsymbol{n}_e)_{\mathscr{E}_h^B}$ vanishes since the exact solution u satisfies $[u]\big|_e = 0, \forall e \in \mathscr{E}_h^B$. Note that $\epsilon_1([u], [v])_{\mathscr{E}_h^B}$ penalizes the jump in the function u, whereas $\epsilon_2([\boldsymbol{\sigma}], [\boldsymbol{q}])_{\mathscr{E}_h^i}$ penalizes the jump in the function $\boldsymbol{\sigma}$. Here ϵ_1 and ϵ_2 are chosen as positive numbers. Unfortunately the third equation of (3.12) loses the locality of discontinuous Galerkin method. Since $\boldsymbol{p}_h$ is function of u_h and $\boldsymbol{\sigma}_h$, $\boldsymbol{p}_h$ can not be eliminated from the third equation. Finally we have to obtain three unknowns u_h, p_{xh}, p_{yh} to be solved. Although such mixed DG method does not eliminate many unknowns of the hybridized DG method, our choice of fluxes makes the error analysis available.

Above and throughout this chapter, we use the notations

$$
(w, v) = \sum_{E \in \mathscr{E}_h} (w, v)_E, \quad (w, v)_{\mathscr{E}_h^i} = \sum_{e \in \mathscr{E}_h^i} (w, v)_e, \quad (w, v)_{\mathscr{E}_h^B} = \sum_{e \in \mathscr{E}_h^B} (w, v)_e.
$$

3.3.1 Dealing with time

We now discretize the time derivative with the method of characteristics based on hybridized discontinuous Galerkin method.

For each positive integer N, let $0 = t^0 < t^1 < \cdots < t^N = T$ be a uniform partition of J into subintervals $J^n = (t^{n-1}, t^n]$ with time step $\Delta t = t^n - t^{n-1}, 1 \le n \le N$. The characteristic tracing back along the field $\boldsymbol{b}$ of a point $\boldsymbol{x} \in \Omega$ at time t^n to t^{n-1} is

62

approximated by [11, 27]

$$\check{x}(x, t^{n-1}) = x - b(x, t^n)\Delta t.$$

Therefore, the approximation for the hyperbolic part of (3.1) at time t^n can be approximated as follows:

$$\psi^n \partial_\tau u^n \approx \frac{u^n - \check{u}^{n-1}}{\Delta t}, \quad \check{u}^{n-1} = u^{n-1}(\check{x}).$$

Remark 3.2. For the time truncation error, under the assumption of (3.17) and the assumption of the solution u of (3.1) (see [27]), there is

$$\| \psi^n \partial_\tau u^n - \frac{u^n - \check{u}^{n-1}}{\Delta t} \|_0^2 \leq C \| \psi^4 \|_{L^\infty(J;L^\infty(\Omega))} \| \partial_{\tau\tau} u \|_{L^2(J^n;L^2(\Omega))}^2 \Delta t.$$

Thus, the fully discrete scheme corresponding to the variational formulation of (3.12) is to find $(u_h^n, \sigma_h^n, p_h^n) \in V_h \times \mathbf{Q}_h \times \mathbf{Q}_h$ for any $(v, \tau, q) \in V_h \times \mathbf{Q}_h \times \mathbf{Q}_h$ such that

$$\begin{cases} \left(\frac{u_h^n - \check{u}_h^{n-1}}{\Delta t}, v\right) + (\sigma_h^n, \nabla v) - (\{\sigma_h^n\} \cdot \boldsymbol{n}_e, [v])_{\mathscr{E}_h^B} + \epsilon_1([u_h^n], [v])_{\mathscr{E}_h^B} = (f^n, v), \\ \\ (\sigma_h^n, \tau) - ((c_1 \mathcal{I}_x^{2-\alpha} p_{xh}^n, c_2 \mathcal{I}_y^{2-\beta} p_{yh}^n), \tau) = 0, \\ \\ (p_h^n, q) - (\nabla u_h^n, q) + ([u_h^n], \{q\} \cdot \boldsymbol{n}_e)_{\mathscr{E}_h^B} + \epsilon_2([\sigma_h^n], [q])_{\mathscr{E}_h^i} = 0, \end{cases} \quad (3.13)$$

where $\check{u}_h^{n-1} = u_h(\check{x}, t^{n-1}), \check{u}_h^0 = u^0$.

Define the bilinear forms by:

$$\mathrm{a}(\sigma_h^n, v) := (\sigma_h^n, \nabla v) - (\{\sigma_h^n\} \cdot \boldsymbol{n}_e, [v])_{\mathscr{E}_h^B},$$

$$\mathrm{c}(p_h^n, q) := (p_h^n, q),$$

$$\mathrm{b}(p_h^n, \tau) := ((c_1 \mathcal{I}_x^{2-\alpha} p_{xh}^n, c_2 \mathcal{I}_y^{2-\beta} p_{yh}^n), \tau),$$

$$\mathrm{d}(u_h^n, v) := \epsilon_1([u_h^n], [v])_{\mathscr{E}_h^B},$$

$$\mathrm{e}(\sigma_h^n, q) := \epsilon_2([\sigma_h^n], [q])_{\mathscr{E}_h^i},$$

and the linear form

$$\mathcal{F}(v) := (f^n, v), \quad \forall v \in V_h.$$

We can rewrite (3.13) as a compact formulation: Find $(u_h^n, \sigma_h^n, p_h^n) \in V_h \times \mathbf{Q}_h \times \mathbf{Q}_h$

63

at time $t = t^n$ such that

$$
\begin{cases}
\left(\frac{u_h^n - \check{u}_h^{n-1}}{\Delta t}, v\right) + a(\boldsymbol{\sigma}_h^n, v) + d(u_h^n, v) = \mathcal{F}(v), \ \forall v \in V_h, \\[2em]
c(\boldsymbol{\sigma}_h^n, \boldsymbol{\tau}) - b(\boldsymbol{p}_h^n, \boldsymbol{\tau}) = 0, \hspace{3em} \forall \boldsymbol{\tau} \in \mathbf{Q}_h, \\[2em]
c(\boldsymbol{p}_h^n, \boldsymbol{q}) - a(\boldsymbol{q}, u_h^n) + e(\boldsymbol{\sigma}_h^n, \boldsymbol{q}) = 0, \hspace{2em} \forall \boldsymbol{q} \in \mathbf{Q}_h.
\end{cases}
\tag{3.14}
$$

Now we introduce a semi-norm that appears in the analysis of these schemes, i.e.

$$
\begin{aligned}
& \left| (u_h^n, \boldsymbol{\sigma}_h^n, \boldsymbol{p}_h^n) \right|_{\mathcal{A}}^2 \\
&= d(u_h^n, u_h^n) + b(\boldsymbol{p}_h^n, \boldsymbol{p}_h^n) + e(\boldsymbol{\sigma}_h^n, \boldsymbol{\sigma}_h^n) \\
&= c_1 \cos(\alpha_1 \pi) \int_c^d \| p_{xh}^n(\cdot, y) \|_{J_{R,0}^{-\alpha_1}(a,b)}^2 \, dy + \epsilon_1 \sum_{e \in \mathscr{E}_h^B} \| [u_h^n] \|_{L^2(e)}^2 \\
&\quad + c_2 \cos(\beta_1 \pi) \int_a^b \| p_{yh}^n(x, \cdot) \|_{J_{R,0}^{-\beta_1}(c,d)}^2 \, dx + \epsilon_2 \sum_{e \in \mathscr{E}_h^i} \| [\boldsymbol{\sigma}_h^n] \|_{L^2(e)}^2 .
\end{aligned}
\tag{3.15}
$$

We end this section by showing that (3.13) is uniquely solvable for the solution $(u_h^n, \boldsymbol{\sigma}_h^n, \boldsymbol{p}_h^n)$ at each time step n.

Lemma 3.4. *(well posedness of the HDG scheme). The HDG method of (3.13) defines a unique approximation solution $(u_h^n, \boldsymbol{\sigma}_h^n, \boldsymbol{p}_h^n) \in V_h \times \mathbf{Q}_h \times \mathbf{Q}_h$.*

Proof. As (3.13) represents a finite system of linear equations, it is enough to show that the unique solution to (3.13) with $f = 0, \check{u}_h^{n-1} = 0$.

Indeed, taking $v = u_h^n, \boldsymbol{\tau} = -\boldsymbol{p}_h^n, \boldsymbol{q} = \boldsymbol{\sigma}_h^n$ into the equations of (3.13), and adding the equations, we get

$$
\frac{1}{\Delta t} \| u_h^n \|_0^2 + \left| (u_h^n, \boldsymbol{\sigma}_h^n, \boldsymbol{p}_h^n) \right|_{\mathcal{A}}^2 = 0,
\tag{3.16}
$$

which implies $u_h^n = 0, \boldsymbol{p}_h^n = 0, [\boldsymbol{\sigma}_h^n] = 0$ on $\mathscr{E}_h^i$. Next we go back to the second equation of (3.13) and take $\boldsymbol{\tau} = \boldsymbol{\sigma}_h^n$, then

$$
\| \boldsymbol{\sigma}_h^n \|_0^2 = 0.
$$

Hence, $\boldsymbol{\sigma}_h^n = 0$, which completes the proof of the uniqueness of the solution. $\qquad\square$

3.4 Stability analysis and error analysis

3.4.1 Stability analysis

In the following, C indicates a generic constant independent of h and Δt, which takes different values in different occurrences.

Throughout this chapter we assume that

$$\boldsymbol{b} \in L^\infty(J; W^{1,\infty}(\Omega)^2). \tag{3.17}$$

Lemma 3.5. [11] Under (3.17), for any function $v \in L^2(\Omega)$ there is

$$\| \, \check{v} \, \|_0^2 - \| \, v \, \|_0^2 \leq C\Delta t \parallel v \parallel_0^2, \tag{3.18}$$

where $\check{v}(\boldsymbol{x}) = v(\boldsymbol{x} - \boldsymbol{b}(\boldsymbol{x}, t^n)\Delta t)$.

Theorem 3.6. (Numerical stability) Let $(u_h^n, \boldsymbol{\sigma}_h^n, \boldsymbol{p}_h^n)$ satisfy (3.13). With (3.17), the scheme is stable for (3.13), i.e., for any integers $N = 1, 2, \cdots$, there is

$$
\begin{aligned}
\| \, u_h^N \, \|_0^2 &+ 2\Delta t \sum_{n=1}^N \left| (u_h^n, \boldsymbol{\sigma}_h^n, \boldsymbol{p}_h^n) \right|_{\mathcal{A}}^2 \\
&\leq C\Delta t \sum_{n=1}^N \| \, f^n \, \|_0^2 + C \| \, u_h^0 \, \|_0^2,
\end{aligned} \tag{3.19}
$$

where the semi-norm $| \cdot |_{\mathcal{A}}$ is defined by formula (3.15), and $u_h^0 = u^0$.

Proof. Let $v = 2\Delta t u_h^n, \boldsymbol{\tau} = -2\Delta t \boldsymbol{p}_h^n, \boldsymbol{q} = 2\Delta t \boldsymbol{\sigma}_h^n$ in equations of (3.14), respectively. By the symmetry of the bilinear forms, adding the above equations we obtain

$$
\begin{aligned}
2\Delta t \mathcal{F}(u_h^n) = 2\Delta t \mathbb{b}(\boldsymbol{p}_h^n, \boldsymbol{p}_h^n) &+ 2\Delta t \mathbb{e}(\boldsymbol{\sigma}_h^n, \boldsymbol{\sigma}_h^n) \\
&+ 2\big(u_h^n - \check{u}_h^{n-1}, u_h^n\big) + 2\Delta t \mathbb{d}(u_h^n, u_h^n).
\end{aligned}
$$

It follows from

$$2\big(u_h^n - \check{u}_h^{n-1}, u_h^n\big) \geq \| \, u_h^n \, \|_0^2 - \| \, \check{u}_h^{n-1} \, \|_0^2,$$

the Young's inequality, the definition of $\mathcal{F}$ and $|\cdot|_{\mathcal{A}}$, Lemma 3.5 that

$$
\begin{aligned}
&\parallel u_h^n \parallel_0^2 - \parallel u_h^{n-1} \parallel_0^2 + 2\Delta t \big| (u_h^n, \boldsymbol{\sigma}_h^n, \boldsymbol{p}_h^n) \big|_{\mathcal{A}}^2 \\
&\leq C\Delta t \parallel u_h^{n-1} \parallel_0^2 + \Delta t \big(\parallel u_h^n \parallel_0^2 + \parallel f^n \parallel_0^2 \big).
\end{aligned}
$$

Summing from $n = 1, 2, \cdots, N$, we get

$$
\begin{aligned}
&\parallel u_h^N \parallel_0^2 + 2\Delta t \sum_{n=1}^{N} \big| (u_h^n, \boldsymbol{\sigma}_h^n, \boldsymbol{p}_h^n) \big|_{\mathcal{A}}^2 \\
&\leq C\Delta t \sum_{n=1}^{N} \parallel u_h^n \parallel_0^2 + (1 + C\Delta t) \parallel u_h^0 \parallel_0^2 + \Delta t \sum_{n=1}^{N} \parallel f^n \parallel_0^2.
\end{aligned}
$$

Using the discrete Gronwall inequality, with $C\Delta t < 1$, $\forall N \geq 1$, there is

$$
\begin{aligned}
&\parallel u_h^N \parallel_0^2 + 2\Delta t \sum_{n=1}^{N} \big| (u_h^n, \boldsymbol{\sigma}_h^n, \boldsymbol{p}_h^n) \big|_{\mathcal{A}}^2 \\
&\leq C \parallel u_h^0 \parallel_0^2 + C\Delta t \sum_{n=1}^{N} \parallel f^n \parallel_0^2.
\end{aligned}
\tag{3.20}
$$

$\square$

3.4.2 Error analysis

In this subsection we state and discuss error bounds for the HDG method. The main steps of our error analysis follow Galerkin orthogonality property. As usual, we denote the error $(e_u^n, \boldsymbol{e}_{\boldsymbol{\sigma}}^n, \boldsymbol{e}_{\boldsymbol{p}}^n) = (u^n - u_h^n, \boldsymbol{\sigma}^n - \boldsymbol{\sigma}_h^n, \boldsymbol{p}^n - \boldsymbol{p}_h^n)$ by the following

$$
(e_u^n, \boldsymbol{e}_{\boldsymbol{\sigma}}^n, \boldsymbol{e}_{\boldsymbol{p}}^n) = (u^n - \Pi u^n, \boldsymbol{\sigma}^n - \boldsymbol{\Pi}\boldsymbol{\sigma}^n, \boldsymbol{p}^n - \boldsymbol{\Pi}\boldsymbol{p}^n) + (\Pi e_u^n, \boldsymbol{\Pi}\boldsymbol{e}_{\boldsymbol{\sigma}}^n, \boldsymbol{\Pi}\boldsymbol{e}_{\boldsymbol{p}}^n),
$$

where Π and $\boldsymbol{\Pi} = (\Pi, \Pi)$ are linear continuous projection operators from V and $\mathbf{Q}$ onto the finite element spaces V_h and $\mathbf{Q}_h$, respectively.

From equation (3.14), we obtain a compact form as follows:

$$
\left(\frac{u_h^n - \check{u}_h^{n-1}}{\Delta t}, v \right) + \mathcal{A}(u_h^n, \boldsymbol{\sigma}_h^n, \boldsymbol{p}_h^n; v, \boldsymbol{\tau}, \boldsymbol{q}) = \mathcal{F}(v),
\tag{3.21}
$$

by setting

$$
\begin{aligned}
&\mathcal{A}(u_h^n, \boldsymbol{\sigma}_h^n, \boldsymbol{p}_h^n; v, \boldsymbol{\tau}, \boldsymbol{q}) \\
&= \mathrm{a}(\boldsymbol{\sigma}_h^n, v) + \mathrm{d}(u_h^n, v) + \mathrm{c}(\boldsymbol{\sigma}_h^n, \boldsymbol{\tau}) - \mathrm{b}(\boldsymbol{p}_h^n, \boldsymbol{\tau}) \\
&\quad + \mathrm{c}(\boldsymbol{p}_h^n, \boldsymbol{q}) - \mathrm{a}(\boldsymbol{q}, u_h^n) + \mathrm{e}(\boldsymbol{\sigma}_h^n, \boldsymbol{q}).
\end{aligned}
\tag{3.22}
$$

Lemma 3.7. *Let* $u \in L^\infty(J; H^2(\Omega)), \partial_t u \in L^2(J; H^1(\Omega)), \partial_{tt} u \in L^2(J; L^2(\Omega))$. *Let* Π *and* $\boldsymbol{\Pi}$ *be linear continuous projection operators from* V *and* $\mathbf{Q}$ *onto the finite element spaces* V_h *and* $\mathbf{Q}_h$, *respectively. Then*

$$
\begin{aligned}
&\left(\psi^n \partial_\tau u^n - \frac{u_h^n - \check{u}_h^{n-1}}{\Delta t}, \Pi e_u^n\right) + \left|(\Pi e_u^n, \boldsymbol{\Pi} e_{\boldsymbol{\sigma}}^n, \boldsymbol{\Pi} e_{\boldsymbol{p}}^n)\right|_{\mathcal{A}}^2 \\
&= \mathcal{A}\left(\Pi u^n - u^n, \boldsymbol{\Pi}\boldsymbol{\sigma}^n - \boldsymbol{\sigma}^n, \boldsymbol{\Pi}\boldsymbol{p}^n - \boldsymbol{p}^n; \Pi e_u^n, -\boldsymbol{\Pi} e_{\boldsymbol{p}}^n, \boldsymbol{\Pi} e_{\boldsymbol{\sigma}}^n\right).
\end{aligned}
\tag{3.23}
$$

Proof. Because of the consistency of the numerical fluxes, the exact solution $(u, \boldsymbol{\sigma}, \boldsymbol{p})$ satisfies equation (3.12) and the approximation solution $(u_h^n, \boldsymbol{\sigma}_h^n, \boldsymbol{p}_h^n)$ satisfies (3.13). Then, subtracting (3.13) from (3.12) and taking $v = \Pi e_u^n, \boldsymbol{\tau} = -\boldsymbol{\Pi} e_{\boldsymbol{p}}^n, \boldsymbol{q} = \boldsymbol{\Pi} e_{\boldsymbol{\sigma}}^n$, the error satisfies

$$
\left(\psi^n \partial_\tau u^n - \frac{u_h^n - \check{u}_h^{n-1}}{\Delta t}, \Pi e_u^n\right) + \mathcal{A}\left(e_u^n, e_{\boldsymbol{\sigma}}^n, e_{\boldsymbol{p}}^n; \Pi e_u^n, -\boldsymbol{\Pi} e_{\boldsymbol{p}}^n, \boldsymbol{\Pi} e_{\boldsymbol{\sigma}}^n\right) = 0,
\tag{3.24}
$$

and

$$
\left|(\Pi e_u^n, \boldsymbol{\Pi} e_{\boldsymbol{\sigma}}^n, \boldsymbol{\Pi} e_{\boldsymbol{p}}^n)\right|_{\mathcal{A}}^2 = \mathcal{A}\left(\Pi e_u^n, \boldsymbol{\Pi} e_{\boldsymbol{\sigma}}^n, \boldsymbol{\Pi} e_{\boldsymbol{p}}^n; \Pi e_u^n, -\boldsymbol{\Pi} e_{\boldsymbol{p}}^n, \boldsymbol{\Pi} e_{\boldsymbol{\sigma}}^n\right).
\tag{3.25}
$$

By Galerkin orthogonality, there is

$$
\begin{aligned}
&\mathcal{A}\left(e_u^n, e_{\boldsymbol{\sigma}}^n, e_{\boldsymbol{p}}^n; \Pi e_u^n, -\boldsymbol{\Pi} e_{\boldsymbol{p}}^n, \boldsymbol{\Pi} e_{\boldsymbol{\sigma}}^n\right) \\
&= \mathcal{A}\left(\Pi e_u^n, \boldsymbol{\Pi} e_{\boldsymbol{\sigma}}^n, \boldsymbol{\Pi} e_{\boldsymbol{p}}^n; \Pi e_u^n, -\boldsymbol{\Pi} e_{\boldsymbol{p}}^n, \boldsymbol{\Pi} e_{\boldsymbol{\sigma}}^n\right) \\
&\quad - \mathcal{A}\left(\Pi u^n - u^n, \boldsymbol{\Pi}\boldsymbol{\sigma}^n - \boldsymbol{\sigma}^n, \boldsymbol{\Pi}\boldsymbol{p}^n - \boldsymbol{p}^n; \Pi e_u^n, -\boldsymbol{\Pi} e_{\boldsymbol{p}}^n, \boldsymbol{\Pi} e_{\boldsymbol{\sigma}}^n\right).
\end{aligned}
\tag{3.26}
$$

Hence, equation (3.23) follows equalities (3.24), (3.25) and (3.26). $\qquad\square$

Thus, in order to prove the error bound, all we need to do is to estimate the first term of the left-side and the right term of equation (3.23), respectively.

The characteristic term

In this subsection, we will estimate the first left-side term of equation (3.23).

Lemma 3.8. *[11] With (3.17), for any function $v \in H^1(\Omega)$ and each n we have*

$$\| v - \check{v} \|_0 \leq C \Delta t \| \nabla v \|_0, \tag{3.27}$$

where $\check{v} = v(\check{\boldsymbol{x}}) = v(\boldsymbol{x} - \boldsymbol{b}^n \Delta t)$.

The following result is a straightforward consequence of the estimate of the first left-side term of equation (3.23).

Theorem 3.9. *Let $u \in L^\infty(J; H^2(\Omega)), \partial_t u \in L^2(J; H^1(\Omega)), \partial_{tt} u \in L^2(J; L^2(\Omega))$ and u_h^n solve equation (3.13). With (3.17), there is*

$$
\begin{aligned}
& \left(\psi^n \partial_\tau u^n - \frac{u_h^n - \check{u}_h^{n-1}}{\Delta t}, \Pi e_u^n \right) \\
& \geq \frac{1}{2\Delta t} \left(\| \Pi e_u^n \|_0^2 - \| \Pi e_u^{n-1} \|_0^2 \right) - C \| \Pi e_u^{n-1} \|_0^2 \\
& \quad - C\Delta t \| \partial_{\tau\tau} u \|_{L^2(J^n; L^2(\Omega))}^2 - \frac{C}{\Delta t} \| \partial_t(\Pi u - u) \|_{L^2(J^n; L^2(\Omega))}^2 \\
& \quad - C \| \nabla(\Pi u^{n-1} - u^{n-1}) \|_0^2 - C \| \Pi e_u^n \|_0^2,
\end{aligned}
\tag{3.28}
$$

where Π is linear continuous projection operator from V onto the finite element space V_h.

Proof. From equation (3.23), we observe that

$$
\begin{aligned}
& \left(\psi^n \partial_\tau u^n - \frac{u_h^n - \check{u}_h^{n-1}}{\Delta t}, \Pi e_u^n \right) \\
& = \left(\frac{\Pi e_u^n - \Pi \check{e}_u^{n-1}}{\Delta t}, \Pi e_u^n \right) + \left(\psi^n \partial_\tau u^n - \frac{u^n - \check{u}^{n-1}}{\Delta t}, \Pi e_u^n \right) \\
& \quad - \left(\frac{(\Pi u^n - u^n) - (\Pi \check{u}^{n-1} - \check{u}^{n-1})}{\Delta t}, \Pi e_u^n \right) \\
& = \sum_{i=1}^3 \mathcal{B}_i.
\end{aligned}
\tag{3.29}
$$

Using Lemma 3.5, we obtain

$$
\begin{aligned}
\mathcal{B}_1 &= \Big(\frac{\Pi e_u^n - \Pi \breve{e}_u^{n-1}}{\Delta t}, \Pi e_u^n \Big) \\
&= \frac{1}{2\Delta t} \big(\parallel \Pi e_u^n \parallel_0^2 - \parallel \Pi \breve{e}_u^{n-1} \parallel_0^2 + \parallel \Pi e_u^n - \Pi \breve{e}_u^{n-1} \parallel_0^2 \big) \\
&\geq \frac{1}{2\Delta t} \big(\parallel \Pi e_u^n \parallel_0^2 - \parallel \Pi \breve{e}_u^{n-1} \parallel_0^2 \big) \\
&\geq \frac{1}{2\Delta t} \big(\parallel \Pi e_u^n \parallel_0^2 - \parallel \Pi e_u^{n-1} \parallel_0^2 \big) - C \parallel \Pi e_u^{n-1} \parallel_0^2,
\end{aligned}
$$

where $\Pi \breve{e}_u^{n-1} = \Pi \breve{u}^{n-1} - \breve{u}_h^{n-1}$. Also by the Taylor expansion and Hölder's inequality,

$$
\begin{aligned}
\mid \mathcal{B}_2 \mid &= \Big| \big(\psi^n \partial_\tau u^n - \frac{u^n - \breve{u}^{n-1}}{\Delta t}, \Pi e_u^n \big) \Big| \\
&\leq C \Delta t \parallel \partial_{\tau\tau} u \parallel_{L^2(J^n; L^2(\Omega))}^2 + C \parallel \Pi e_u^n \parallel_0^2,
\end{aligned}
$$

and

$$
\begin{aligned}
-\mathcal{B}_3 &= \Big(\frac{(\Pi u^n - u^n) - (\Pi \breve{u}^{n-1} - \breve{u}^{n-1})}{\Delta t}, \Pi e_u^n \Big) \\
&= \Big(\frac{(\Pi u^n - u^n) - (\Pi u^{n-1} - u^{n-1})}{\Delta t}, \Pi e_u^n \Big) \\
&+ \Big(\frac{(\Pi u^{n-1} - u^{n-1}) - (\Pi \breve{u}^{n-1} - \breve{u}^{n-1})}{\Delta t}, \Pi e_u^n \Big) = \mathcal{S}_1 + \mathcal{S}_2,
\end{aligned} \tag{3.30}
$$

where

$$
\begin{aligned}
\mathcal{S}_1 &= \Big(\frac{(\Pi u^n - u^n) - (\Pi u^{n-1} - u^{n-1})}{\Delta t}, \Pi e_u^n \Big) \\
&\leq \frac{1}{\Delta t} \parallel \Pi e_u^n \parallel_0 \int_{t^{n-1}}^{t^n} \parallel \partial_t (\Pi u - u) \parallel_0 dt \\
&\leq C \parallel \Pi e_u^n \parallel_0^2 + \frac{C}{\Delta t} \parallel \partial_t (\Pi u - u) \parallel_{L^2(J^n; L^2(\Omega))}^2,
\end{aligned} \tag{3.31}
$$

and

$$
\begin{aligned}
\mathcal{S}_2 &= \Big(\frac{(\Pi u^{n-1} - u^{n-1}) - (\Pi \breve{u}^{n-1} - \breve{u}^{n-1})}{\Delta t}, \Pi e_u^n \Big) \\
&\leq C \parallel \Pi e_u^n \parallel_0^2 + C \parallel \nabla (\Pi u^{n-1} - u^{n-1}) \parallel_0^2,
\end{aligned} \tag{3.32}
$$

follow from Cauchy-Schwarz's inequality, Young's inequality and Lemma 3.8. Substituting $\mathcal{B}_1, \mathcal{B}_2, \mathcal{B}_3$ into (3.29), we finish the proof. $\qquad\square$

69

The right hand side term

In this subsection, we will use general analytic methods to get the bound of the right hand side term of equation (3.23).

Theorem 3.10. *Let u be sufficiently smooth and solve (3.9). Assume that $(\Pi u^n, \boldsymbol{\Pi\sigma}^n, \boldsymbol{\Pi p}^n)$ are standard L^2-projection operators of $(u^n, \boldsymbol{\sigma}^n, \boldsymbol{p}^n)$, and $(u_h^n, \boldsymbol{\sigma}_h^n, \boldsymbol{p}_h^n)$ solves (3.13). Under the assumption of (3.17), there is*

$$
\left| \mathcal{A}\big(\Pi u^n - u^n, \boldsymbol{\Pi\sigma}^n - \boldsymbol{\sigma}^n, \boldsymbol{\Pi p}^n - \boldsymbol{p}^n; \Pi e_u^n, -\boldsymbol{\Pi e_p^n}, \boldsymbol{\Pi e_\sigma^n}\big) \right|
$$

$$
\leq Cc_1\epsilon_\alpha \int_c^d \| \Pi e_{p_x}^n(\cdot, y) \|_{J_{R,0}^{-\alpha_1}(a,b)}^2 \, dy + (\frac{C}{\epsilon_1} + C\epsilon_1)h^{2k+1} + \frac{C}{\epsilon_\alpha}h^{2k+2}
$$

$$
+ Cc_2\epsilon_\beta \int_a^b \| \Pi e_{p_y}^n(x, \cdot) \|_{J_{R,0}^{-\beta_1}(c,d)}^2 \, dx + (\frac{C}{\epsilon_2} + C\epsilon_2)h^{2k+1} + \frac{C}{\epsilon_\beta}h^{2k+2}
$$

$$
+ \frac{\epsilon_1}{2} \sum_{e \in \mathscr{E}_h^B} \| [\Pi e_u^n] \|_{L^2(e)}^2 + \frac{\epsilon_2}{2} \sum_{e \in \mathscr{E}_h^i} \| [\boldsymbol{\Pi e_\sigma^n}] \|_{L^2(e)}^2 .
$$

(3.33)

Proof. From the definition of $\mathcal{A}$, we have

$$
\mathcal{A}\big(\Pi u^n - u^n, \boldsymbol{\Pi\sigma}^n - \boldsymbol{\sigma}^n, \boldsymbol{\Pi p}^n - \boldsymbol{p}^n; \Pi e_u^n, -\boldsymbol{\Pi e_p^n}, \boldsymbol{\Pi e_\sigma^n}\big)
$$

$$
\leq \left| \mathrm{a}(\boldsymbol{\Pi\sigma}^n - \boldsymbol{\sigma}^n, \Pi e_u^n) \right| + \left| \mathrm{b}(\boldsymbol{\Pi p}^n - \boldsymbol{p}^n, \boldsymbol{\Pi e_p^n}) \right| + \left| \mathrm{d}(\Pi u^n - u^n, \Pi e_u^n) \right|
$$

$$
+ \left| \mathrm{e}(\boldsymbol{\Pi\sigma}^n - \boldsymbol{\sigma}^n, \boldsymbol{\Pi e_\sigma^n}) \right| + \left| \mathrm{a}(\boldsymbol{\Pi e_\sigma^n}, \Pi u^n - u^n) \right| + \left| \mathrm{c}(\boldsymbol{\Pi\sigma}^n - \boldsymbol{\sigma}^n, -\boldsymbol{\Pi e_p^n}) \right|
$$

$$
+ \left| \mathrm{c}(\boldsymbol{\Pi p}^n - \boldsymbol{p}^n, \boldsymbol{\Pi e_\sigma^n}) \right|
$$

$$
= \sum_{i=1}^7 \mathcal{T}_i.
$$

(3.34)

Using Hölder's, Young's inequalities and the property of projection operator $\boldsymbol{\Pi}$, from Lemma 1.6 we obtain

$$
\mathcal{T}_1 = \left| \mathrm{a}(\boldsymbol{\Pi\sigma}^n - \boldsymbol{\sigma}^n, \Pi e_u^n) \right| = \left| (\{\boldsymbol{\Pi\sigma}^n - \boldsymbol{\sigma}^n\} \cdot \boldsymbol{n}_e, [\Pi e_u^n])_{\mathscr{E}_h^B} \right|
$$

$$
\leq \sum_{e \in \mathscr{E}_h^B} \| \{\boldsymbol{\Pi\sigma}^n - \boldsymbol{\sigma}^n\} \cdot \boldsymbol{n}_e \|_{L^2(e)} \| [\Pi e_u^n] \|_{L^2(e)}
$$

$$
\leq \sum_{e \in \mathscr{E}_h^B} \big(\frac{1}{\epsilon_1} \| \{\boldsymbol{\Pi\sigma}^n - \boldsymbol{\sigma}^n\} \cdot \boldsymbol{n}_e \|_{L^2(e)}^2 + \frac{\epsilon_1}{4} \| [\Pi e_u^n] \|_{L^2(e)}^2 \big)
$$

$$
\leq \frac{C}{\epsilon_1}h^{2k+1} + \frac{\epsilon_1}{4} \sum_{e \in \mathscr{E}_h^B} \| [\Pi e_u^n] \|_{L^2(e)}^2 .
$$

70

From the property of projection operator Π and Lemma 1, Definition 3.1, Definition 3.3, Theorem 3.3, it follows that

$$
\begin{aligned}
\mathcal{T}_2 &= \left| c_1(\Pi p_x^n - p_x^n, {}_x\mathcal{I}_b^{2-\alpha}\Pi e_{p_x}^n) + c_2(\Pi p_y^n - p_y^n, {}_y\mathcal{I}_d^{2-\beta}\Pi e_{p_y}^n) \right| \\
&\leq c_1 \parallel \Pi p_x^n - p_x^n \parallel_0 \Big(\int_c^d \parallel \Pi e_{p_x}^n(\cdot, y) \parallel_{J_{R,0}^{-(2-\alpha)}(a,b)}^2 \, dy \Big)^{\frac{1}{2}} \\
&\quad + c_2 \parallel \Pi p_y^n - p_y^n \parallel_0 \Big(\int_a^b \parallel \Pi e_{p_y}^n(x, \cdot) \parallel_{J_{R,0}^{-(2-\beta)}(c,d)}^2 \, dx \Big)^{\frac{1}{2}} \\
&\leq Cc_1 \parallel \Pi p_x^n - p_x^n \parallel_0 \Big(\int_c^d \parallel \Pi e_{p_x}^n(\cdot, y) \parallel_{J_{R,0}^{-\alpha_1}(a,b)}^2 \, dy \Big)^{\frac{1}{2}} \\
&\quad + Cc_2 \parallel \Pi p_y^n - p_y^n \parallel_0 \Big(\int_a^b \parallel \Pi e_{p_y}^n(x, \cdot) \parallel_{J_{R,0}^{-\beta_1}(c,d)}^2 \, dx \Big)^{\frac{1}{2}} \\
&\leq \frac{C}{\epsilon_\alpha} h^{2k+2} + Cc_1\epsilon_\alpha \int_c^d \parallel \Pi e_{p_x}^n(\cdot, y) \parallel_{J_{R,0}^{-\alpha_1}(a,b)}^2 \, dy \\
&\quad + \frac{C}{\epsilon_\beta} h^{2k+2} + Cc_2\epsilon_\beta \int_a^b \parallel \Pi e_{p_y}^n(x, \cdot) \parallel_{J_{R,0}^{-\beta_1}(c,d)}^2 \, dx,
\end{aligned}
$$

where ϵ_α and ϵ_β are chosen as sufficiently small numbers such that $C\epsilon_\alpha \leq cos(\alpha_1\pi)$ and $C\epsilon_\beta \leq cos(\beta_1\pi)$.

With the same deduction of $\mathcal{T}_1$, there is

$$
\begin{aligned}
\mathcal{T}_3 &= \left| \mathrm{d}(\Pi u^n - u^n, \Pi e_u^n) \right| \\
&\leq \epsilon_1 \sum_{e \in \mathscr{E}_h^B} \Big(\parallel [\Pi u^n - u^n] \parallel_{L^2(e)}^2 + \frac{1}{4} \parallel [\Pi e_u^n] \parallel_{L^2(e)}^2 \Big) \\
&\leq Ch^{2k+1}\epsilon_1 + \frac{\epsilon_1}{4} \sum_{e \in \mathscr{E}_h^B} \parallel [\Pi e_u^n] \parallel_{L^2(e)}^2 .
\end{aligned}
$$

By Lemma 1.6, there is

$$
\begin{aligned}
\mathcal{T}_4 &= \left| \mathrm{e}(\boldsymbol{\Pi}\boldsymbol{\sigma}^n - \boldsymbol{\sigma}^n, \boldsymbol{\Pi}e_{\boldsymbol{\sigma}}^n) \right| \\
&\leq \epsilon_2 \sum_{e \in \mathscr{E}_h^i} \parallel [\boldsymbol{\Pi}\boldsymbol{\sigma}^n - \boldsymbol{\sigma}^n] \parallel_{L^2(e)} \parallel [\boldsymbol{\Pi}e_{\boldsymbol{\sigma}}^n] \parallel_{L^2(e)} \\
&\leq \epsilon_2 \sum_{e \in \mathscr{E}_h^i} \Big(\parallel [\boldsymbol{\Pi}\boldsymbol{\sigma}^n - \boldsymbol{\sigma}^n] \parallel_{L^2(e)}^2 + \frac{1}{4} \parallel [\boldsymbol{\Pi}e_{\boldsymbol{\sigma}}^n] \parallel_{L^2(e)}^2 \Big) \\
&\leq C\epsilon_2 h^{2k+1} + \frac{\epsilon_2}{4} \sum_{e \in \mathscr{E}_h^i} \parallel [\boldsymbol{\Pi}e_{\boldsymbol{\sigma}}^n] \parallel_{L^2(e)}^2 .
\end{aligned}
$$

Integrating the first term of $a(\boldsymbol{\Pi e_\sigma^n}, \Pi u^n - u^n)$ by parts, and using the orthogonal property of projection operator $\boldsymbol{\Pi}$, we get

$$
\begin{aligned}
\mathcal{T}_5 &= \left| a(\boldsymbol{\Pi e_\sigma^n}, \Pi u^n - u^n) \right| \\
&= \left| \left([\boldsymbol{\Pi e_\sigma^n}], \{\Pi u^n - u^n\} \boldsymbol{n_e} \right)_{\mathscr{E}_h^i} \right| \\
&\leq \sum_{e \in \mathscr{E}_h^i} \| [\boldsymbol{\Pi e_\sigma^n}] \|_{L^2(e)} \| \{\Pi u^n - u^n\} \boldsymbol{n_e} \|_{L^2(e)} \\
&\leq \sum_{e \in \mathscr{E}_h^i} \left(\frac{1}{\epsilon_2} \| \{\Pi u^n - u^n\} \boldsymbol{n_e} \|_{L^2(e)}^2 + \frac{\epsilon_2}{4} \| [\boldsymbol{\Pi e_\sigma^n}] \|_{L^2(e)}^2 \right) \\
&\leq \frac{C}{\epsilon_2} h^{2k+1} + \frac{\epsilon_2}{4} \sum_{e \in \mathscr{E}_h^i} \| [\boldsymbol{\Pi e_\sigma^n}] \|_{L^2(e)}^2 .
\end{aligned}
$$

Note that $\mathcal{T}_6$ and $\mathcal{T}_7$ vanish because of the orthogonal property of projection $\boldsymbol{\Pi}$. Substituting $\mathcal{T}_i, i = 1, \cdots, 7$ into (3.34), we complete the proof. $\qquad\square$

Error bound

Assume that the corresponding analytical solution is sufficiently regular and satisfies $u \in L^\infty(J; H^2(\Omega))$, $\partial_t u \in L^2(J; H^1(\Omega))$, $\partial_{tt} u \in L^2(J; L^2(\Omega))$.

Theorem 3.11. *Let $(u^n, \boldsymbol{\sigma}^n, \boldsymbol{p}^n)$ be the exact solution of (3.9), and $(u_h^n, \boldsymbol{\sigma}_h^n, \boldsymbol{p}_h^n)$ be numerical solution of the HDG scheme corresponding to equation (3.13). Under the assumption of (3.17), for any integer $N = 1, 2, \cdots$, the following inequality holds*

$$
\begin{aligned}
&\| u^N - u_h^N \|_0^2 + \Delta t \sum_{n=1}^{N} \Big(\epsilon_1 \sum_{e \in \mathscr{E}_h^B} \| [u^n - u_h^n] \|_{L^2(e)}^2 + \epsilon_2 \sum_{e \in \mathscr{E}_h^i} \\
&\| [\boldsymbol{\sigma}^n - \boldsymbol{\sigma}_h^n] \|_{L^2(e)}^2 \Big) + 2\Delta t \sum_{n=1}^{N} c_1 K_\alpha \int_c^d \| (p_x^n - p_{xh}^n)(\cdot, y) \|_{J_{R,0}^{-\alpha_1}(a,b)}^2 \, dy \\
&+ 2\Delta t \sum_{n=1}^{N} c_2 K_\beta \int_a^b \| (p_y^n - p_{yh}^n)(x, \cdot) \|_{J_{R,0}^{-\beta_1}(c,d)}^2 \, dx \\
&\leq C(\Delta t)^2 \sum_{n=1}^{N} \| \partial_{\tau\tau} u \|_{L^2(J^n; L^2(\Omega))}^2 + C \sum_{n=1}^{N} \| \partial_t(\Pi u - u) \|_{L^2(J^n; L^2(\Omega))}^2 \\
&+ C_\epsilon h^{2k+1} + C\Delta t \sum_{n=1}^{N} | \Pi u^{n-1} - u^{n-1} |_1^2,
\end{aligned} \tag{3.35}
$$

where $K_\alpha = \cos(\alpha_1 \pi) - C\epsilon_\alpha \geq 0$, $K_\beta = \cos(\beta_1 \pi) - C\epsilon_\beta \geq 0$, C_ϵ is dependent of ϵ_1, ϵ_2,

and ϵ_α and ϵ_β are chosen as above.

Remark 3.3. Note that $C_\epsilon = C\epsilon_1 + \frac{C}{\epsilon_1} + C\epsilon_2 + \frac{C}{\epsilon_2}$ is independent on h for some suitable choices of ϵ_1, ϵ_2. But if $\epsilon_1 = \epsilon_2 = h^{-1}$, then $C_\epsilon = \mathcal{O}(h^{-1})$ (see next section).

Proof. Substituting the results of Theorem 3.9 and Theorem 3.10 into equation (3.23), there is

$$
\begin{aligned}
& \frac{1}{2\Delta t} \big(\parallel \Pi e_u^n \parallel_0^2 - \parallel \Pi e_u^{n-1} \parallel_0^2 \big) + \frac{\epsilon_1}{2} \sum_{e \in \mathscr{E}_h^B} \parallel [\Pi e_u^n] \parallel_{L^2(e)}^2 + \frac{\epsilon_2}{2} \sum_{e \in \mathscr{E}_h^i} \parallel [\boldsymbol{\Pi e_\sigma^n}] \parallel_{L^2(e)}^2 \\
& + c_1 (cos(\alpha_1 \pi) - C\epsilon_\alpha) \int_c^d \parallel \Pi e_{p_x}^n(\cdot, y) \parallel_{J_{R,0}^{-\alpha_1}(a,b)}^2 \, dy \\
& + c_2 (cos(\beta_1 \pi) - C\epsilon_\beta) \int_a^b \parallel \Pi e_{p_y}^n(x, \cdot) \parallel_{J_{R,0}^{-\beta_1}(c,d)}^2 \, dx \\
& \leq C \parallel \Pi e_u^{n-1} \parallel_0^2 + C \parallel \Pi e_u^n \parallel_0^2 + C\Delta t \parallel \partial_{\tau\tau} u \parallel_{L^2(J^n; L^2(\Omega))}^2 \\
& + \frac{C}{\Delta t} \parallel \partial_t (\Pi u - u) \parallel_{L^2(J^n; L^2(\Omega))}^2 + C \mid \Pi u^{n-1} - u^{n-1} \mid_1^2 + C_\epsilon h^{2k+1}.
\end{aligned}
$$

With $\Pi e_u^0 = 0$, multiplying the above inequality by $2\Delta t$ for both sides, summing over n from 1 to N, and using the discrete Gronwall inequality, we obtain

$$
\begin{aligned}
& \parallel \Pi e_u^N \parallel_0^2 + \Delta t \sum_{n=1}^N \Big(\epsilon_1 \sum_{e \in \mathscr{E}_h^B} \parallel [\Pi e_u^n] \parallel_{L^2(e)}^2 + \epsilon_2 \sum_{e \in \mathscr{E}_h^i} \parallel [\boldsymbol{\Pi e_\sigma^n}] \parallel_{L^2(e)}^2 \Big) \\
& + 2\Delta t \sum_{n=1}^N c_1 (cos(\alpha_1 \pi) - C\epsilon_\alpha) \int_c^d \parallel \Pi e_{p_x}^n(\cdot, y) \parallel_{J_{R,0}^{-\alpha_1}(a,b)}^2 \, dy \\
& + 2\Delta t \sum_{n=1}^N c_2 (cos(\beta_1 \pi) - C\epsilon_\beta) \int_a^b \parallel \Pi e_{p_y}^n(x, \cdot) \parallel_{J_{R,0}^{-\beta_1}(c,d)}^2 \, dx \qquad\qquad (3.36) \\
& \leq C(\Delta t)^2 \sum_{n=1}^N \parallel \partial_{\tau\tau} u \parallel_{L^2(J^n; L^2(\Omega))}^2 + C \sum_{n=1}^N \parallel \partial_t (\Pi u - u) \parallel_{L^2(J^n; L^2(\Omega))}^2 \\
& + C\Delta t \sum_{n=1}^N \mid \Pi u^{n-1} - u^{n-1} \mid_1^2 + C_\epsilon h^{2k+1}.
\end{aligned}
$$

By the triangle inequality, we complete the proof. □

3.5 Numerical experiments

In this section, we shall illustrate numerical performance of our proposed scheme by numerical simulation of two examples. In the first example, we verify the accuracy of our scheme with exact smooth solution u combining with fractional Riemann-Liouville derivatives with respect to x-variable and y-variable, respectively. When computing the fractional integral part in triangular meshes (see Figures 3.1-3.2), we use Gauss points and weights to deal with the terms relating with the fractional operators element-by-element (see [48]). Since this part needs more time and memory (see [41]), we only used the piecewise linear basis functions to simulate the solutions in triangular meshes. TABLE 3.1 and TABLE 3.2 illustrate that our scheme has a good convergence order with piecewise linear basis function. In the second example, Figures 3.3-3.10 justify that our scheme simulates the solution very well.
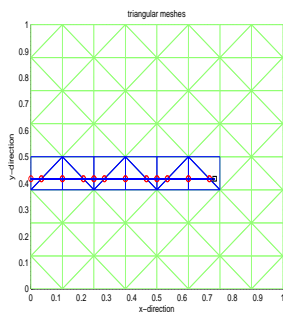

Fig. 3.1: All triangles in x-direction affected by Gauss point (denoted by black square).
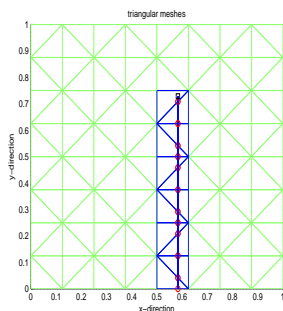

Fig. 3.2: All triangles in y-direction affected by Gauss point (denoted by black square).

Example 3.1. Consider the two-dimensional space-fractional convection-diffusion prob-

74

lem (3.1) in the unit square $\Omega = [0,1] \times [0,1]$. The initial condition and the exact solution are specified as:

$$\begin{cases} u(\boldsymbol{x}, t) = e^{-t} x^2 (x-1)^2 y^2 (y-1)^2, \\ u_0(\boldsymbol{x}) = x^2 (x-1)^2 y^2 (y-1)^2, \\ \boldsymbol{b}(\boldsymbol{x}, t) = (0,0). \end{cases} \tag{3.37}$$

Then the exact solution has the homogeneous boundary value, and the force term $f(\boldsymbol{x}, t)$ is determined accordingly from (3.1) for given c_1, c_2. For our numerical simulation, in order to validate stability and accuracy of the presented HDG scheme, we choose the time-step, $\Delta t = \mathcal{O}(h)$, used to advance the discrete formulation from t^{n-1} to $t^n, n = 1, 2, \cdots, N$. The experimental convergence rate is given by

$$rate = \frac{log\big(\parallel u(t) - u_{h_1}(t) \parallel_{L^2(\mathscr{E}_{h_1})} / \parallel u(t) - u_{h_2}(t) \parallel_{L^2(\mathscr{E}_{h_2})} \big)}{log(h_1/h_2)}.$$

h	$\parallel e_u \parallel_0$	$rate$	$\parallel e_u \parallel_1$	$rate$	$\parallel \partial_x e_u \parallel_0$	$rate$	$\parallel \partial_y e_u \parallel_0$
	$(\alpha, \beta) = (1.2, 1.4)$, $\epsilon_1 = 1, \epsilon_2 = 1$						
1/6	2.23e-04	–	1.28e-04	–	2.22e-03	–	6.52e-03
1/8	1.45e-04	1.5	8.12e-05	1.6	1.79e-03	0.8	6.77e-03
1/10	1.03e-04	1.5	5.67e-05	1.6	1.45e-03	1.0	6.86e-03
1/12	7.83e-05	1.5	4.18e-05	1.7	1.16e-03	1.2	6.90e-03
1/14	5.86e-05	1.9	3.21e-05	1.7	9.75e-04	1.1	6.94e-03
1/16	4.27e-05	2.4	2.41e-05	2.2	9.72e-04	0.2	6.98e-03
	$(\alpha, \beta) = (1.2, 1.4)$, $\epsilon_1 = h^{-1}, \epsilon_2 = h^{-1}$						
1/6	2.14e-04	–	1.28e-04	–	2.10e-03	–	6.50e-03
1/8	1.38e-04	1.5	7.95e-05	1.7	1.65e-03	0.8	6.74e-03
1/10	1.02e-04	1.4	6.25e-05	1.1	1.47e-03	0.5	6.88e-03
1/12	7.51e-05	1.7	4.65e-05	1.6	1.25e-03	0.9	6.92e-03
1/14	5.53e-05	2.0	3.47e-05	1.9	9.44e-04	1.8	6.94e-03
1/16	3.72e-05	3.0	2.27e-05	3.2	7.83e-04	1.4	6.95e-03

Tab. 3.1: Errors and convergence orders of Example 3.1 with $c_1 = \frac{\Gamma(5-\alpha)}{\Gamma(6)}, c_2 = \frac{\Gamma(3-\beta)}{\Gamma(2)}$.

Table 3.1 and Table 3.2 display the numerical L^2, L^1-errors and derivative errors with respect to x-variable and y-variable, respectively, at $t = 0.1$. Note that with different

choices of ϵ_1, ϵ_2, the HDG scheme has good errors (i.e. $10e - 5$), and almost has a convergence of an order 1.5 in L^2-norm. The errors and rates of Table 3.2 are better than Table 3.1.

	$(\alpha, \beta) = (1.9, 1.6), \epsilon_1 = 0.01, \epsilon_2 = 0.01$						
h	$\| e_u \|_0$	$rate$	$\| e_u \|_1$	$rate$	$\| \partial_x e_u \|_0$	$rate$	$\| \partial_y e_u \|_0$
1/6	7.94e-05	–	4.87e-05	–	1.17e-03	–	6.38e-03
1/8	5.88e-05	1.0	3.77e-05	0.9	7.52e-04	1.5	6.66e-03
1/10	4.49e-05	1.2	2.82e-05	1.3	5.23e-04	1.6	6.78e-03
1/12	3.61e-05	1.2	2.26e-05	1.2	4.02e-04	1.4	6.85e-03
1/14	2.98e-05	1.2	1.82e-05	1.4	3.20e-04	1.5	6.90e-03
1/16	2.42e-05	1.6	1.47e-05	1.6	2.63e-04	1.5	6.93e-03
	$(\alpha, \beta) = (1.9, 1.6), \epsilon_1 = h^{-1}, \epsilon_2 = h^{-1}$						
h	$\| e_u \|_0$	$rate$	$\| e_u \|_1$	$rate$	$\| \partial_x e_u \|_0$	$rate$	$\| \partial_y e_u \|_0$
1/6	7.24e-05	–	3.60e-05	–	1.15e-03	–	6.39e-03
1/8	5.06e-05	1.2	2.39e-05	1.4	7.58e-04	1.5	6.67e-03
1/10	3.88e-05	1.2	2.04e-05	0.7	5.43e-04	1.5	6.79e-03
1/12	3.08e-05	1.3	1.72e-05	0.9	4.23e-04	1.4	6.86e-03
1/14	2.39e-05	1.7	1.29e-05	1.9	3.46e-04	1.3	6.90e-03
1/16	1.69e-05	2.6	8.54e-05	3.1	2.79e-04	1.6	6.93e-03

Tab. 3.2: Errors and convergence orders of Example 3.1 with $c_1 = \frac{\Gamma(2-\alpha)}{\Gamma(6)}, c_2 = \frac{\Gamma(2-\beta)}{\Gamma(6)}$.

Example 3.2. In this example, we shall investigate the approximation solution of problem (3.1). For convenience, we still choose the domain is the unit square $\Omega = (0,1) \times (0,1)$, and the initial condition, exact solution u, the vector function $\boldsymbol{b}$ are given by:

$$\begin{cases} u(\boldsymbol{x},t) = e^{-t}x^2(x-0.5)^2(x-1)^2 y^2(y-0.5)^2(y-1)^2, \\ u_0(\boldsymbol{x}) = x^2(x-0.5)^2(x-1)^2 y^2(y-0.5)^2(y-1)^2, \\ \boldsymbol{b}(\boldsymbol{x},t) = ((x-0.5), -(y-0.5)). \end{cases} \quad (3.38)$$

For the second example, in order to further support the theoretical convergence and justify the powerful HDG scheme, we give some approximation solutions with the refining space-step h to compare with exact solutions. It is clear that the exact solution of Example 3.2 is nonnegative with four hills. In our simulation, our $\mathbb{P}^1$-DG solution recovers the exact solution perfectly with all four hills in coarse meshes.

In these numerical experiments, we choose $\Delta t = \mathcal{O}(h), \epsilon_1 = \epsilon_2 = h^{-1}$. Figures 3.3-3.6

give the exact solution u and the numerical solutions u_h based on different space step $h = \frac{1}{4}, \frac{1}{8}, \frac{1}{16}$ at $t = 0.05$, $\alpha = 1.2, \beta = 1.4, c_1 = \frac{\Gamma(5-\alpha)}{\Gamma(6)}, c_2 = \frac{\Gamma(3-\beta)}{\Gamma(2)}$. Figures 3.7-3.10 give the exact solution u and the numerical solutions u_h based on different space step $h = \frac{1}{4}$, $\frac{1}{8}$, $\frac{1}{16}$ at $t = 0.1, \alpha = 1.9, \beta = 1.6, c_1 = \frac{\Gamma(2-\alpha)}{\Gamma(6)}, c_2 = \frac{\Gamma(2-\beta)}{\Gamma(6)}$. Note that the numerical results display that the approximations are more and more accurate with the refining of the meshes.
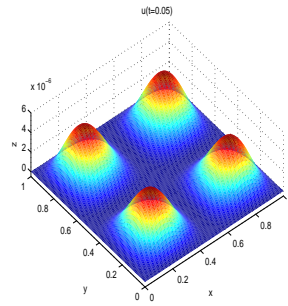
Fig. 3.3: Exact solution $u(t = 0.05)$.
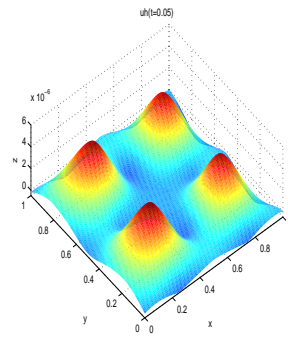

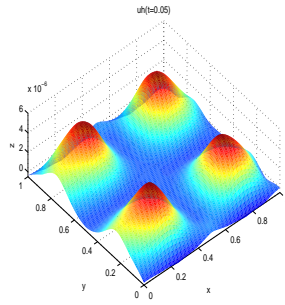Fig. 3.4: Numerical solution $u_h(t = 0.05), h = \frac{1}{4}$.

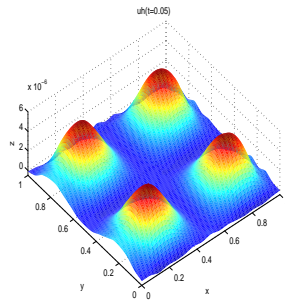Fig. 3.5: Numerical solution $u_h(t = 0.05), h = \frac{1}{8}$.

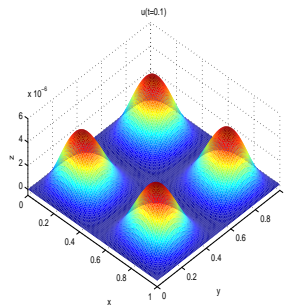Fig. 3.6: Numerical solution $u_h(t = 0.05), h = \frac{1}{16}$.
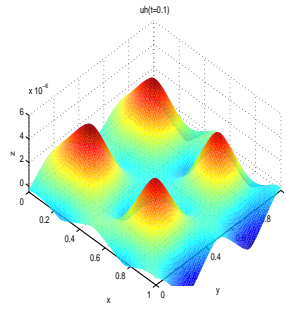

Fig. 3.7: Exact solution $u(t = 0.1)$.

Fig. 3.8: Numerical solution $u_h(t = 0.1), h = \frac{1}{4}$.

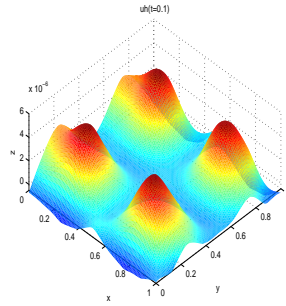Fig. 3.9: Numerical solution $u_h(t = 0.1), h = \frac{1}{8}$.
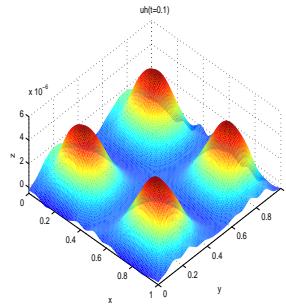

Fig. 3.10: Numerical solution $u_h(t = 0.1), h = \frac{1}{16}$.

Chapter 4

Conclusions and perspectives

In this thesis, we finished two work from two areas, i.e., characteristic local discontinuous Galerkin method for the incompressible Navier-Stokes equations proposed in Chapter 2 and hybridized discontinuous Galerkin method for space-fractional convection-diffusion equations in 2D shown in Chapter 3, respectively.

- S. Q. Wang, W. H. Deng, J. Y. Yuan, Y. J. Wu, Characteristic local discontinuous Galerkin method for incompressible Navier-Stokes equations. submitted.

- S. Q. Wang, J. Y. Yuan, W. H. Deng, Y. J. Wu, A hybridized discontinuous Galerkin method for 2D fractional convection-diffusion equations. submitted.

The first work is concerning on a problem of mathematical physical fluid computation. In this work we extended the work of local discontinuous Galerkin methods for the Stokes system [15] with characteristic local discontinuous Galerkin (CLDG) method. By carefully constructing the numerical fluxes, adding the penalty terms, and using the method of characteristics to discretize the time derivative and nonlinear convective term, we design the effective LDG scheme to solve the time-dependent incompressible Navier-Stokes equations in $\mathbb{R}^2$. Besides the general advantages of the LDG scheme, the proposed scheme is theoretically proved or numerically verified to have the following benefits: 1) it is symmetric, so easy to do theoretical analysis and numerical computation; 2) theoretically proved to be nonlinear stable; 3) numerically verified to have the suboptimal convergence rates; 4) the scheme is efficient for a wide range of Reynolds numbers, such as $Re = 10^2, 10^3, 10^6, 10^8, 10^{12}, 10^{15}, 10^{16}$.

For the characteristic local discontinuous Galerkin method for the incompressible Navier-Stokes equations, we did not complete all problems of considered equations. In

our work, we just recasted the solutions with one time accuracy and obtained suboptimal convergence by simulating some simple examples. In future work, we will consider combining second order modified characteristics with some discontinuous Galerkin methods to recast the time-dependent incompressible Navier-Stokes equations. In numerical implementation, the benchmark problem which is fundamental problem in Navier-Stokes equations will be performed.

The second work focus on numerical analysis and implementation of fractional equations with discontinuous Galerkin method. By carefully introducing the auxiliary variables and constructing the numerical fluxes, adding the penalty terms, and using the method of characteristics to deal with the time derivative and convective term, we design the effective HDG scheme to solve 2D space-fractional convection-diffusion equations with triangular meshes. As we know, this work is the first time to deal 2D space-fractional convection-diffusion equations with triangular mesh by the DG method. The stability and error analysis are investigated. Besides the general advantages of HDG method, the presented scheme is proved to have the following benefits: 1) it is symmetric, so easy to deal with fractional operators; 2) theoretically, the stability was proved more easily; 3) the penalty terms made the error analysis more convenient; 4) numerically verified to have efficient approximation; 5) the scheme was performed very well in triangular meshes; 6) it is possible to use this scheme to solve nonlinear equations.

As our knowledge, there are few works on applying discontinuous Galerkin method for fractional equations in 2D, and much less on fractional equations with complicated domains. In the future, we will extend the work to some space-fractional equations in some complicated domains, such as triangle, polygonal domains. As we stated that we performed the simulations only with $\mathbb{P}^1$-DG method (linear piecewise polynomial approximation) because of the expensive memory and time. In next work, the numerical performance will be improved up to simulate problems with quadratic piecewise or cubic piecewise polynomial. I think some other interesting fractional problems will be considered further.

Bibliography

[1] A. Allievi, R. Bermejo, Finite element modified method of characteristics for the Navier-Stokes equations, *Int. J. Numer. Meth. Fluids*, 32: 439-464, 2000.

[2] T. Arbogast, C.-S. Huang, A fully mass and volume conserving implementation of a characteristic method for transport problems, *SIAM J. Sci. Comput.*, 28: 2001-2022, 2006.

[3] T. Arbogast, M. F. Wheeler, A characteristics-mixed finite element method for advection-dominated transport problems, *SIAM J. Numer. Anal.*, 32: 404-424, 1995.

[4] F. Bassi, S. Rebay, A high-order accurate discontinuous finite element method for the numerical solution of the compressible Navier-Stokes equations, *J. Comput. Phys.*, 131: 267-279, 1997.

[5] D. A. Benson, S. W. Wheatcraft, M. M. Meerschaert, The fractional-order governing equation of Lévy motion, *Water Resour. Res.*, 36: 1413-1423, 2000.

[6] K. Boukir, Y. Maday, B. Métivet, E. Razafindrakoto, A high order characteristics/finite element method for the incompressible Navier-Stokes equations, *Int. J. Numer. Meth. Fluids*, 25: 1421-1454, 1997.

[7] S. C. Brenner, L. R. Scott, *The Mathematical Theory of Finite Element Methods*, third edition, Springer, 2008.

[8] B. A. Carreras, V. E. Lynch, G. M. Zaslavsky, Anomalous diffusion and exit time distribution of particle tracers in plasma turbulence model, *Phys. Plasmas*, 8: 5096-5103, 2001.

[9] P. Castillo, B. Cockburn, I. Perugia, and D. Schötzau, An a priori error analysis of the local discontinuous Galerkin method for elliptic problems, *SIAM J. Numer. Anal.*, 38: 1676-1706, 2000.

[10] M. H. Chen, W. H. Deng, A second-order numerical method for two-dimensional two-sided space fractional convection diffusion equation, *Appl. Math. Model.*, 38: 3244-3259, 2014.

[11] Z. X. Chen, Characteristic mixed discontinuous finite element methods for advection-dominated diffusion problems, *Comput. Meth. Appl. Mech. Engrg.*, 191: 2509-2538, 2002.

[12] Z. X. Chen, R. E. Ewing, Q. Y. Jiang, and A. M. Spagnuolo, Error analysis for characteristics-based methods for degenerate parabolic problems, *SIAM J. Numer. Anal.*, 40: 1491-1515, 2002.

[13] A. J. Chorin, J. E. Marsden, *A Mathematical Introduction to Fluid Mechanics*, Springer, 1990.

[14] P. G. Ciarlet, *The Finite Element Method for Elliptic Problems*, SIAM, 2002.

[15] B. Cockburn, G. Kanschat, D. Schötzau, C. Schwab, Local discontinuous Galerkin methods for the Stokes system, *SIAM J. Numer. Anal.*, 40: 319-343, 2002.

[16] B. Cockburn, G. Kanschat, D. Schötzau, The local discontinuous Galerkin method for the Ossen equations, *Math. Comp.*, 73: 569-593, 2003.

[17] B. Cockburn, G. Kanschat, D. Schötzau, A locally conservative LDG method for the incompressible Navier-Stokes equations, *Math. Comp.*, 74: 1067-1095, 2005.

[18] B. Cockburn, G. Kanschat, D. Schötzau, A note on discontinuous Galerkin divergence-free solutions of Navier-Stokes equations, *J. Sci. Comput.*, 31: 61-73, 2007.

[19] B. Cockburn, G. E. Karniadakis, C. -W. Shu, *The Development of Discontinuous Galerkin Methods*, Springer, 2000.

[20] B. Cockburn, J. Gopalakrishnan, F. -J. Sayas, A projection-based error analysis of HDG methods, *Math. Comp.*, 79: 1351-1367, 2010.

[21] B. Cockburn, C. -W. Shu, The local discontinuous Galerkin method for time-dependent convection-diffusion systems, *SIAM J. Numer. Anal.*, 35: 2440-2463, 1998.

[22] B. Cockburn, C. -W. Shu, Runge-Kutta discontinuous Galerkin methods for convection-dominated problems, *J. Sci. Comput.*, 16: 173-261, 2001.

[23] M. R. Cui, A high-order compact exponential scheme for fractional convection-diffusion equations, *J. Comput. Appl. Math.*, 255: 404-416, 2014.

[24] C. N. Dawson, T. F. Russell and M. F. Wheeler, Some improved error estimates for the modified method of characteristics, *SIAM J. Numer. Anal.*, 26: 1487-1512, 1989.

[25] W. H. Deng, Finite element method for the space and time fractional Fokker-Plank equations, *SIAM J. Numer. Anal.*, 47: 204-226, 2008.

[26] W. H. Deng, J. S. Hesthaven, Local discontinuous Galerkin methods for fractional diffusion equations, *ESAIM: M2AN*, 47: 1845-1864, 2013.

[27] J. Douglas, JR. and T. F. Russell, Numerical methods for convection-dominated diffusion problems based on combining the method of characteristics with finite element or finite difference procedures, *SIAM J. Numer. Anal.*, 19: 871-885, 1982.

[28] V. J. Ervin, J. P. Roop, Variational formulation for the stationary fractional advection dispersion equation, *Numer. Meth. Part. D. E.*, 22: 558-576, 2006.

[29] V. Girault, B. Rivière, M. F. Wheeler, A splitting method using discontinuous Galerkin for the transient incompressible Navier-Stokes equations, *ESAIM: M2AN*, 39: 1115-1147, 2005.

[30] V. Girault, P. A. Raviart, *Finite Element Approximations for the Navier-Stokes Equations*, Springer-Verlag Berlin Heidelberg, 1979.

[31] J. L. Guermond, J. Shen, On the error estimates for the rotational pressure-correction projection method, *Math. Comp.*, 73: 1719-1737, 2003.

[32] Y. He, A fully discrete stabilized finite-element method for the time-dependent Navier-Stokes problem, *IMA J. Numer. Anal.*, 23: 665-691, 2003.

[33] J. S. Hesthaven, T. Warburton, *Nodal Discontinuous Galerkin Methods: Algorithms, Analysis, and Applications*, Springer, 2008.

[34] X. Ji, H. Z. Tang, High-order accurate Runge-Kutta (local) discontinuous Galerkin methods for one- and two-dimensional fractional diffusion equations, *Numer. Math. Theor. Meth. Appl.*, 5: 333-358, 2012.

[35] J. W. Kirchner, X. H. Feng, C. Neal, Fractal stream chemistry and its implications for contaminant transport in catchments, *Nature*, 403: 524-527, 2000.

[36] Y. M. Lin, C. J. Xu, Finite difference/spectral approximations for the time-fractional diffusion equation, *J. Comput. Phys.*, 225: 1533-1552, 2007.

[37] M. E. Liu, Y. X. Ren, H. X. Zhang, A class of fully second order accurate projection methods for solving the incompressible Navier-Stokes equations, *J. Comput. Phys.*, 200: 325-346, 2004.

[38] F. Liu, P. Zhuang, V. Anh, I. Turner, K. Burrage, Stability and convergence of the difference methods for the space-time fractional advection-diffusion equation, *Appl. Math. Comp.*, 191: 12-20, 2007.

[39] R. L. Magin, *Fractional Calculus in Bioengineering*, Begell House, 2006.

[40] W. McLean, K. Mustapha, Convergence analysis of a discontinuous Galerkin method for a sub-diffusion equation, *Numer. Algor.*, 52: 69-88, 2009.

[41] W. McLean, Fast summation by interval clustering for an evolution equation with memory, *SIAM J. Sci. Comput.*, 34: A3039-A3056, 2012.

[42] K. Mustapha, W. McLean, Superconvergence of a discontinuous Galerkin method for fractional diffusion and wave equations, *SIAM J. Numer. Anal.*, 51: 491-515, 2013.

[43] K. Mustapha, W. McLean, Piecewise-linear, discontinuous Galerkin method for a fractional diffusion equation, *Numer. Algor.*, 56: 159-184, 2011.

[44] R. H. Nochetto, J. -H. Pyo, The Gauge-Uzawa finite element method. Part I: The Navier-Stokes Equations, *SIAM J. Numer. Anal.*, 43: 1043-1068, 2005.

[45] K. B. Oldham, J. Spanier, *The Fractional Calculus: Theory and Applications of Differentiation and Integration to Arbitrary*, Academic Press, 1974.

[46] O. Pironneau, On the transport-diffusion algorithm and its applications to the Navier-Stokes equations, *Numer. Math.*, 38: 309-332, 1982.

[47] I. Podlubny, *Fractional Differential Equations*, Academic Press, 1999.

[48] L. L. Qiu, W. H. Deng, J. S. Hesthaven, Nodal discontinuous Galerkin methods for fractional diffusion equations on 2D domain with triangualr meshes. submitted.

[49] W. H. Reed and T. R. Hill, Triangular mesh methods for the neutron transport equation, Los Alamos Scientific Laboratory report LA-UR-73-479, Los Alamos, NM, 1973.

[50] B. Rivière, *Discontinuous Galerkin Methods for Solving Elliptic and Parabolic Equations: Theory and Implementation*, SIAM, 1999.

[51] B. Rivière, V. Girault, Discontinuous finite element methods for incompressible flows on subdomains with non-matching interfaces, *Comput. Meth. Appl. Mech. Engrg.*, 195: 3274-3292, 2006.

[52] J. Sabatier, O. P. Agrawal, J. A. T. Machado, *Advances in Fractional Calculus: Theoretical Developments and Applications in Physics and Engineering*, Springer, 2007.

[53] M. F. Shlesinger, B. J. West, J. Klafter, Lévy dynamics of enhanced diffusion: application to turbulence, *Phys. Rev. Lett.*, 58: 1100-1103, 1987.

[54] Z. Y. Si, X. G. Song, P. Z. Huang, Modified characteristics Gauge-Uzawa finite element method for time dependent conduction-convection problems, *J. Sci. Comput.*, 58: 1-24, 2014.

[55] E. Süli, Convergence and nonlinear stability of the Lagrange-Galerkin method for the Navier-Stokes equations, *Numer. Math.*, 53: 459-483, 1988.

[56] R. Temam, *Navier-Stokes Equations: Theory and Numerical Analysis*, North-Holland, Amsterdam, 1984.

[57] K. X. Wang, H. Wang, M. Al-Lawatia, H. X. Rui, A family of characteristic discontinuous Galerkin methods for transient advection-diffusion equations and their optimal-order L^2 error estimates, *Commun. Comput. Phys.*, 6: 203-230, 2009.

[58] Z. B. Wang, S. W. Vong, A high-order exponential ADI scheme for two dimensional time fractional convection-diffusion equations, *Comput. Math. Appl.*, 68: 185-196, 2014.

[59] Q. Xu, J. S. Hesthaven, Discontinuous Galerkin method for fractional convection-diffusion equations, *SIAM J. Numer. Anal.*, 52: 405-423, 2014.

[60] S. Z. Zhai, X. H. Feng, Y. N. He, An unconditionally stable compact ADI method for three-dimensional time-fractional convection-diffusion equations, *J. Comput. Phys.*, 269: 138-155, 2014.